A barley gene cluster for the biosynthesis of diterpenoid phytoalexins

Dissertation

zur Erlangung des

Doktorgrades der Naturwissenschaften (Dr. rer. nat.)

vorgelegt der

Naturwissenschaftlichen Fakultät I
Biowissenschaften

der Martin-Luther-Universität Halle-Wittenberg

von

Herrn Yaming Liu

Gutachter:

1. Prof. Dr. Alain Tissier
2. Prof. Dr. Jörg Degenhardt
3. Prof. Dr. Corinna Dawid

Tag der Verteidigung: 30.06.2023, Halle (Saale)

For the ideal that I hold dear to my heart, I would not regret a thousand times to die.

亦余心之所善兮，虽九死其犹未悔。

Qu Yuan

Table of Contents

Abbreviations

3-DXAs	3-deoxyanthocyanidins
ATR1	*Arabidopsis thaliana* cytochrome reductase 1
B. sorokiniana or *Bs*	*Bipolaris sorokiniana*
bp	base pair
CcKS	*Coffea canephora ent*-kaurene synthase
CPP	copalyl diphosphate
CPS	copalyl diphosphate synthase
CRISPR/Cas9	clustered regularly interspaced short palindromic repeats and CRISPR-associated protein 9
$CuCl_2$	Copper(II) chloride
CYP(s)	cytochrome P450(s)
DAMPs	damage-associated molecular patterns
diTPS	diterpene synthase
DMAPP	dimethylallyl diphosphate
DNA	deoxyribonucleic acid
dpi	days post-infection
DXS	1-deoxy-d-xylulose 5-phosphate synthase
E. coli	*Escherichia coli*
EI	electron ionization
ESI	electrospray ionization
ETI	effector-triggered immunity
ETS	effector-triggered susceptibility
FPP	farnesyl diphosphate
GAs	gibberellins
GC-MS	gas chromatography-mass spectrometry
GGPP	geranylgeranyl diphosphate
GPP	geranyl diphosphate
HMGR	hydroxymethylglutaryl CoA-reductase
IPP	isopentenyl diphosphate
KS	kaurene synthase

KSL	kaurene synthase-like
LC-MS	liquid chromatography-mass spectrometry
LPP	labda-13-en-8-ol diphosphate
m/z	mass-to-charge ratio
MAPK	mitogen-activated protein kinase
MeJA	methyl jasmonate
MEP	methylerythritol phosphate
monoTPS	monoterpene synthase
MS	mass spectrometry
MVA	mevalonate
NB-LRR or NLR	nucleotide binding and leucine-rich repeat
NMR	nuclear magnetic resonance
OD	optical density
PAMPs/MAMPs	pathogen- or microbe-associated molecular patterns
PCR	polymerase chain reaction
PDA	pisatin demethylase
PPP	peregrinol diphosphate
PRRs	pattern recognition receptors
PTI	pattern-triggered immunity
PTMs	post-translational modifications
QToF	quadrupole time-of-flight
R	resistance
RNA	ribonucleic acid
RoMiS	*Rosmarinus officinalis* miltiradiene synthase
ROS	reactive oxygen species
RPKM	reads per kilobase of transcript per million mapped reads
S. vermifera or *Sv*	*Serendipita vermifera*
SA	salicylic acid
SEM	standard error of the mean
sesquiTPS	sesquiterpene synthase
T-DNA	transfer DNA
Ta[gene name]	*Triticum aestivum* [gene name]

TIC	total ion chromatogram
TPS	terpene synthase
UV	ultraviolet

List of Figures

List of Tables

1. Introduction

The increasing human population worldwide and climate change has led to many concerns about food security. A recent meta-analysis projected that global food demand will increase by 35% to 56% between 2010 and 2050 (van Dijk *et al.*, 2021). The increase in food productivity is fundamental for this challenge, together with other solutions, such as reducing poverty or decreasing food waste. Phytopathogens and pests limit the potential of agricultural production and reduce food quality. A study estimated global crop losses ranging between 17 and 23% for wheat, maize, potato, and soybean due to pathogen infection and pests, while for rice, the number is even higher (30%) (Savary *et al.*, 2019). The use of agrochemicals is helpful in pathogen control. However, excessive usage of these chemicals leads to residual accumulation and these eventually pose detrimental effects to humans and the ecosystem in general, which are incompatible with a sustainable agriculture. Alternatively, the adoption of elite crop varieties and the use of biocontrol agents are strongly required to promote green farming. To meet this demand, exploring plant resistance traits and a deeper understanding of the interaction between plants and pathogens is needed.

1.1 Plant abiotic and biotic stress

Plant stress refers to external conditions that adversely affect plants' growth, development, or productivity (Verma *et al.*, 2013), and can be classified into two major categories, abiotic stress and biotic stress. Plants being sessile organisms cannot escape from the environment where they grow. Therefore, they have evolved various mechanisms to adapt to or combat these threats. Plant responses to different stress factors are highly complex and involve altered gene expression, cellular metabolism, changes in growth rates, crop yields, and so on. (Gull *et al.*, 2019). They sense or recognize external stress, get elicited, and then generate an appropriate cellular and molecular response. The sensors on the cell surface or cytoplasm transfer the stimuli to the transcriptional machinery located in the nucleus via signal transduction pathways. Phytohormones, calcium, kinases, and reactive oxygen species (ROS) are critical components of the signaling networks (Peck & Mittler, 2020). This results in a

changed transcriptome and synthesis of protective proteins or compounds, helping plants to acclimate or become resistant to the specific stress.

Abiotic factors such as water availability, temperature, salinity, nutrients, and toxic metals under extreme conditions can cause stress to plants. Stress due to drought, salt, and temperature are the three major stress factors that affect geographical distribution of plants in nature, reduce plant productivity in agriculture, and threaten food security (Zhu, 2016). These adverse effects are expected to be aggravated by more frequent extreme weather due to climate change (Fedoroff *et al.*, 2010; Stott, 2016). Plants have adapted to quickly adjust to changes in physical or chemical conditions such as osmotic potential, ion concentration or temperature. These adaptions consist of complex internal signaling pathways that involves the employment of nonspecific or stress specific sensors followed by cell signaling and a cascade of events involving transcription, translation and post-translation modifications (PTMs), resulting in ionic and water homeostasis and cellular stability for the plant under abiotic stress (Zhu, 2016; Zhang *et al.*, 2022). With the knowledge, many genetic and chemical approaches have been explored to enhance resistance of plants towards abiotic stress (Morran *et al.*, 2011; Cao *et al.*, 2017; Gupta *et al.*, 2018; Wang *et al.*, 2018; Vaidya *et al.*, 2019). It is known that microbes in the rhizosphere, also called root microbiota, can benefit host plants by improving resistance to drought and other abiotic stress (Lugtenberg & Kamilova, 2009; Reinhold-Hurek *et al.*, 2015; Hou *et al.*, 2021). Therefore, new strategies employing beneficial soil microbes, possibly combined with genetic or chemical approaches, are becoming more appealing to scientists for the sake of environmental friendliness and sustainability (Zhang *et al.*, 2022).

Biotic stress of plants is caused by deleterious microorganisms like viruses, bacteria, fungi, viroids, phytoplasma, and nematodes. These aggressors, also named pathogens, deploy virulence factors that facilitate infection under defined environmental conditions to cause diseases on the leaf, stem, root, vascular system, and fruit of a susceptible plant (Wang, Y *et al.*, 2022). Unlike vertebrates, plants do not have an adaptive immune system due to a lack of circulatory system with mobile immune cells (Han, 2019). Though lacking the adaptive immune system, plants have

evolved a robust innate immune system. The immune response to pathogen invasion can be divided into three phases: immune recognition, signal integration, and defense execution (Wang, Y *et al.*, 2022) (**Fig. 1.1**). Plants use numerous cell-surface pattern recognition receptors (PRRs) to perceive pathogen- or microbe-associated molecular patterns (PAMPs/MAMPs), such as bacteria flagellin and peptidoglycan (Liu *et al.*, 2014; Buscaill *et al.*, 2019). Recognition of a microbe at the cell surface elicits pattern-triggered immunity (PTI). PTI usually activates early resistance responses, including stomatal closure, mitogen-activated protein kinase (MAPK) cascades, transcription of resistance-related genes, accumulation of antimicrobial secondary metabolites, ROS burst, and callose deposition (Luna *et al.*, 2011; Meng & Zhang, 2013; Jh, 2015; Sang & Macho, 2017). PTI is sufficient to provide complete host protection against non-adapted pathogens and partial protection against host-adapted pathogens (Wang, Y *et al.*, 2022). However, successful pathogens have evolved strategies to suppress PTI by specialized proteins, termed effectors, that alter host resistance signaling, thus contributing to pathogen virulence. This brings about effector-triggered susceptibility (ETS). In turn, plants have developed more specialized mechanisms to defend against adapted pathogens. Plants deploy nucleotide binding and leucine-rich repeat (NLR) proteins encoded by most resistance (R) genes (Dangl & Jones, 2001) to sense microbial effectors either directly or indirectly, resulting in effector-triggered immunity (ETI). ETI is a form of accelerated and amplified PTI response, accompanied by a hypersensitive response and programmed cell death. Diverse effectors from the pathogens can evolve to escape from the specific ETI, but new R proteins from the host plants can counteract this adaption hence triggering ETI again (Jones & Dangl, 2006).

In nature, plants grow in field environments where they are often exposed to multiple stress factors simultaneously, such as drought and salinity, drought and heat, or abiotic stress factors and pathogen infection. Different from how they respond to single stress, plants uniquely react to combination of two or more stress (Atkinson & Urwin, 2012; Suzuki *et al.*, 2014). Rather than simply being additive, one stress factor can have either positive or detrimental effects on the second layer of stress, which is imposed on the same host plant. This interaction is mediated by hormone signaling pathways that may induce or inhibit one another, particularly that of abscisic acid

(Anderson *et al.*, 2004; Asselbergh *et al.*, 2008). Transcription factors, kinase cascades, and ROS are critical components of this cross-talk (Atkinson & Urwin, 2012). An understanding of the mechanism underlying this interaction will help crop protection and production.

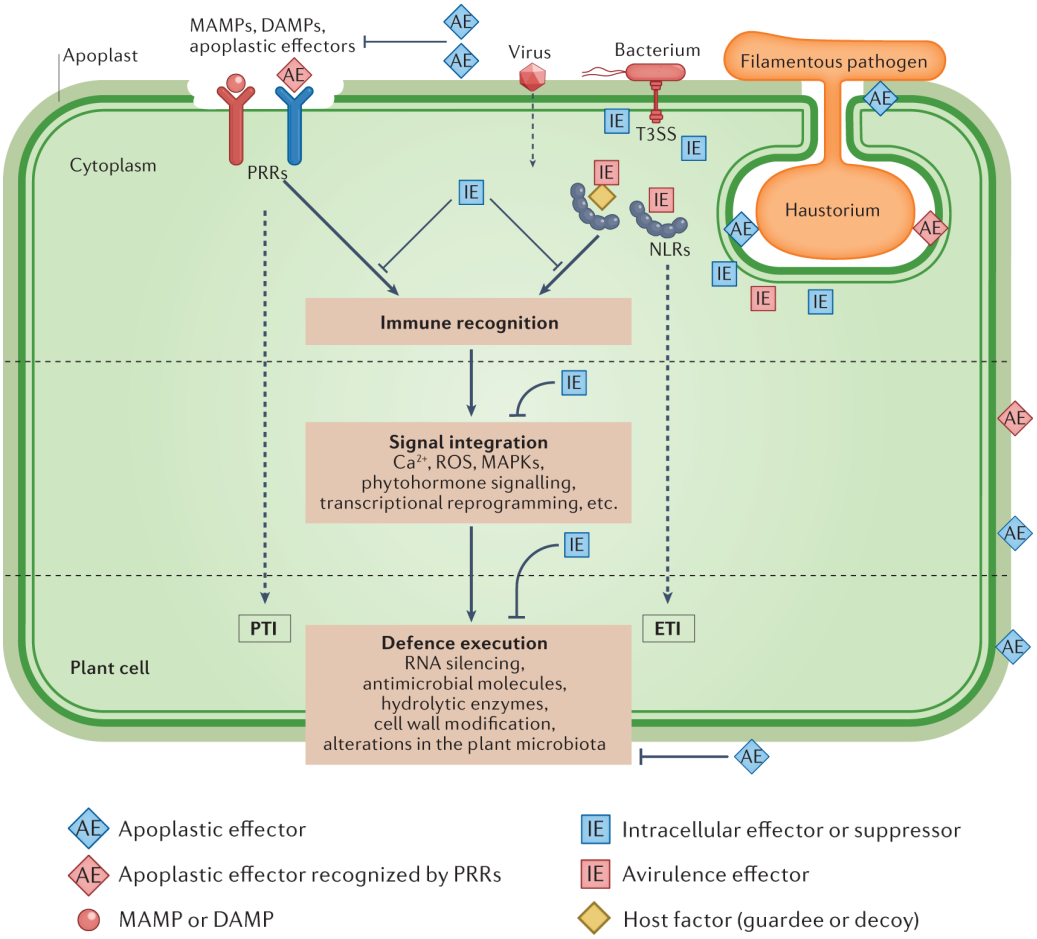

Figure 1.1 The activation of plant innate immunity

The activation of plant innate immunity can be divided into three stages: immune recognition, signal integration, and defense execution. PRR-mediated recognition of MAMPs or damage-associated molecular patterns (DAMPs) elicits pattern-triggered immunity. NLR-mediated pathways trigger effector-triggered immunity. Plant immune responses include cell wall reinforcement, ROS production, RNA interference, protease and protease inhibitor secretion, antimicrobial compound biosynthesis, and plant microbiota homeostasis. This figure is originally from (Wang, Y *et al.*, 2022).

1.2 *Bipolaris sorokiniana* as a cereal pathogen

Bipolaris sorokiniana (syn. *Helminthosporium sorokinianum*, *Drechslera sorokiniana*, and *Helminthosporium sativum*) is an ascomycete fungus. It is distributed worldwide but is more prevalent in warm, dry regions. The genus *Bipolaris* has brown conidiophores, producing conidia through the apical pore. The conidia are brown,

multiple-celled, elliptical, straight, or curved, germinating by one germ tube at each end (Navathe *et al.*, 2020; Al-Sadi, 2021) (**Fig. 1.2**). *B. sorokiniana* has thick-walled, olive-brown, elliptical conidia (60–120 µm × 12–20 µm) with five to nine cells (Kumar *et al.*, 2002; Al-Sadi, 2021). In axenic culture, the mycelium is composed of loose cotton-like hypha, with white or light to dark grey color depending on the isolates (Kumar *et al.*, 2002).

B. sorokiniana has a broad host spectrum in the Poaceae family, including common cereals, such as wheat and barley, though rye and oat are less susceptible. A literature survey (Sprague, 1950) included more than 100 grass species in the host plant family, including *Avena sativa*, *Bromus catharticus*, *Dactylis glomerata*, *Festuca elatior*, *Festuca rubra*, *Hordeum vulgare*, *Lolium perenne*, *Phleum pratense*, *Poa pratensis*, *Secale cereale*, *Triticum aestivum*, *Triticum spelta*, and *Zea mays*. *B. sorokiniana* has no host specialization, while some isolates were reported to show different aggressiveness in the infection of wheat and barley (Al-Sadi, 2016).

B. sorokiniana induces several plant diseases, including head blight and seeding blight of wheat and barley, as well as leaf spot blotch, common root rot, and black point on grains (Kumar *et al.*, 2002; Al-Sadi, 2021) (**Fig. 1.2**). Seedings can get the infection from contaminated seeds, then die or develop brown necroses on the coleoptile and the primary leaf. Young plants wither and die afterward. Leaf blade and sheath infections of older plants start with numerous small spots. They are dark brown, first rounded, later elongated, and surrounded by a yellow halo. These individual spots grow together over time, destroying the whole sheet. Leaf spotting appears more frequently in wet weather, on lower leaves. In proper conditions, especially in warm, dry areas, the fungus also infects roots and crowns. They turn brown and rot; the infection can be so severe that the plants dry out without producing any seed (Kumar *et al.*, 2002). *B. sorokiniana* can also survive as a saprophyte in soil. However, it shows little competitive saprophytic activity. Spore formation and germination are also inhibited in the soil (Simmonds *et al.*, 1950).

Barley (*Hordeum vulgare*) is a prominent cereal grain grown in temperate climates worldwide, ranking fourth in quantity produced behind maize, rice, and wheat (Ullrich,

2010). The production of barley is commonly used for bread and health product, though it is primarily used as animal feed and as a source of substrate for alcoholic beverages, especially beer (Newton *et al.*, 2011). The first draft of the barley genome was published in 2016 and was recently updated (Beier, Sebastian *et al.*, 2017; Monat *et al.*, 2019; Mascher *et al.*, 2021). As a self-pollinating species with a diploid (2n) genome and a haploid complement of only seven chromosomes, it has proven to be an excellent model organism for basic and applied research. Furthermore, a wealth of natural genetic diversity constitutes a valuable resource to breed varieties that are adapted to various environmental challenges such as drought, salinity, and cold (Dawson *et al.*, 2015; Pham *et al.*, 2019). Genetic transformation and an extensive collection of molecular tools are now well-established in this species (Rotasperti *et al.*, 2020). All these make it an ideal model crop for functional genomics studies.

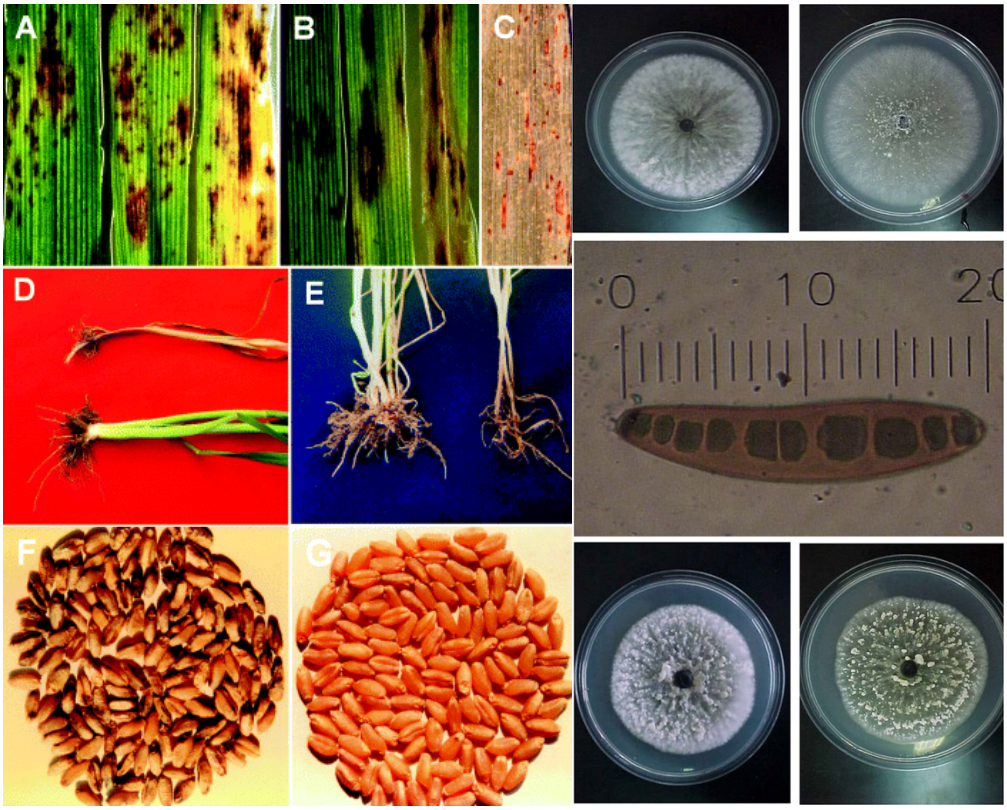

Figure 1.2 Disease caused by *B. sorokiniana*; Morphology of *B. sorokiniana* culture and spores

Spot blotch caused by *B. sorokiniana* on primary leaves of barley (A), wheat (B), and flag leaf of wheat (C). Common root rot (D), crown rot (E), black point (F), healthy grain seeds (G) (Kumar *et al.*, 2002). *B. sorokiniana* culture and spores (1 scale is 5 µm) grow on potato dextrose agar. The mycelial growth of four isolates shows mixed color (white and black), with varying intensities of the black color among the isolates (Al-Sadi, 2021).

1.3 Plant chemical defense

In parallel to PTI and ETI, plants also employ a wide range of secondary metabolites (synonymous with specialized metabolites) that play roles in the interactions of plants with the biotic and abiotic environment, including the essential part of chemical defense against insects and pathogens. Plant secondary metabolites are highly diverse in chemical structures comprising over 200,000 compounds, varying in composition and concentration at the individual and population level, as well as within different development stages and plant tissues (Hartmann, 2007). The differentiation between primary and secondary metabolism (metabolites) was first introduced by Albrecht Kossel in 1891 (Mothes, 1980; Hartmann, 2007). In contrast to a primary metabolite that is directly involved in growth, development, and reproduction, a secondary metabolite is formed during metabolism but is no longer used in the formation of new cells (Sachs, 1874). It has no direct role in these primary functions (Seigler, 1998). Therefore, for a long time, they were just considered as by- or detoxification products of primary metabolism with only accidental biological function (Reznik, 1960; Paech, 2013). The study of plant secondary compounds can be traced back to 1806 when Friedrich Wilhelm Sertürner isolated morphine from the opium poppy. This is the first demonstration that the active component of a plant drug can be isolated and attributed to a single chemical compound. Over the last several decades, research has illuminated the ecological importance of plant secondary metabolites in chemical defense (fungi, bacteria, viruses, herbivores), attraction and stimulation (pollination, seed dispersal, symbiosis), and protection (ultraviolet, evaporation, extreme temperature, drought) of plants (Hartmann, 1996; Chomel *et al.*, 2016). These activities are fulfilled by three major classes of secondary metabolites: (1) terpenoids, (2) phenolic and polyphenolic compounds, and (3) nitrogen-containing (i.e., alkaloids) or sulfur-containing (e.g., glucosinolates) compounds.

Phytoalexins are defined as antimicrobial low-molecular-weight secondary metabolites that are synthesized *de novo* and accumulated in plants after exposure to biotic or abiotic stresses. The concept of phytoalexins was introduced over 70 years ago by Müller and Börger. They demonstrated that prior infection of potato tuber with an incompatible race (results in resistance) of *Phytophthora infestans* induced host resistance to a compatible race (results in disease) of *P. infestans* or to a tuber-

infecting *Fusarium* (Mueller & Börger, 1939). Based on the finding, they hypothesized that in response to the incompatible race, the tuber produced nonspecific substances, which they called phytoalexins, that inhibited further growth of the pathogen and protected the tissue against later infection by other compatible pathogens. Phytoalexins are absent in healthy tissues or present only in trace amounts, while they accumulate in significant quantities after pathogen infection. Other factors like temperature, humidity, and water availability also affect the synthesis of phytoalexins. Their biosynthesis is not restricted to a specific organ. Almost every organ, such as roots, stems, leaves, flowers, and seeds, can produce phytoalexins (Ahuja *et al.*, 2012). However, often these substances are produced in small amounts, and it makes it difficult to isolate them from plant sources. The development of chemical synthesis and the usage of their analogs facilitate studying their environmental function and biological activity (Pedras *et al.*, 2004b).

Phytoalexins from the Poaceae

The most studied Poaceae crop plants known to produce phytoalexins are rice (*Oryza sativa*), maize (*Zea mays*), sorghum (*Sorghum bicolor*), wheat (*Triticum aestivum*), and barley (*Hordeum vulgare*). Rice and maize produce many diterpenoid phytoalexins, while flavonoid phytoalexins are characterized from rice and sorghum. In wheat and barley, several phenylamides are induced in response to pathogen attack.

Fifteen phytoalexins, including fourteen diterpenoids and one flavonoid, have been characterized in rice by the treatment with elicitors such as chitin, fungal cerebroside, and cholic acid; leaf infection with the blast fungus *Magnaporthe grisea* or irradiation with ultraviolet (UV) light (UEHARA, 1958; Koga *et al.*, 2006; Schmelz *et al.*, 2014). These diterpenoid phytoalexins are classified into four groups based on the structure of their backbone precursors, phytocassanes A-E, oryzalexins A-F, momilactones A and B, and oryzalexin S (Okada, 2011) (**Fig. 1.3**). As well as diterpenoids, the UV-inducible flavonoid sakuranetin is a major phytoalexin in rice (Kodama *et al.*, 1992; Shimizu *et al.*, 2012). It was considered the only phenolic phytoalexin in rice until studies identified several phenylamides by infection of rice with brown spot fungus *Bipolaris oryzae* or UV stress (Ishihara *et al.*, 2008; Park *et al.*, 2014). Their antimicrobial activity against rice pathogens suggested their role as phytoalexins.

These phenylamides include *N*-cinnamoyltyramine, *N*-cinnamoyltryptamne, *N*-feruloyltyramine, *N*-*p*-coumaroylserotonin, and *N*-feruloylserotonin (Cho & Lee, 2015).

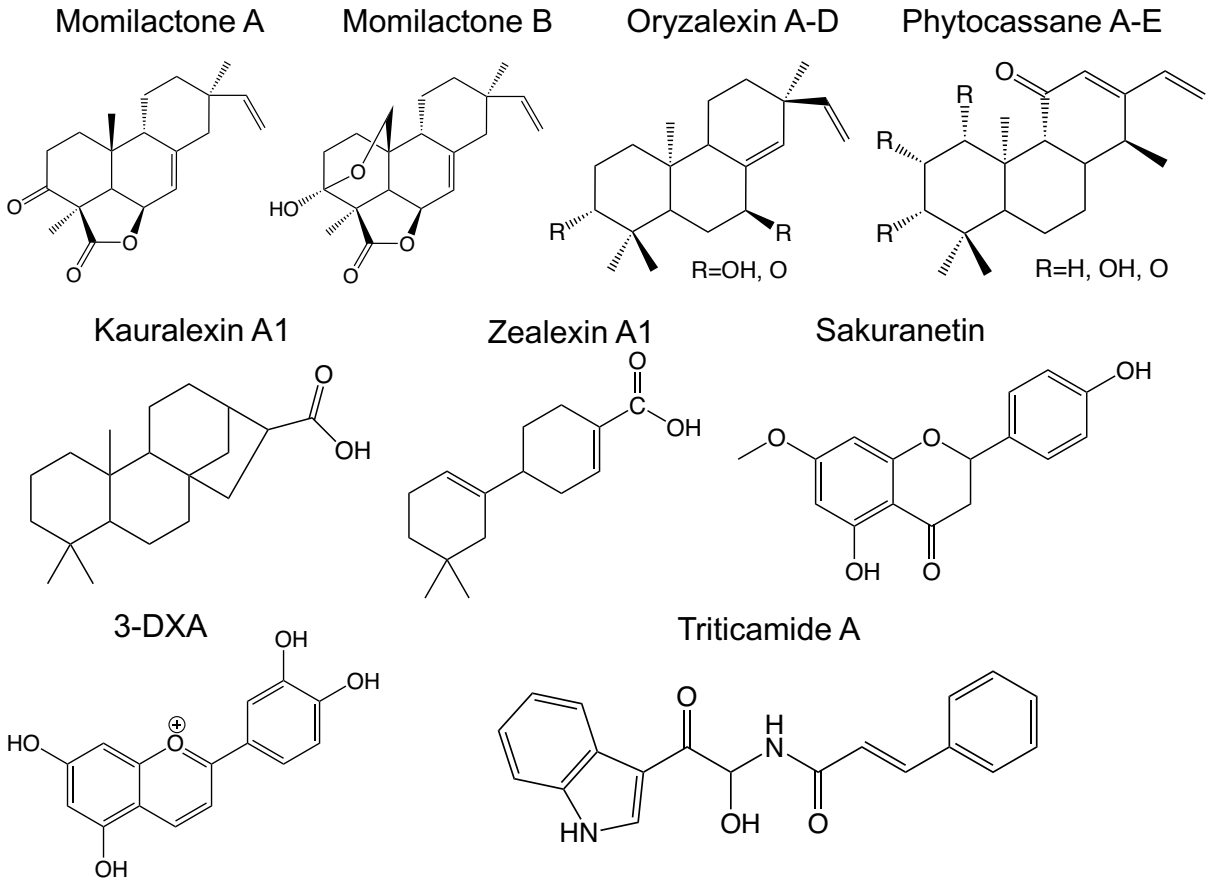

Figure 1.3 Structures of selected phytoalexins from members of the Poaceae

Several groups of diterpenoid phytoalexins including momilactones, oryzalexins, and phytocassanes were identified in rice. Terpenoid phytoalexins including kauralexins and zealexins were identified in maize.

Maize is one of the most abundant crops on earth and is the staple food for many populations, especially in the Americas and Africa. Maize is cultivated worldwide and has a variety of industrial applications, such as animal feed, cosmetics, and biofuel production. Maize stems produce labdane-type diterpenoid phytoalexins, termed kauralexins, and acidic sesquiterpenoids, known as zealexins, in response to fungal attack (Ejike *et al.*, 2013) (**Fig. 1.3**). In addition, insects, pathogen attack, and phytohormones trigger the biosynthesis and accumulation of the kauralexins (Huffaker *et al.*, 2011; Schmelz *et al.*, 2011). In addition to terpenoids, another important class of phytoalexins in maize are benzoxazinoids represented by 2-hydroxy-4,7-dimethoxy-

1,4-benzoxazin-3-one-glucoside (HDMBOA-Glc) and 4-dihydroxy-7-methoxy-1,4-benzoxazin-3-one-glucoside (DIMBOA-Glc) (Oikawa *et al.*, 2004; Meihls *et al.*, 2013).

Sorghum synthesizes a distinctive class of flavonoid phytoalexins named 3-deoxyanthocyanidins (3-DXAs) (**Fig. 1.3**) upon fungal infection (Lo *et al.*, 1999), including apigeninidin, luteolinidin, tricetinidin, columnidin, and diosmetinidin. The 3-DXAs are a rare class of plant pigments with distinct chemical properties from their anthocyanin analogs. For instance, 3-DXAs are more stable to light, heat, and change in pH than anthocyanins. The 3-DXAs were demonstrated to exhibit *in vitro* toxicity toward some bacteria (Stonecipher *et al.*, 1993) and fungi including the pathogen of sorghum, *Colletotrichum sublineolum* (Nicholson *et al.*, 1987; Schutt & Netzly, 1991; Lo *et al.*, 1996). The 3-DXAs can be induced in sorghum roots by methyl jasmonate (MeJA), but salicylic acid (SA) antagonizes the stimulation (Liu *et al.*, 2010). Biosynthesis of 3-DXAs is independent of light and occurs in the dark, in contrast to that of anthocyanins which are light-dependent (Weiergang *et al.*, 1996).

The accumulation of phenylamide phytoalexins was detected upon wheat leaf inoculation with *Bipolaris sorokiniana*, the causal agent of spot blotch of Poaceae species. These phenylamides were also induced by *Fusarium graminearum* infection and by treatment with elicitors like $CuCl_2$, jasmonic acid, and isopentenyladenine. The bioactivity of these amides, like the inhibition of conidial germination and germ tube elongation of *F. graminearum* and *Alternaria brassicicola,* indicates their antifungal activity and roles as phytoalexins (Ube, Naoki *et al.*, 2019). Later, two of the same phenylamides, triticamide A and B, and a new one, triticamide C, were identified in barley roots infected by a root pathogen, *Fusarium culmorum* (Ube, N. et al., 2019) (**Fig. 1.3**). Very recently, two methoxylchalcone phytoalexins were characterized in barley leaves in response to $CuCl_2$ treatment and pathogen infection (Ube *et al.*, 2021). The accumulation of methoxylchalcones was observed in seven barley cultivars tested in the study but was absent in wild *Hordeum* species, wheat, and rice, indicating their specificity to cultivated barley. To date, no diterpenoid phytoalexins have been identified from wheat and barley. However, the results from different studies suggested that this group of specialized metabolites also exist in the two species. Wheat contains copalyl diphosphate synthase (*CPS*) and kaurene synthase-like (*KSL*)

gene families that encode diterpene synthases, known to act sequentially in the biosynthesis pathway of labdane-related diterpenoids (Wu *et al.*, 2012; Zhou, K. *et al.*, 2012). More details were discussed in section **3.4**. Moreover, UV-inducible transcription of *TaCPS1* and *TaCPS2* suggests that they potentially play a role in phytoalexin biosynthesis. Like wheat, barley also contains multiple copies of *CPS*, *KSL*, and kaurene oxidase-like genes. The barley *CPS* and *KSL* genes are in regions of the chromosome known to be syntenic with the rice momilactones biosynthesis gene cluster (Spielmeyer *et al.*, 2004; Wu *et al.*, 2012; Wu *et al.*, 2022). Therefore, although no diterpenoid products have yet been reported, it appears that they also exist in wheat and barley and function as defense compounds.

Phytoalexins from the Brassicaceae

The Brassicaceae (common name crucifers), containing some 338 genera and more than 3700 species, is a plant family of much economic importance, including oilseeds, vegetables, and condiments that have been cultivated and consumed worldwide for centuries. Furthermore, some wild cruciferous species, including *Arabidopsis thaliana* and *Thellungiella* species, are model organisms of paramount importance in almost every scientific aspect, and some have great potential for industrial utilization. More than 40 phytoalexins have been isolated from the plant family, and most of the phytoalexins are alkaloids derived from the amino acid tryptophan and contain sulfur (Pedras & Yaya, 2010; Pedras *et al.*, 2011). Since indole- and sulfur-containing phytoalexins were firstly and mostly reported in the *Brassicaceae* species, it is considered a characteristic feature of the family. Brassinin, cyclobrassinin, and 1-methoxybrassinin are indole phytoalexins first isolated from Chinese cabbage infected by the *Pseudomonas cichorii* bacterium (Takasugi *et al.*, 1986) (**Fig. 1.4**). Camalexin, the major phytoalexin in *Arabidopsis*, was first isolated from camelina (*Camelina sativa*) then was also detected in *Arabidopsis* and a few related species (Browne *et al.*, 1991; Bednarek *et al.*, 2011). The production of camalexin can be induced in *Arabidopsis* leaves by biotrophic and necrotrophic plant pathogens or elicitors like autoclaved baker's yeast suspension and fungal toxins (Bouizgarne *et al.*, 2006). Phytoalexins from crucifers have beneficial effects on plant protection but also on human health. For instance, brassinin a phytoalexin from crucifers is known to exhibit anticancer activity (Chripkova *et al.*, 2014).

Phytoalexin from the Fabaceae

Fabaceae or Leguminosae, commonly known as the legume, pea, or bean family, is the third largest family among the angiosperms after Orchidaceae and Asteraceae, consisting of more than 700 genera and about 20,000 species of trees, shrubs, vines, and herbs (Christenhusz & Byng, 2016). This family is distributed worldwide; most woody species are in tropical regions, while the herbaceous plants and shrubs are predominant in temperate areas. The Fabaceae includes several plants that are common in agriculture, including soybeans (*Glycine max*), garden peas (*Pisum sativum*), peanuts (*Arachis hypogaea*), chickpea (*Cicer arietinum*), and alfalfa (*Medicago sativa*).

Phytoalexins are extensively studied in the Fabaceae. Most phytoalexins produced by the family belong to six isoflavonoid classes: isoflavones, isoflavanones, pterocarpans, pterocarpenes, isoflavans, and coumestans (Jeandet *et al.*, 2013). Pisatin (**Fig. 1.4**) was the first phytoalexin to be purified and chemically identified from pods of *Pisum sativum* (Cruickshank & Perrin, 1960) and is the major one of garden pea plants. It can be stimulated by many biotic and abiotic factors such as fungi, spore germination fluids, UV radiation, and antibiotics (Schwochau & Hadwiger, 1968; Hadwiger & Schwochau, 1971; Pueppke & VanEtten, 1976; SHIRAISHI *et al.*, 1978). In the study of *P. sativum* and pathogen *Nectria haematococca*, fungal isolates which can detoxify pisatin showed high virulence, suggesting pisatin is an effective barrier to defense against microbial attack (Preisig *et al.*, 1990). Soybeans are well studied, mainly due to their ability to produce proteins and health-promoting compounds such as genistein and daidzein (Sun *et al.*, 2016; Goh *et al.*, 2022). Stress-challenged soybean tissues produce a group of flavonoids called glyceollins. In addition to their function as plant defense compounds, some members, including glyceollins I, II, and III (**Fig. 1.4**), have demonstrated potential antidiabetic activity and antitumor effects in the human breast and prostate cancer (Bamji & Corbitt, 2017). Plants of *A. hypogaea* synthesize and accumulate a group of stilbene-derived antimicrobial compounds termed stilbenoids after being challenged by different biotic agents (Sobolev *et al.*, 2011). Inoculation of peanut seeds with an *Aspergillus caelatus* strain produced stilbenes and stilbenoids (arahypin 1-7) and pterocarpenes, which showed defensive roles against several pathogens (Sobolev *et al.*, 2009; Sobolev, Victor S. *et al.*, 2010; Sobolev, V. S. *et al.*,

2010). Germinated peanuts were shown to produce phytoalexins, including resveratrol, arachidins (**Fig. 1.4**), and a large number of stilbenoids derivatives after inoculation with the food-grade fungus *Rhizopus oligosporus* (Wu et al., 2011). An analysis of peanut kernels infected with different *Aspergillus* fungal strains showed that phytoalexin profiles varied in a temporal, spatial, and strain-specific manner (Sobolev, 2008). The reduced form of glutathione elicits the formation not only of the pterocarpan phytoalexins medicarpin and maackiain but also that of the constitutive isoflavones biochanin A and formononetin, and in seedings older than four days, that of the isoflavanones homoferreirin and cicerin (Armero *et al.*, 2001). These secondary metabolites do not accumulate in plant root tissue; instead, they are released into the surrounding external medium.

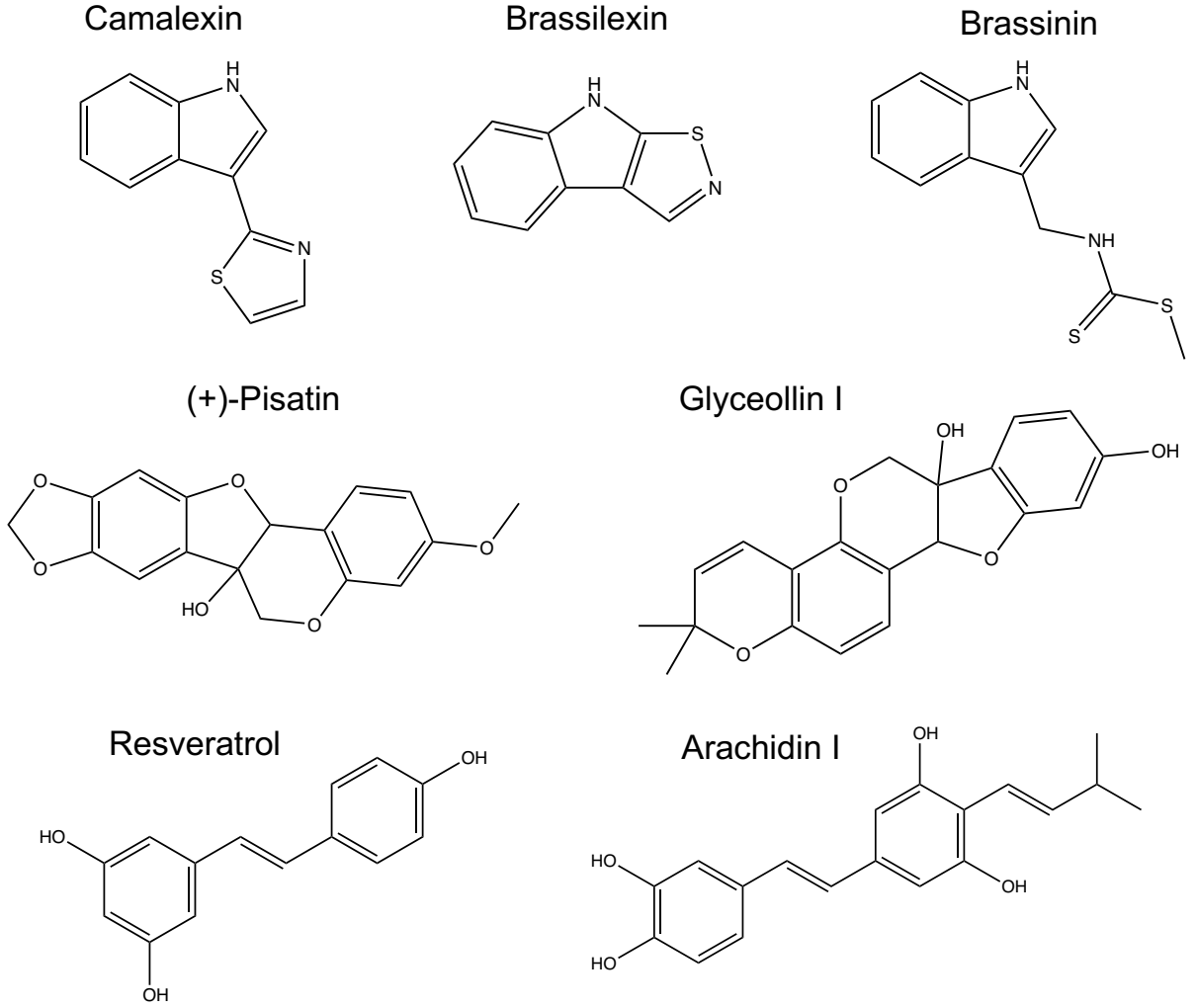

Figure 1.4 Structures of selected phytoalexins from members of the Brassicaceae and Fabaceae

Indole- and sulfur-containing phytoalexins including camalexin, brassilexin and brassinin were characterized from members of the Brassicaceae. Pterocarpan and stilbenoid phytoalexins were identified in plants of the Fabaceae.

Detoxification of phytoalexins

Since phytoalexins can be toxic not only to the pathogen but also to the plant cell, they can accumulate in plants only transiently, and then they are degraded oxidatively or polymerized by enzymes, such as peroxidases, cytochrome P450s (CYPs) (VanEtten *et al.*, 1982; Camagna *et al.*, 2020). Detoxification of phytoalexins by phytopathogens is of great interest due to its potential application in controlling of plant pathogens (VanEtten *et al.*, 2001). Many studies on phytoalexin tolerance in pathogenic fungi have demonstrated a clear relationship between virulence and their ability to detoxify phytoalexins. It is suggestive that such detoxification of plant phytoalexins is a general mechanism of fungi to overcome phytoalexin-mediated plant defenses. Therefore, the degradation of phytoalexins may be a necessary component of successful fungal pathogenicity.

The metabolism and detoxification of the phytoalexin brassinin from the Cruciferae family by virulent isolates of *Leptosphaeria maculans* led to indole-3-carboxylic acid via indole-3-carboxaldehyde, employing the brassinin oxidase enzyme (Pedras & Taylor, 1991; Pedras *et al.*, 2008). In *Sclerotinia sclerotiorum*, this detoxification is mediated by a glucosyltransferase (Pedras *et al.*, 2004a). Brassilexin, another phytoalexin from the same family, can also be detoxified by *L. maculans* or *S. sclerotiorum* (Pedras & Suchy, 2005; Pedras & Hossain, 2006). Camalexin produced by the model species *Arabidopsis thaliana* is one of the most studied phytoalexins. *Rhizoctonia solani* degrades and detoxifies camalexin through 5'-hydroxylation of the indole ring or the formation of an oxazoline derivate (Pedras & Khan, 2000). The stem rot phytopathogen *S. sclerotiorum* is able to transform camalexin into the glycosylated derivate at N-1 or C-6 of the indole ring (Pedras *et al.*, 2004a).

Pisatin, the first chemically characterized phytoalexin, has been widely studied regarding its degradation by fungal pathogens. Pea pathogen *Ascochyta pisi* or *Nectria haematococca* can metabolize pisatin to 6a-hydroxymaackiain by demethylation, which is catalyzed by pisatin demethylase (PDA) (Fuchs *et al.*, 1980; VanEtten *et al.*, 1980). PDA is a microsomal cytochrome P450 monooxygenase and is inducible in *N. haematococca* (Desjardins et al., 1984). Naturally occurring isolates of *N. haematococca* that lack the ability to demethylate pisatin are not pathogenic to

pea, and this deficiency in virulence was complemented by introducing a PDA-encoding gene into *pda*$^-$ isolates (Ciuffetti & VanEtten, 1996). It indicates that the ability to detoxify pisatin is required for the pathogenicity of *N. haematococca* on the pea. It has been demonstrated that when PDA-encoding genes were transformed into and highly expressed in *Cochliobolus heterostrophus*, a fungal pathogen of maize but not pea plants, this recombinant fungus acquired the ability to cause symptoms on pea and retained its virulence on maize (Schäfer *et al.*, 1989). This suggests that PDAs help recombinant *C. heterostrophus* develop pathogenicity on a new host plant.

1.4 Terpenoids *in planta*

Terpenoids represent the chemically and functionally most diversified class of natural products in living organisms. More than 36,000 members of this class have been reported, and this number is continuously increasing at a rate of about 1000 per year (Ashour *et al.*, 2010). Terpenoids can be highly diverse in structure, exhibiting hundreds of carbon skeletons and a wide range of functional groups. The classification of terpenoids is based on the number of isoprenoid units present in the structure, with compounds having two isoprenoid units (monoterpenes), three isoprenoid units (sesquiterpenes), four isoprenoid units (diterpenes), five isoprenoid units (sesterterpenes), six isoprenoid units (triterpenes), eight isoprenoid units (tetraterpenes) and more than eight isoprenoid unit (polyterpenes). Terpenoids play roles in almost all basic plant processes, including growth, development, reproduction, and defense (Wink & Van Wyk, 2008). For instance, gibberellins (GAs), a group of diterpenoid plant hormones, are involved in the control of seeds germination, stem elongation, and flower induction (Thomas *et al.*, 2005). Carotenoids, such as lutein and β-carotene, are the essential constituents of photosynthetic tissues. And the hormones abscisic acid and strigolactones are derived from the degradation of carotenoids. Phylloquinone (Vitamin K1), tocopherols (Vitamin E), and chlorophylls contain a prenyl side chain with all or all but one of the double bonds reduced. Many terpenoids act as defense compounds against microorganisms and herbivores and or are signal molecules to attract pollinating insects, fruit-dispersing animals, or predators that can destroy insect herbivores. Furthermore, some terpenoids have marked pharmacological activities and are interesting for medicine and biotechnology.

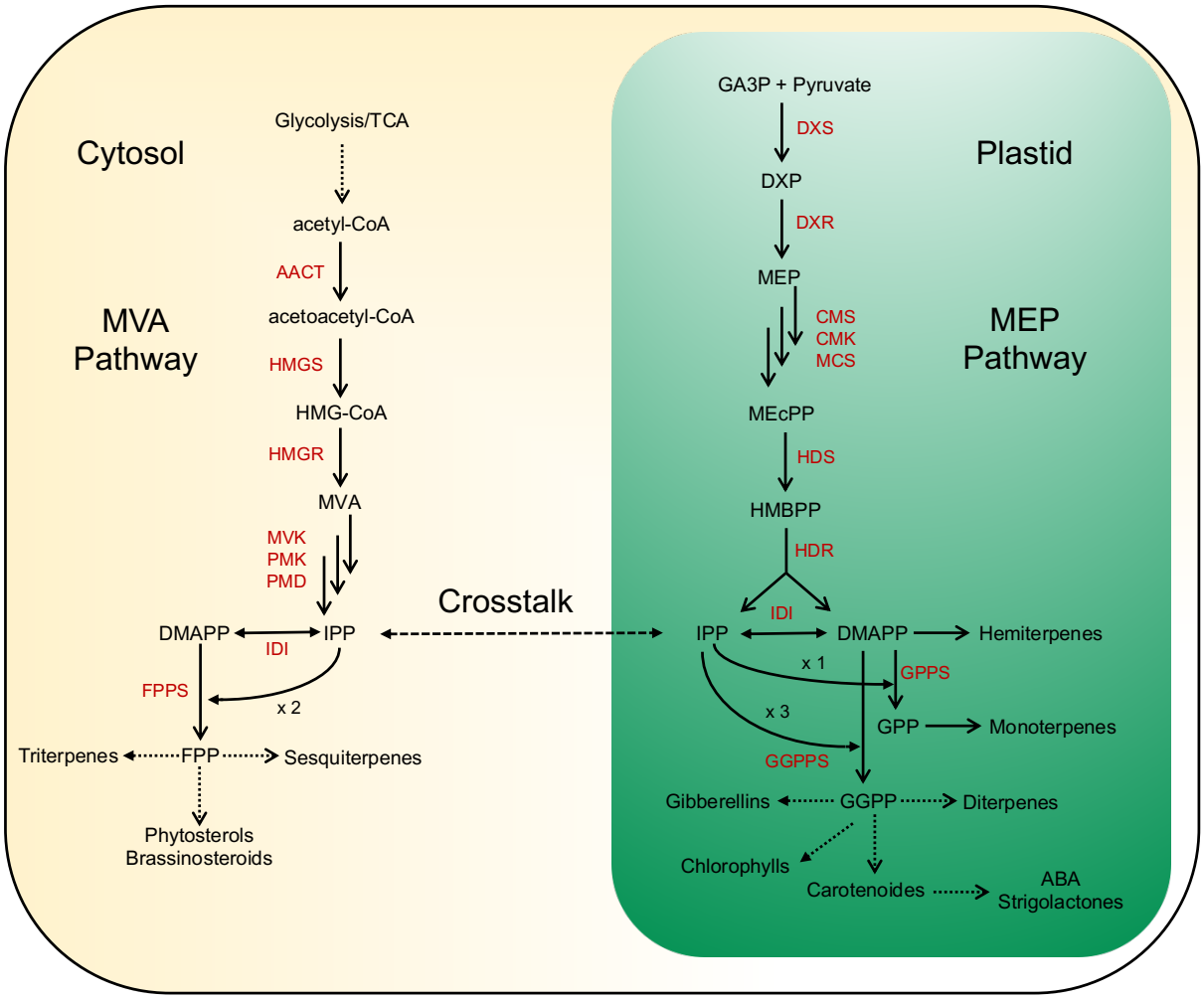

Figure 1.5 Isoprenoids metabolism in a plant cell

In the plant cell, two pathways, the cytosolic MVA pathway and plastidial MEP pathway are present, providing the precursors, IPP and DMAPP, for the biosynthesis of isoprenoids. **Metabolites**: **HMG-CoA**: 3-hydroxy-3-methylglutary-CoA, **MVA**: mevalonic acid, **IPP**: isopentenyl diphosphate, **DMAPP**: dimethylallyl diphosphate, **FPP**: famesyldiphosphate, **GA3P**: glyceraldehyde-3-phosphate, **DXP**: 1-deoxy-D-xylulose5-phosphate, **MEP**: methylerythritol phosphate, **MEcPP**: 2-C-Methyl-d-erythritol-2,4-cyclopyrophosphate, **HMBPP**: 4-hydroxy-3-methylbut-2-enyl diphosphate, **GPP**: geranyl diphosphate, **GGPP**: geranylgeranyl diphosphate, **ABA**: abscisic acid. **Enzymes**: **AACT**: acetoacetyl CoA thiolase, **HMGS**: 3-hydroxy-3-methylglutaryl-CoA synthase, **HMGR**: 3-hydroxy-3-methylglutaryl-CoA reductase, **MVK**: mevalonate kinase, **PMK**: phosphomevalonate kinase, **PMD**: mevalonic acid 5-diphoshate decarboxylase, **IDI**: isopentenyl diphosphate isomerase, **FPPS**: farnesyl-diphosphate synthase, **DXS**: 1-deoxy-D-xylulose5-phosphate synthase, **DXR**: 1-deoxy-D-xylulose5-phosphate reductoisomerase, **CMS**: 4-diphosphocytidyl-2-C-methyl-D-erythritol synthase, **CMK**: 4-diphosphocytidyl-2-C-methyl-D-erythritol kinase, **MCS**: 2-C-methyl-d-erythritol-2,4-cyclodiphosphate synthase, **HDS**: 4-hydroxy-3-methylbut-2-enyl diphosphate synthase, **HDR**: 4-hydroxy-3-methylbut-2-enyl diphosphate reductase, **GPPS**: geranyl diphosphate synthase, **GGPPS**: geranyl geranyl diphosphate synthase. **TCA:** tricarboxylic acid.

Terpenoids are derived from a basic five-carbon unit, isopentenyl diphosphate (IPP), and its allylic isomer, dimethylallyl diphosphate (DMAPP). DMAPP is sequentially condensed with IPP to yield short-chain isoprenoid precursors such as geranyl

diphosphate (GPP), farnesyl diphosphate (FPP), and geranylgeranyl diphosphate (GGPP), which are further metabolized to monoterpenes, sesquiterpenes, and diterpenes respectively, employing terpene synthase (TPS). In plant cells, biosynthesis of IPP and DMAPP occurs via two distinct pathways (**Fig. 1.5**): the cytosolic mevalonate (MVA) pathway, first reported in yeast and mammals, and the plastidic methylerythritol phosphate (MEP) pathway, identified afterward in eubacteria and plants (Rohmer *et al.*, 1996; Estévez *et al.*, 2000; Estévez *et al.*, 2001). In plants, these two pathways are metabolically separated and provide IPP and DMAPP for the biosynthesis of distinct sets of terpenes in different subcellular compartments (**Fig. 1.5**). The plastidial MEP pathway provides the precursors for the synthesis of monoterpenes, diterpenes, and carotenoids, whereas the cytosolic MVA pathway plays roles in the production of sesquiterpenes and triterpenes (**Fig. 1.5**). However, some studies suggest that there is crosstalk of a small fraction of the terpene precursors, including IPP and DMAPP, between the MVA pathway and the MEP pathway (Kasahara *et al.*, 2002; Laule *et al.*, 2003). As the MEP pathway is absent in animals and fungi, it also draws significant attention to being a target for the development of new herbicides and antimicrobial drugs with broad-spectrum activity and no toxicity in humans (Rodríguez-Concepción, 2004; Rohdich *et al.*, 2005). In addition, metabolic engineering of the MEP pathway in plants has successfully increased the production of some terpenoids with nutritional and economic relevance, such as carotenoids, tocopherols, and monoterpenes (Mahmoud & Croteau, 2001; Rodríguez-Concepción, 2006; Misawa, 2011).

Terpene synthase (TPS) are the gatekeepers in generating diversity of terpenoids by catalyzing complex carbocation-driven cyclization, rearrangement, and elimination reactions that enable the transformation of a few acyclic prenyl diphosphate substrates into a vast chemical library of hydrocarbon and for a few enzymes, oxygenated terpene skeleton (Karunanithi & Zerbe, 2019). Most full-length TPSs contain two conserved domains with Pfam ID PF01397 (N-terminal) and PF03936 (C-terminal) (Starks *et al.*, 1997; Finn *et al.*, 2016). The N-terminal domain has a conserved RRx_8W (x, alternative amino acid) motif, and the C-terminal domain has two highly conserved aspartate-rich motifs. One of them is the DDxxD motif, involving the coordination of divalent ions, water molecules, and the stabilization of the active site (Rynkiewicz *et al.*, 2001;

Whittington *et al.*, 2002). The second motif in the C-terminal domain is the NSE/DTE motif. The plant TPS family is clustered into seven subfamilies according to phylogenetic analysis, namely TPS-a, -b, -c, -d, -e/f, -g, and -h (Chen *et al.*, 2011; Jiang *et al.*, 2019). The TPS-a subfamily mainly encodes sesquiTPSs in both monocots and dicots, whereas the angiosperm-specific TPS-b subfamily encodes monoTPSs. The TPS-g subfamily is another angiosperm monoTPS subfamily but encodes TPSs without the R(R)x_8W motif. These TPSs catalyze the biosynthesis of acyclic monoterpenes, usually presenting in floral volatile organic compounds (VOCs) (Dudareva *et al.*, 2013). The TPS-c subfamily, consisting of diterpene synthases (diTPSs), is present in land plants and is characterized by the DxDD motif instead of the common DDxxD in the encoded proteins. The TPS-d subfamily is gymnosperm-specific and encodes mono-, sesqui-, and diTPSs. The TPS-e/f is mainly present in vascular plants and is responsible for gibberellic acid biosynthesis. The TPS-h family is specific to *Selaginella moellendorffii*, and members in the cluster contain both DxDD and DDxxD motifs (Chen *et al.*, 2011).

Diterpene synthases are vital for generating diverse diterpene scaffolds (Zerbe & Bohlmann, 2015). The diTPS enzymes are organized modularly, comprising two or three conserved α-helical domains α, β, and γ (Zhou, Ke *et al.*, 2012). Variations in the components of these domains, along with that in the associated active sites and motifs, define three main diTPS classes: monofunctional class I and class II diTPSs, and bifunctional class I/II diTPSs. Class II diTPSs contain an N-terminal active site formed by $\beta\gamma$ domains with a conserved DxDD motif that is critical for the cyclization of GGPP into bicyclic prenyl diphosphates including copalyl diphosphate (CPP) of *ent* (9*R*, 10*R*) (Sun & Kamiya, 1994), normal (9*S*, 10*S*) (Brückner *et al.*, 2014), or *syn* (9*S*, 10*R*) (Xu *et al.*, 2007), as well as the oxygenated labda-13-en-8-ol diphosphate (LPP) (Falara *et al.*, 2010) and peregrinol diphosphate (PPP) (Zerbe *et al.*, 2014). Class I diTPSs possess a functional α domain that harbors two catalytic motifs, DDxxD and NSE/DTE, which coordinate the Mg^{2+} mediated substrate binding (Gao *et al.*, 2012). Most class I diTPSs convert products of class II diTPS into a variety of diterpene skeletons. Bifunctional class I/II diTPSs combine the two reactions in a single protein (Hayashi *et al.*, 2006). Some class I diTPSs act directly on GGPP or its stereoisomer nerylneryl

diphosphate (NNPP) to produce linear or macrocyclic diterpenes without requiring prior cyclization by class II diTPS (Herde *et al.*, 2008; Vaughan *et al.*, 2013).

The cytochrome P450s (CYPs), as a superfamily of heme monooxygenases, are major players in generating the structural diversity of terpenoids and their corresponding bioactivity (Guo *et al.*, 2016). CYPs representing the biggest superfamily of enzymes in plants, catalyze various biological reactions. While hydroxylation is the most common catalyzed reaction, CYPs can also catalyze many more reactions, such as phenol-coupling reactions, oxidative rearrangements, oxidative C-C bond cleavage, etc. (Mizutani & Sato, 2011; Banerjee & Hamberger, 2018). In addition to the typical regio- and stereospecific hydroxylation reactions, there are many examples of CYPs exhibiting promiscuity by accepting multiple substrates and/or producing multiple products (Seki *et al.*, 2011; Wang, Q *et al.*, 2012; Wu *et al.*, 2013). The high abundance of CYPs in plant genomes, comprising an average of more than 200 genes in an individual plant genome (Karunanithi & Zerbe, 2019), together with their promiscuity, is one of the main drivers of the chemical diversity of terpenoids. In addition to P450s, several other enzyme families contribute to the biosynthesis of bioactive terpenoids. This includes but is not limited to the function of 2-oxoglutarate/Fe(II)-dependent dioxygenases (2-ODDs) in GAs phytohormone metabolism (Farrow & Facchini, 2014), as well as members of methyl-, glycosyl-, and acetyl-transferases (Bathe & Tissier, 2019).

1.5 Aim of this study

Plants use a variety of specialized metabolites, namely phytoalexins, to counter-attack threats caused by pests and pathogens. Exploring new phytoalexins produced by cereal plants is highly interesting to researchers and breeders, because of the potential these phytoalexins exhibit in elevating plant resistance to biotic stress and in increasing yield and productivity. A range of diterpenoid phytoalexins have been identified in the Poaceae family, mainly from rice and maize. However, barley, another important cereal plant from the same plant family, has not yet been reported to produce such diterpenoids for chemical defense. A recent study (Sarkar *et al.*, 2019) has shown the induction of two putative diterpene synthases upon pathogen infection, and they were co-expressed with genes of the MEP pathway. Jointly, this infers the presence of yet unknown diterpenoids in barley and their potential roles as phytoalexins. Several objectives were defined based on this hypothesis:

1. Identifying diterpenoids from barley roots upon pathogen infection using an untargeted metabolomic approach;
2. Elucidating the biosynthesis pathway of the diterpenoids by heterologous expression in *Saccharomyces cerevisiae* and *Nicotiana benthamiana*;
3. Elucidating the biological function of the diterpenoids by *in vitro* antifungal assay or using diterpenoid deficiency mutants.

Addressing these questions would expand the current knowledge of phytoalexins in cereals and enzymes in the biosynthesis pathway of diterpenoids and help to understand the ecological roles of diterpenoids in the interaction of the host plant and fungal pathogen.

2. Results

2.1 Identification of a gene cluster for diterpenoid biosynthesis

Previous work by Sarkar et al. reported that two diTPSs, along with several cytochrome P450s, were strongly induced in barley roots inoculated with a fungal pathogen, *Bipolaris sorokiniana* (*Bs*) but only moderately when inoculated with a beneficial endophyte, *Serendipita vermifera* (*Sv*) (Sarkar *et al.*, 2019) (**Fig. 2.1**). We observed that these pathogen-induced genes are located at close vicinity at a region in barley chromosome 2. Combined with two annotation versions of the barley genome, Morex V1 (Beier, S. *et al.*, 2017) and Morex V2 (Monat *et al.*, 2019), we created our own gene annotation in this region, as shown in **Fig. 2.1** and **Tab. S1**. This cluster spans over 600 kb and contains genes encoding a copalyl diphosphate synthase (CPS), a kaurene-synthase like (KSL), one asparaginase, and nine CYPs, together with several pseudogenes. As the CYP-encoding genes share high similarity in sequence and some of them are present in duplicates or triplicates, it may have caused difficulties in genome assembly and gene identification when this region was sequenced. Therefore, the annotation of genes in this region is still not final, though three versions of the barley genome are available now. New genes may emerge as more accurate genome sequences become available.

Phylogenetic analysis of two diTPSs and the CYPs in the gene cluster

To briefly understand their possible biochemical activity and evolutionary events, we performed a phylogenetic analysis based on protein sequences. HvCPS1 was identified and biochemically characterized as an *ent*-CPP synthase (Wu *et al.*, 2012). In the phylogenetic tree, it is clustered with TaCPS3 and TaCPS4, both of which are *ent*-CPP synthases and located at a branch that is exclusively for *ent*-CPP synthase (**Fig. 2.2**). This indicates a distinct evolutionary conservation of *ent*-CPP synthases in monocots. One possible explanation for it could be that *ent*-CPP synthase produces the substance for the biosynthesis of gibberellins, a hormone class present in a wide range of plant species. The CPS in the barley gene cluster has not been characterized yet, and we proposed to name it HvCPS2. HvCPS2 is highly similar to TaCPS2 (90% identity in protein sequence), a (+)-CPP synthase, and is located at a different branch to OsCPS4, a *syn*-CPP synthase (**Fig. 2.2**). These data allow us to hypothesize that

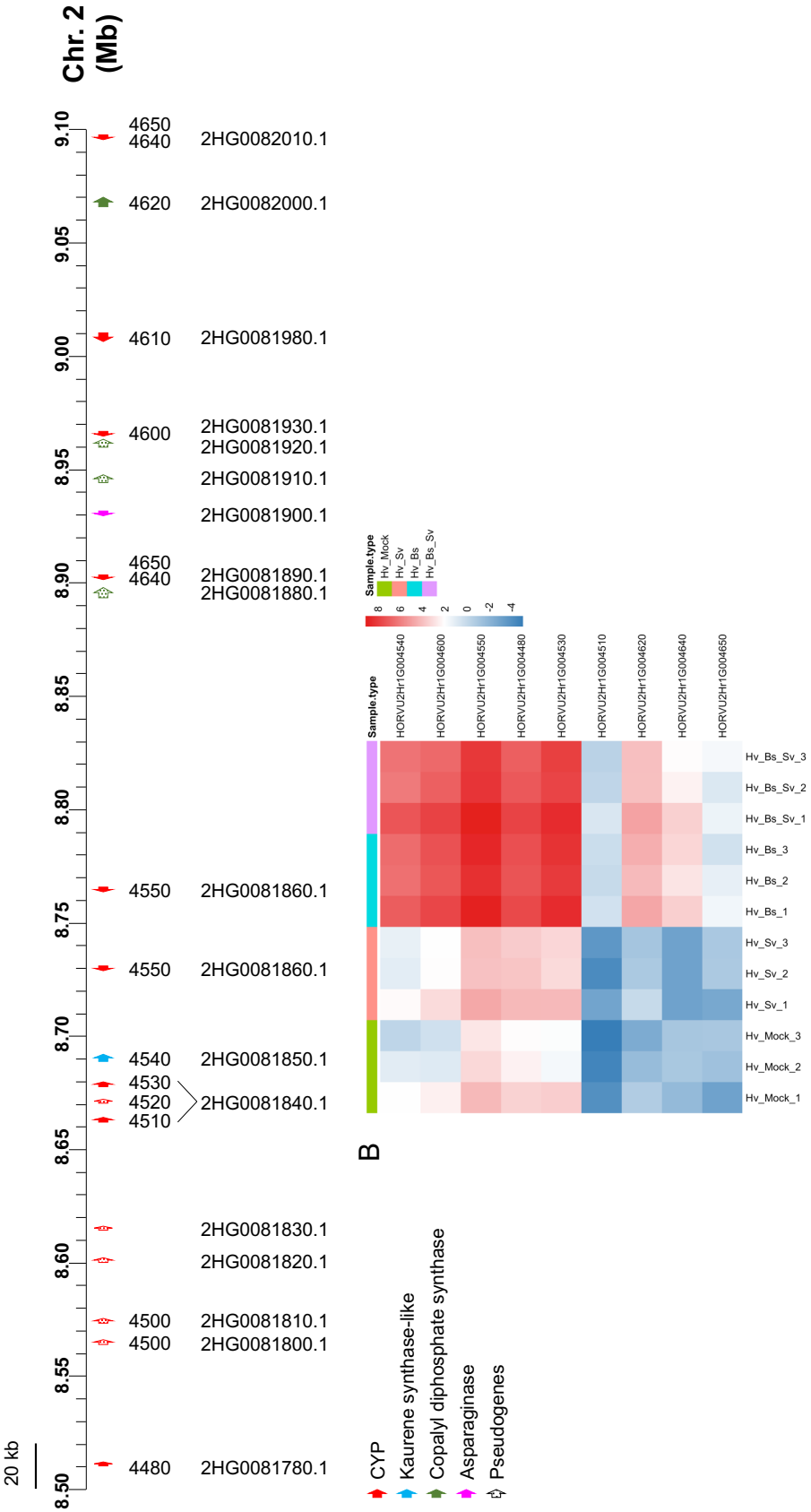

Figure 2.1 Overview of the barley chromosome 2 gene cluster for diterpenoid biosynthesis

(A) The scale on top indicates the position on chromosome 2 based on the Morex V2 annotation of the barley genome (Monat *et al.*, 2019). The genes are represented by arrows underneath the scale. The color code indicates to which gene family they belong, and the dotted pattern the presence of a pseudogene. The first row of numbers below the scale indicates the last 4 digits of the gene ID according to Morex V1 gene models, and the second row gives the gene identification in the Morex V2 version of the barley genome. (B) The colors in the heatmap represent gene expression values as log2-transformed RKPM values for genes that show differential gene expression (|fold change| > 2, data from Sarkar *et al.*, 2019). The samples types are indicated by the following color code: purple: barley root co-inoculated with *Bs* and *Sv*; turquoise blue: barley roots inoculated with *Bs*; pink: barley roots inoculated with *Sv*; green: barley root mock-inoculated.

the product of HvCPS2 is (+)-CPP, and that it may play a role in specialized metabolism of diterpenes. Further validation by biochemical assay was described in section **2.3**. The kaurene synthase-like of gene cluster has been previously identified and named HvKSL4 (Li *et al.*, 2016). In the phylogenetic tree, it aligns with the branch of TaKSL1, TaKSL4, and OsKSL4 (**Fig. 2.2**). The substrate of TaKSL1 and TaKSL4 is (+)-CPP (Zhou, K. *et al.*, 2012), while that of OsKSL4 is *syn*-CPP (Otomo *et al.*, 2004). The clear separation from kaurene synthase (KS) that uses *ent*-CPP as substrate, including HvKS, indicates that HvKSL4 likely uses either (+)-CPP or *syn*-CPP as substrate. However, HvKSL4 does not show high similarity in protein sequence with either one of TaKSL1, TaKSL4, and OsKSL4, indicating possibly a different product of HvKSL4.

Eight of the nine CYP-encoding genes in the gene cluster were expressed at significantly high levels and displayed an expression pattern like that of *HvCPS2* and *HvKSL4*, except the 2Hr1G004510, which was induced but was expressed at a rather low level (average RPKM in root samples < 1). High redundancy of the CYPs in the cluster was observed; for example, two CYPs, 2Hr1G004550 and 2Hr1G004640, are present in duplicates, and the amino acid sequences of the three CYPs, 2Hr1G004600, 2Hr1G004610, and 2Hr1G004640, are identical except for one amino acid change in 2Hr1G004600 (**Fig. 2.1** and **Tab. S1**). With all these factors considered, we ended up with four individual CYPs encoded by the genes 2Hr1G004480, 2Hr1G004530, 2Hr1G004550, and 2Hr1G004600. Their official names according to the CYP nomenclature were assigned by Dr. Nelson, the curator of the CYP database, Cytochrome P450 Homepage (https://drnelson.uthsc.edu/). A phylogenetic analysis of these four CYPs shows that three of them are most similar to OsCYP99A2 and OsCYP99A3 from rice (**Fig. S1**), both of which have known function in the biosynthesis of momilactones by oxidizing *syn*-pimaradiene at the C19 position to generate a carboxylic acid function (Wang *et al.*, 2011; Kitaoka *et al.*, 2015). Interestingly, OsCYP99A2 and OsCYP99A3 are in the same tandem cluster next to OsCPS4 and OsKSL4, a situation highly reminiscent of the barley cluster presented here. A further study into the correlation of these two biosynthesis gene clusters was described in section **3.4**. The fourth CYP, CYP89E31, shares the strongest similarity to enzymes of the CYP89 clan, including CYP89A2 in *Arabidopsis thaliana* and two from the grass

plants *Triticum aestivum* and *Setaria viridis* (**Fig. S1**), but none of them has a known function.

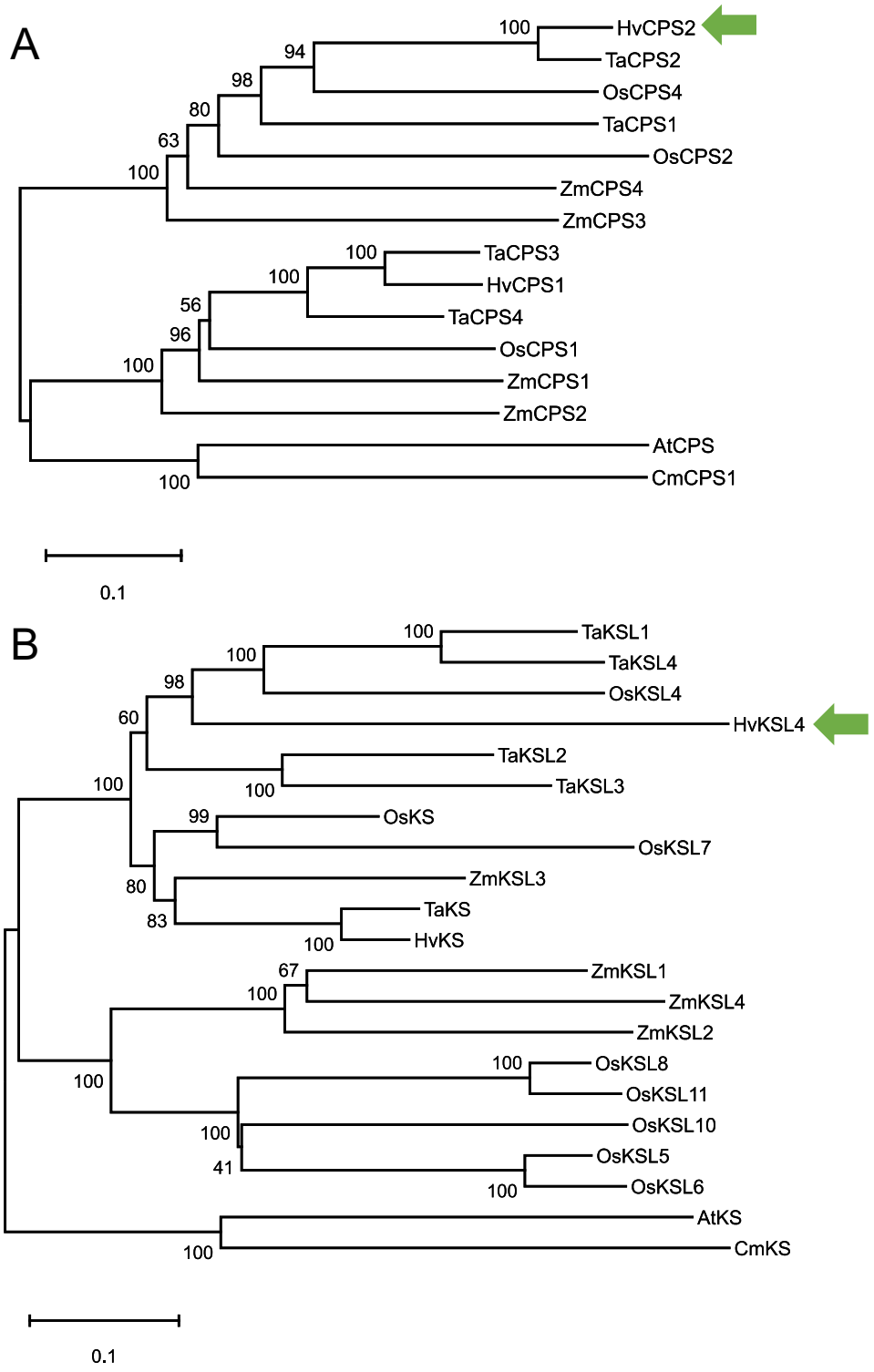

Figure 2.2 Phylogenetic analysis of HvCPS2 and HvKSL4

The protein sequences indicated were aligned by ClustalW and further processed with the MEGA X software (Kumar *et al.*, 2018) using the maximum likelihood method and 500 bootstrap replications. The tree with the highest log likelihood is shown. For other parameters, default settings were used. The list of sequences used is provided in **Table S2** and **S3**.

2.2 Untargeted metabolome profiling of barley roots

Mass spectrometry (MS) is a technique that is widely used to measure a single or limited number of known metabolites by a targeted method, or to acquire all signals from the sample generated by a mass spectrometer, termed metabolome profiling. Often, a mass spectrometer is coupled with a chromatography device. Two well-developed MS platforms are gas chromatography-mass spectrometry (GC-MS) and liquid chromatography-mass spectrometry (LC-MS). Arguably, GC-MS is more suitable for detecting volatile apolar compounds, while LC-MS is more desirable for measuring medium-polar and polar compounds. Diterpenoids vary in polarity, from apolar to medium-polar, depending on the type and number of functional groups on the skeletons. A single MS method is difficult to cover all diterpenoids of complex biological samples, therefore, two methods employing GC-MS or LC-MS/MS are used in this thesis.

Detection/identification of diterpenoids from barley roots by GC-MS

Barley roots infected with the pathogen *B. sorokiniana,* together with mock-treated root samples, were extracted for metabolites and analyzed by GC-MS. We searched for diterpenoids from our GC-MS data using the theoretical mass of labdane-related diterpenoids, which are well characterized from rice, maize, and other species. The masses we used include m/z 270, 272 indicating a diterpene backbone, and 284, 286, 300, 302, 304, indicating once or more oxidized diterpenoids. They are supposed to be well detected by GC-MS. By this strategy, we identified five diterpenoids both from infected and mock-treated barley roots, and they were significantly upregulated after pathogen infection (**Fig. 2.3**). Their possible structures were inferred by their molecular mass, together with a search of a spectra library. The typical mass for a diterpene skeleton is 272, but no such diterpene was detected in our datasets. However, compound **5**, with a mass of 270, indicating one more double bond in the skeleton, was clearly detected. A spectra library search shows the most similar compound to **5** is abietariene, an abietane diterpene with three double bonds. Compound **8**, showing the highest abundance among the five diterpenoids, has a mass of 286 and shows a similar fragment pattern to compound **5** (**Fig. S2**). Their mass difference of 16 and MS spectra similarity suggests compound **8** possibly derives from **5** by a hydroxylation.

The other two low abundant diterpenoids, **9** and **13,** also show similarities with **5** and **8** in their MS spectra (**Fig. S2**).

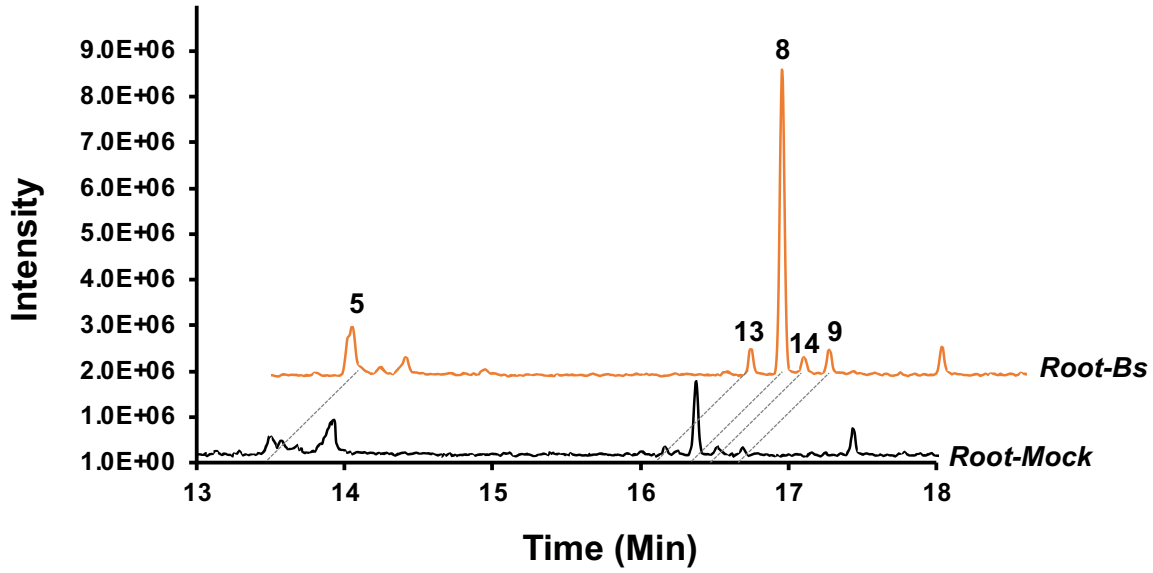

Figure 2.3 GC-MS chromatograms of extracts from barley roots infected with *B. sorokiniana* or mock treatment

Extracted ion chromatograms (m/z 270, 284, 286, 300, 302) of extracts from barley roots infected with *B. sorokiniana* (Root-Bs) or mock-inoculated (Root-Mock). MS Spectra of these diterpenoids are presented in **Fig. S2**.

Detection/identification of diterpenoids from barley roots by LC-MS

To better detect more oxidized diterpenes, which are more polar, we performed an untargeted LC-QToF-MS/MS (negative mode) analysis of extracts from the root and the medium. Using the same strategy as for GC-MS data, we searched for m/z corresponding to additional oxidations of **8** (**Fig. 2.3**), i.e., 313.2, 315.2, 317.2, and 331.2. Several peaks could be detected with a strong increase in roots and medium of plants infected with *B. sorokiniana* (**Fig. 2.4**). Some diterpenoids are present in mock control samples as well, but at much lower levels. Among all the diterpenoids detected, only a few are present at a relatively high level, i.e., compounds **21**, **26**, **32** (**Fig. 2.4**). However, in roots if all metabolites are considered, they are very low abundant (data not shown). Interestingly, these diterpenoids were also secreted into the medium, and for most of them, most of the total production is in the medium rather than in the roots.

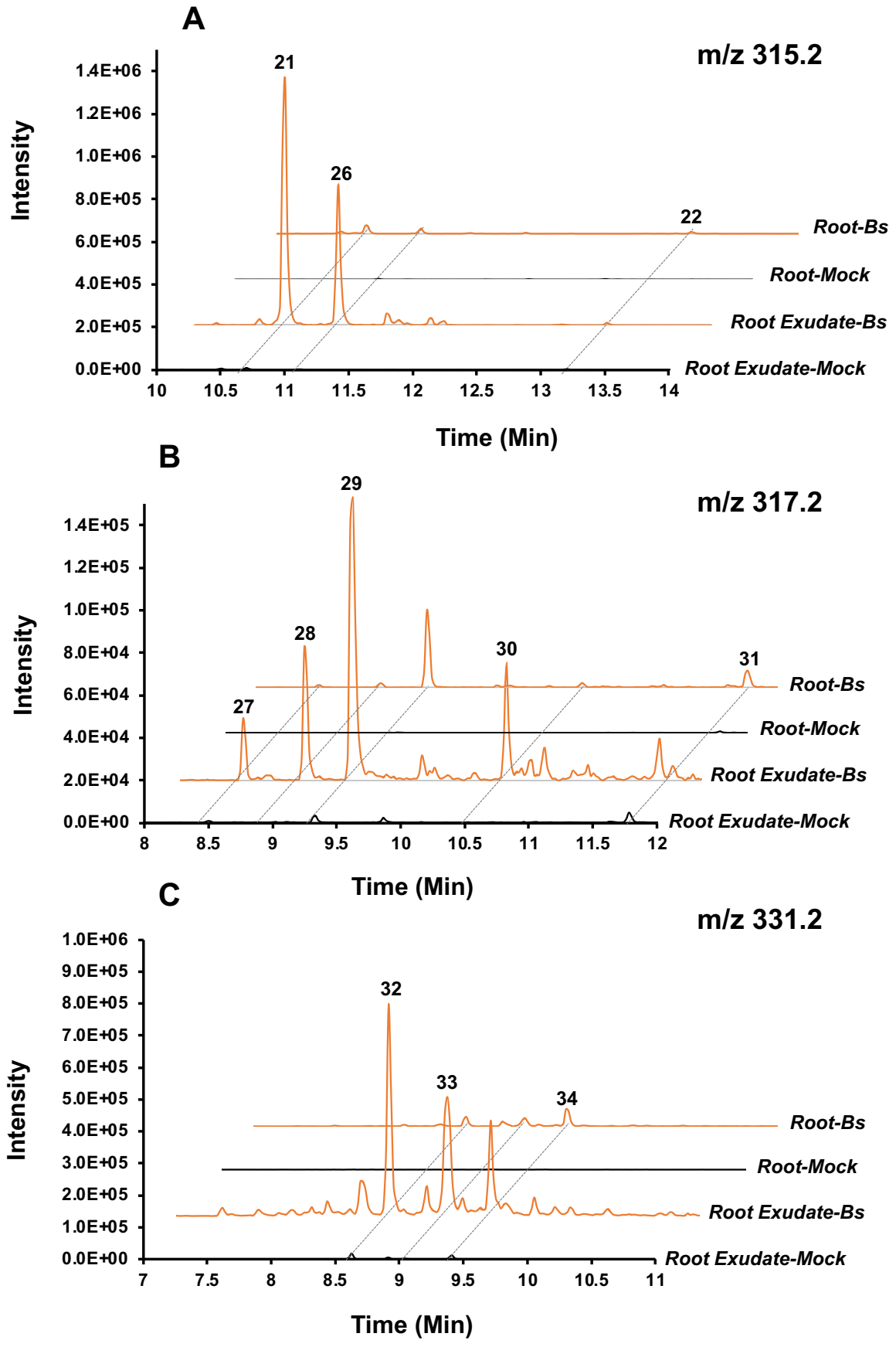
A
m/z 315.2
Intensity
1.4E+06
1.2E+06
1.0E+06
8.0E+05
6.0E+05
4.0E+05
2.0E+05
0.0E+00
21
26
22
Root-Bs
Root-Mock
Root Exudate-Bs
Root Exudate-Mock
10
10.5
11
11.5
12
12.5
13
13.5
14
Time (Min)
B
m/z 317.2
Intensity
1.4E+05
1.2E+05
1.0E+05
8.0E+04
6.0E+04
4.0E+04
2.0E+04
0.0E+00
29
28
30
31
27
Root-Bs
Root-Mock
Root Exudate-Bs
Root Exudate-Mock
8
8.5
9
9.5
10
10.5
11
11.5
12
Time (Min)
C
m/z 331.2
Intensity
1.0E+06
9.0E+05
8.0E+05
7.0E+05
6.0E+05
5.0E+05
4.0E+05
3.0E+05
2.0E+05
1.0E+05
0.0E+00
32
33
34
Root-Bs
Root-Mock
Root Exudate-Bs
Root Exudate-Mock
7
7.5
8
8.5
9
9.5
10
10.5
11
Time (Min)

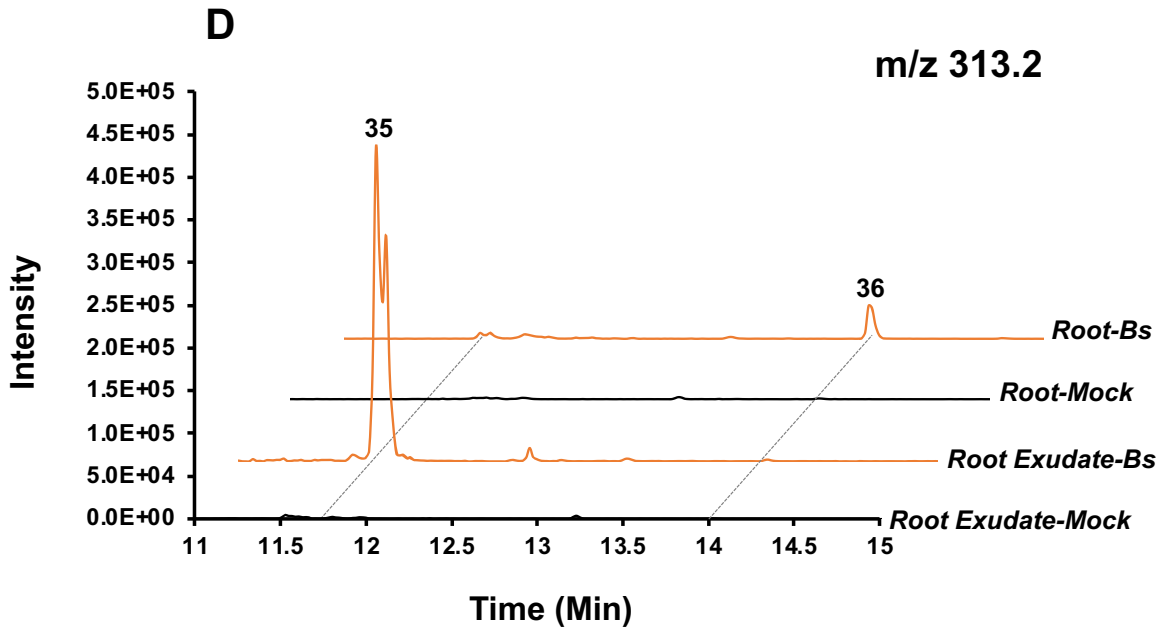

Figure 2.4 LC-ESI-QToF-MS of major diterpenoid metabolites in roots and root exudates of barley 6 dpi with *B. sorokiniana* and mock-infected controls

Extracted ion chromatograms of m/z 315.2 (A), 317.2 (B), 331.2 (C), 313.2 (D) of extracts from barley roots or medium inoculated with *B. sorokiniana* (Root/Root Exudate-*Bs*) or mock-inoculated (Root/Root Exudate-Mock). MS/MS spectra are presented in **Fig. S2.**

Multiple diterpenoids with the same mass were observed, which is quite common for diterpenoids, given that positional isomers reflect oxygenation of the diterpene backbone at different carbon atoms. MS/MS spectra of these compounds imply diterpenoids based on characteristic fragment ions 269.19, 271.21, 287.20, and 301.1 (**Fig. S2**). Many diterpenoids, for instance, **21**, **22**, **26**, **32**, **34**, and **35** (**Fig. S2**), have neutral losses of 43.99 and 46.01, suggesting the presence of carboxyl groups. Moreover, a neutral loss of 18.01, indicating the presence of a hydroxyl group, also was often observed in the spectra of identified diterpenoids.

2.3 Heterologous expression of the diTPSs and CYPs in *S. cerevisiae* and *N. benthamiana*

Heterologous expression of proteins in the model organisms is a fast and efficient way to characterize enzyme activity instead of testing it in a non-model system. *Saccharomyces cerevisiae* (yeast), *Nicotiana benthamiana*, and *Escherichia coli* are probably the three most used hosts. Yeast and *N. benthamiana* can be a better option

in some cases, for example, for expressing CYPs, due to their anchoring in membranes, a feature specific to eukaryotes.

HvCPS2 is a (+)-CDP synthase, and HvKSL4 produces a cleistanthane-type backbone

To determine the biochemical activity of HvCPS2, we expressed it in yeast using the Golden Gate yeast cloning system (Scheler *et al.*, 2016), together with the miltiradiene synthase from *Rosmarinus officinalis* (RoMiS) (Brückner *et al.*, 2014), with an *ent*-kaurene synthase from *Coffea canephora* (CcKS), or with HvKSL4. No *ent*-kaurene

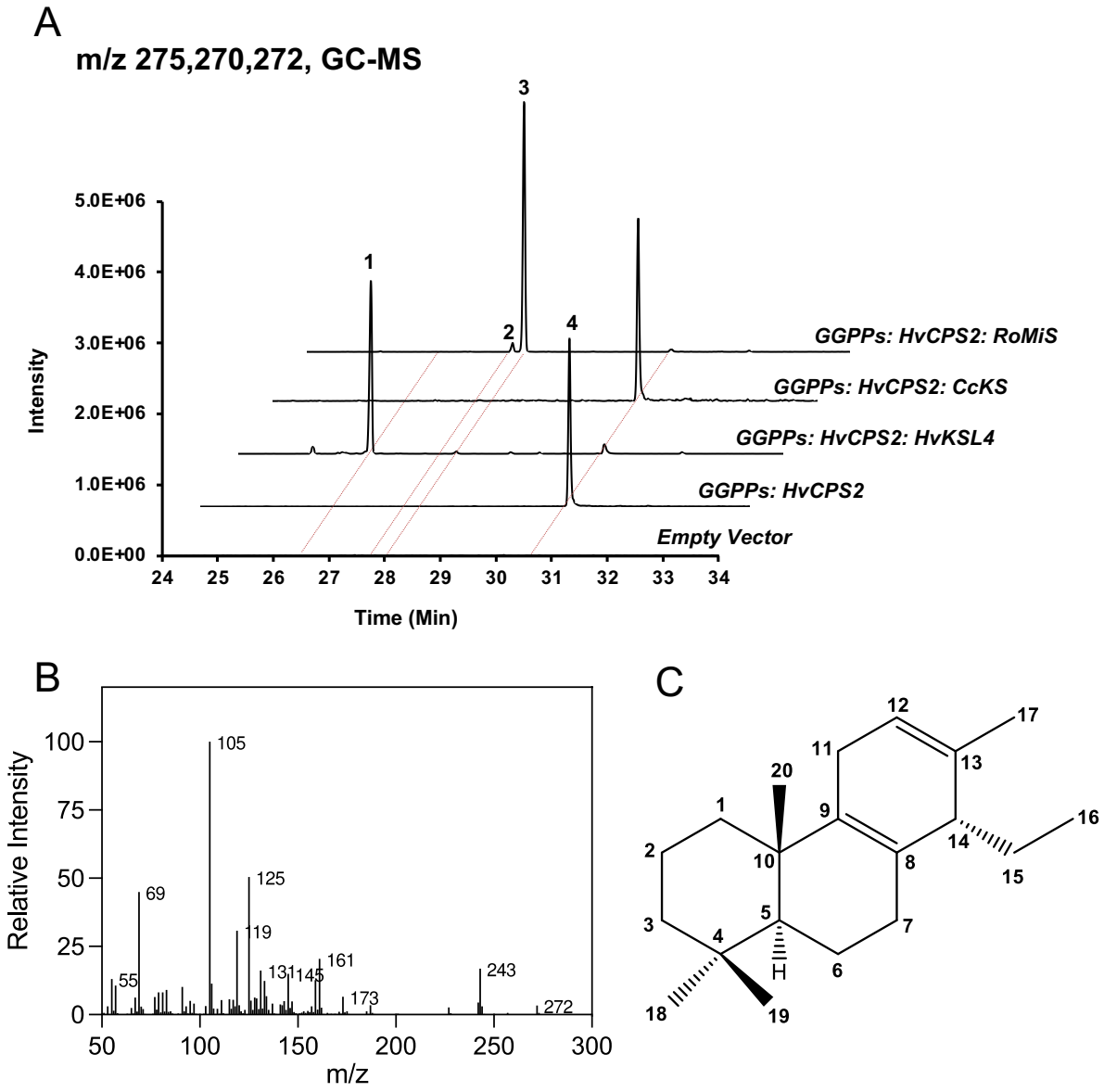

Figure 2.5 Characterization of HvCPS2 and HvKSL4 in yeast

(A) Selected ion (*m/z* 270, 272, and 275) GC-MS chromatograms of extracts of yeast strains expressing the gene combinations indicated on the right. CcKS: ent-kaurene synthase from coffee (*Coffea*

canephora); RoMiS, miltiradiene synthase from rosemary (*Rosmarinus officinalis*). **1**: hordediene; **2**: abietatriene; **3**: miltiradiene; **4**: (+)-copalol. (B) EI mass spectrum of hordediene. (C) Structure of hordediene determined by NMR. MS or MS/MS Spectra of products are presented in **Fig. S2**.

was detected, when HvCPS2 was co-expressed with CcKS, ruling out that HvCPS2 produces *ent*-CPP (**Fig. 2.5**). By contrast, co-expression HvCPS2 with RoMiS, which is known to accept (+)-CPP, yielded the expected diterpene product in normal configuration, miltiradiene, together with the product by spontaneous oxidation, abietatriene (**Fig. 2.5**). These results indicate that HvCPS2 produces (+)-CPP. Co-expression of HvCPS2 and HvKSL4 in yeast yielded a novel product with a molecular mass of 272 (**Fig. 2.5**), suggesting that it is a diterpene olefin. When expressing the truncated version of HvCPS2 and HvKSL4 together with a cytosolic geranylgeranyl diphosphate synthase (GGPPs) and a truncated version of hydroxymethylglutaryl CoA-reductase (trHMGR) in *Nicotiana benthamiana* the same product could be detected (**Fig. S3**). Since there was no confident match in the NIST database (Mass Spectrometry Data Center, http://chemdata.nist.gov), we purified the main product and determined its structure by nuclear magnetic resonance (NMR) spectroscopy (**Tab. S5**). The product was determined to have a cleistanthane backbone with two double bonds in the C-ring at positions C8-C9 and C12-C13 (**Fig. 2.5**). Cleistanthanes constitute a relatively small group of diterpenoids that are identified in some plants and fungi (C. Pinto *et al.*, 1985; Kaufman *et al.*, 1987; Shiono *et al.*, 2010; Zheng *et al.*, 2018). Since no identical structure was reported, we named it cleistantha-8(9), 12(13)-diene, or hordediene (Liu *et al.*, 2021).

Characterization of HvCYP89E31, HvCYP99A66, HvCYP99A67, and HvCYP99A68 in yeast and *N. benthamiana*

The four CYPs identified from the chromosome 2 cluster were characterized in yeast. The yeast-optimized sequence of individual CYP was cloned into a vector together with HvCPS2 and HvKSL4 and in addition with the cytochrome P450 reductase (CPR) from Arabidopsis. CPR is required for electron transfer from NADPH to cytochrome P450. The products extracted from the yeast culture were measured by GC/EI-MS and LC/ESI-MS/MS separately. Co-expression of HvCYP89E31 with the two diTPSs from the cluster resulted in two major products, **5** and **8,** with an *m/z* 270 and 286, respectively, suggesting another double bond formation and one additional oxygenation of hordediene (**1**) (**Fig. 2.6**). A minor product **9** was also detected,

exhibiting the same *m/z* and nearly identical mass spectrum to product **8** (**Fig. 2.6** and **Fig. S2**), indicating that these two compounds are isomers. Products **6** and **7** were

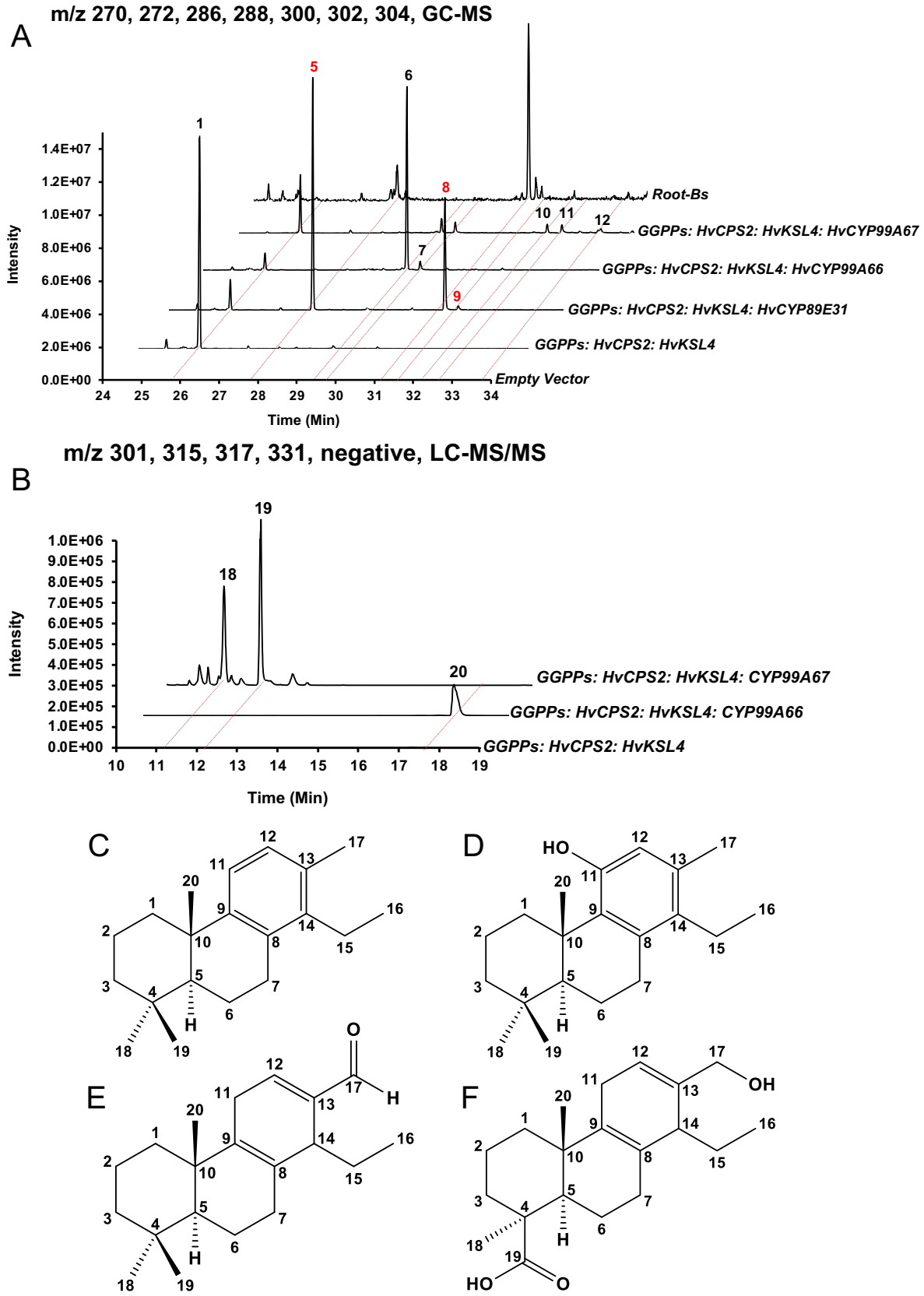

Figure 2.6 Characterization of HvCYP89E31, HvCYP99A66, HvCYP99A67, and HvCYP99A68 in yeast

(A) Selected ion chromatograms (m/z 270, 272, 286, 288, 300, 302, 304; GC-MS) of extracts of yeast strains expressing the gene combinations indicated on the right. (B) Selected ion chromatograms (m/z 301.2, 315.2, 317.2, 331.2; negative mode, LC-MS/MS) of extracts of yeast strains expressing the gene combinations indicated on the right. Products that were detected in barley root are colored red. (C), (D), (E), (F) Structure of products **5**, **8**, **6**, and **19,** respectively, which was determined by NMR. MS or MS/MS Spectra of products are presented in **Fig. S2**.

detected when either one of HvCYP99A66 and HvCYP99A67 was co-expressed with HvCPS2 and HvKSL4. Several more oxidized compounds including **10**, **11**, **12** detected by GC-MS and **18, 19** detected by LC-MS, were produced when HvCYP99A67 was co-expressed (**Fig. 2.6** and **Fig. S2**). However, when HvCYP99A66 was co-expressed, only one more product (**20**, **Fig. 2.6**) was detected. Notably, products **5**, **8**, and **9** were detected in pathogen-infected barley roots. No product was detected when HvCYP99A68 was co-expressed with HvCPS2 and HvKSL4. We also expressed the gene combinations in *N. benthamiana* that we tested in yeast. All the same products that we described above were detected in the extracts of leaf discs after infiltration, except product **18** (**Fig. S4**).

In order to describe which positions of the substrate are oxidized by the individual CYPs, we purified products **5**, **6**, **8**, **19** that showed higher abundance in the extracts of a large-scale yeast culture. Next, their structures were determined by NMR (**Fig. 2.6** and **Tab. S6-S9**). The structure of product **6** was determined to have an aldehyde group at C-17 of hordediene, as catalyzed by HvCYP99A66. With this information, product **7,** with a mass of 288 and a very close retention time of **6**, is predicted to be 17-hydroxy-hordediene. In addition, product **20**, with a mass of 302, is predicted to be a further oxidized **6**, with a carboxyl group at position 17. The structure of product **19** indicates that HvCYP99A67 can oxidize hordediene not only at position 17, which is the same as the function of HvCYP99A66 but also at position 19. Three products were detected when HvCYP89E31 was co-expressed, and two (**5** and **8**) of them were elucidated by NMR. Product **5** has an aromatized C-ring, whereas **8** additionally shows one more hydroxyl group at position 11. These two products are named hordetriene (**5**) and 11-hydroxy-hordetriene (**8**).

Co-expression of two or three CYPs in yeast and *N. benthamiana*

Many diterpenoids with higher masses, indicating more steps of biosynthesis, were detected in infected barley roots. It is also common that more than one CYP is needed for the biosynthesis of diterpenoids. For instance, four CYPs are involved in the biosynthesis of momilactone B (De La Peña & Sattely, 2021). Therefore, with the aim to elucidate the biosynthesis pathway of higher oxidized diterpenoids, an array of combinations of two or three out of these four CYPs were tested in yeast and *N. benthamiana*, while only the combinations that showed products which were also detected in barley root, are presented here.

The gene combinations were first tested in yeast, and the products were analyzed by GC-MS and LC-MS/MS separately. A similar product profile, including products **8**, **9**, **13**, **14**, **15**, and **16**, was observed in GC-MS measurement (**Fig. 2.7**) when either HvCYP99A66 or HvCYP99A67 were co-expression with HvCYP89E31. Product **14,** with an *m/z* of 286, shows a close retention time and a high similarity in MS spectrum to products **8** and **9**, indicating they are isomers. As HvCYP99A66 can oxidize hordediene at C-17, we assume it oxidized hordetriene at the same position. Jointly, we predicted **14** as 17-hydroxy-hordetriene (**Fig. S2**). In addition, product **13,** with an *m/z* of 284, is supposed to have undergone one more step of oxidization, and it resulted in an aldehyde group (**Fig. S2**). Products **13** and **14** were detected in barley roots after infection. Together with **8** and **9**, they provide evidence that HvCYP89E31, HvCYP99A66, and HvCYP99A67 from the chromosome 2 cluster are the enzymes in the biosynthesis pathway of induced diterpenoids. In addition to **15** and **16**, several peaks near them are also assumed to be diterpenoid products from the combination of HvCYP89E31 and HvCYP99A67, but it was not possible to predict their structures due to the large set of possible oxidations. Co-expression of HvCYP89E31 and HvCYP99A68 resulted in three new products (**17**, **22**, **24**, **Fig. 2.7**), in comparison with none when HvCYP99A68 was solely expressed, together with HvCPS2 and HvKSL4. This indicates that the biosynthesis of diterpenoids is a sequential process. One enzyme relies on the product of the previous one. Another example is the proposed biosynthesis pathway of **25**. HvCYP99A66 conducted three steps of oxidation at the same position of hordetriene, forming a carboxyl group at C-17. The two intermediates, **14** and **13**, supported this hypothesis. And the four compounds including **5**, **13**, **14**, **25** were all detected in barley roots. Product **21**, one of the most abundant diterpenoids

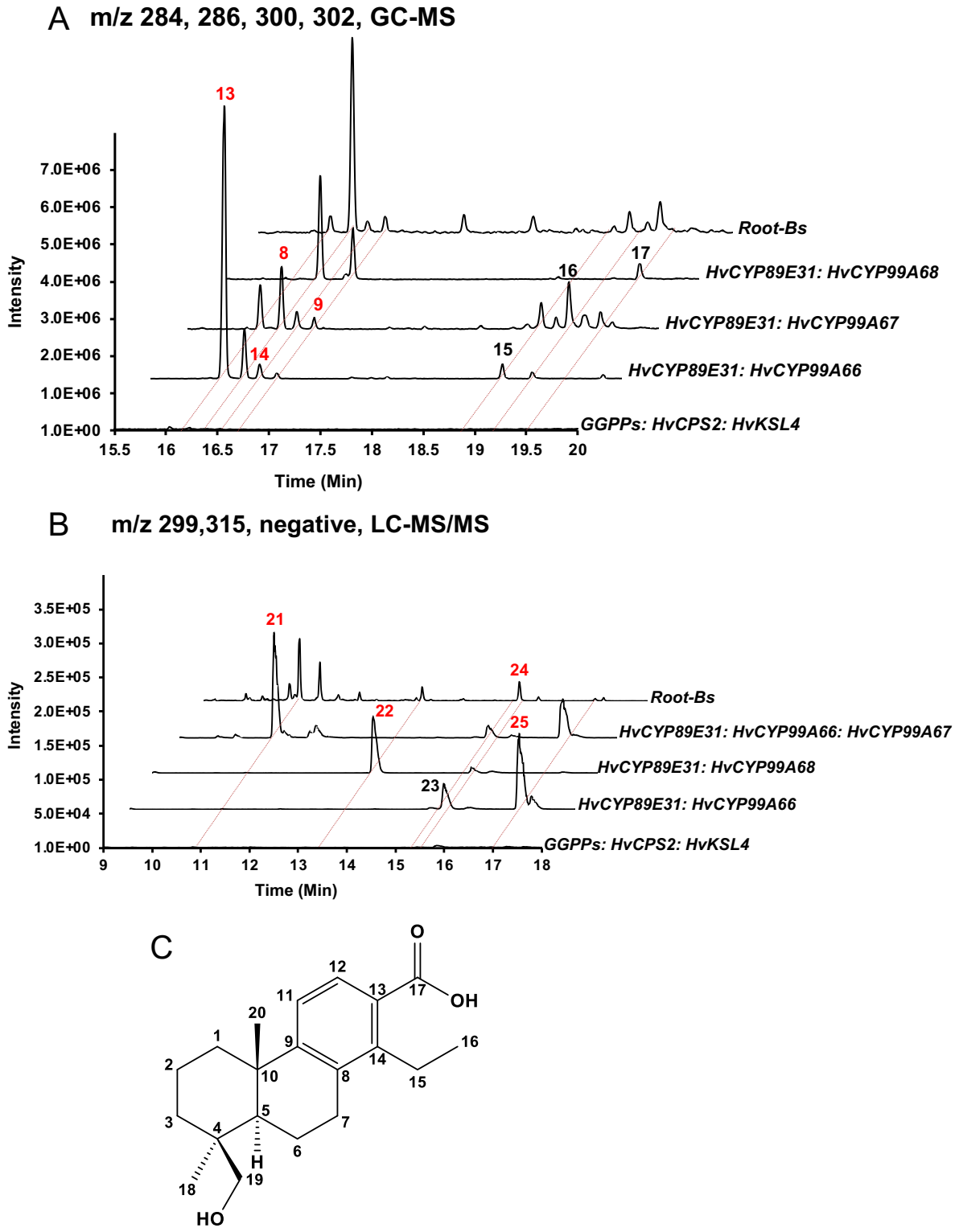

Figure 2.7 Co-expression of multiple CYPs in yeast

(A) Selected ion (m/z 284, 286, 300, 302) chromatograms (GC-MS) of extracts of yeast strains expressing the gene combinations indicated on the right. (B) Selected ion (m/z 299.2, 315.2, negative mode) chromatograms (LC-MS/MS) of extracts of yeast strains expressing the gene combinations indicated on the right. When *CYPs* were expressed, they were always co-expressed together with *HvCPS2* and *HvKSL4*, though it was not written in the figure. Products that were detected in barley root

are colored red. (C) Structure of product **21**, which was determined by NMR. MS or MS/MS Spectra of products are presented in **Fig. S2**.

in both roots and exudates of barley after pathogen infection (**Fig. 2.4** and **Fig 2.7**), can be reconstituted by co-expression of HvCYP89E31, HvCYP99A66, and HvCYP99A67. We purified it from the culture of yeast and determined its structure by NMR (**Fig 2.7** and **Tab. S10**). The structure shows it has a hordetriene backbone, owning a carboxyl group at position 17 and a hydroxyl group at position 19. All the combinations of CYPs which were expressed in yeast, were tested in *N. benthamiana* too, and the same products were detected, except that products **17** and **22** were not detected at a significant level (**Fig. S5**).

2.4 Biosynthesis pathway of pathogen induced diterpenoids in barley

Biosynthesis of diterpenoids starts by the conversion of the typical precursor all-*trans*-geranylgeranyl diphosphate (GGPP) by diterpene synthases (diTPSs) to either linear or cyclic diterpenes or diterpene alcohols, though in some cases, the precursor is the all-*cis*-isomer, nerylneryl diphosphate (Zi *et al.*, 2014). Class II diTPSs initiate the reaction by protonation-initiated cyclization of GGPP, which proceeds via cationic carbon-carbon double bond addition (Wendt & Schulz, 1998; Peters, 2010). The main products of class II diTPSs are *ent*-copalyl diphosphate (*ent*-CPP), the precursor of the gibberellins, and two other stereoisomers *syn*-copalyl diphosphate (*syn*-CPP) and normal-CPP. In addition, there are other products of class II diTPSs, such as clerodienyl or halimadienyl diphosphates as well as products with an alcohol function (Nakano *et al.*, 2005; Sallaud *et al.*, 2012; Pelot *et al.*, 2017). Class I diTPSs can convert the products of class II diTPSs to olefinic diterpenes or diterpene alcohols. Very often, these diterpene backbones are then oxidized at different positions and in a stereospecific way. Cytochrome P450 oxygenases (CYPs) are most frequently involved in these oxidations but other classes of enzymes such as 2-oxoglutarate dependent dioxygenases in gibberellin biosynthesis (Hedden & Kamiya, 1997) or short-chain dehydrogenases/reductases as in momilactone biosynthesis (Kitaoka *et al.*, 2016) can also play a role in functionalizing diterpenes. These oxidations can but rarely lead to backbone rearrangements and, importantly provide anchoring groups such as hydroxyl or carboxyl groups, for further modification by conjugating enzymes (Long *et al.*, 2008; Rontein *et al.*, 2008). Thus, sugar, acyl, or benzoyl groups can decorate the oxidized diterpene core and provide additional functionalities.

Here we elucidated the biosynthesis pathways (**Fig. 2.8**) of diterpenoid phytoalexins in barley, with six genes in a biosynthesis cluster. HvCPS2 catalyzed the first step of cyclization to a CPP (**4**) with normal configuration using GGPP, followed by a second cyclization by HvKSL4 to a new diterpene olefin, named hordediene (**1**), using normal-CPP as substrate. Hordediene belongs to the cleistanthane group of labdane-related diterpenes which is characterized by an ethyl group attached to C14. Four CYPs identified from the cluster, including three of the CYP99 family and one of the CYP89 family, were characterized by heterologous expression in yeast and *N. benthamiana*. CYP89E31 catalyzed the aromatization of ring C of hordediene and further oxidization of hordetriene (**5**) at the C11 position. Three CYPs from the CYP99 family show the same type of activities. They catalyzed multiple steps of oxidation, resulting in a carboxyl group at different positions of hordediene or hordetriene. The activities of CYP99A66 and CYP99A67 were determined by the elucidated structures of **6**, **19**, **21** based on NMR spectroscopy. The activity of CYP99A68 was inferred based on the products of **17**, **24**, **22**. In the literature (Silva *et al.*, 2001), the EI spectrum of compound **5** was thoroughly studied. The same fragment pattern in the EI spectra was observed for hordetriene (**5**) and for oxidized compounds with the same backbone, where three fragments representing the intact ring C and the partial ring B of an intact diterpene are conserved (**Fig. 2.9**). The three conserved fragments are very informative and useful to speculate about the possible decorations in ring C and ring B. Analyzing the spectrum of **17**, the mass of 302 indicates that **17** has two hydroxyl group. Since **17** was produced by co-expression of CYP89E31 and CYP99A68 (**Fig. 2.7A**) and we know CYP89E31 oxidizes the C ring at position 11, one hydroxyl group introduced by CYP89E31 is supposed to be at C11 position. The three fragments (m/z 191, 205, 217; **Fig. 2.9**) representing ring B and C of **17** indicates that another hydroxyl group introduced by CYP99A68 is at ring C or the side groups attached to ring C. Since products **24** and **22** were identified from the same extracts of **17** (**Fig. 2.7B**) and neutral loss of 44 indicating a carboxyl group was observed from the MS/MS spectrum of **22** (**Fig. S2**), the second hydroxyl group probably has been further oxidized to a carboxyl group. Therefore, this hydroxyl group should be at one of the two primary carbons of the side groups attached to ring C, C16 or C17. The primary carbon, C17, is ruled out because product **16** with two -OH groups at C11 and C17 showed different

retention time with **17** (**Fig. 2.7A**). Therefore, logically, the second -OH group of **17** can only be at C16.

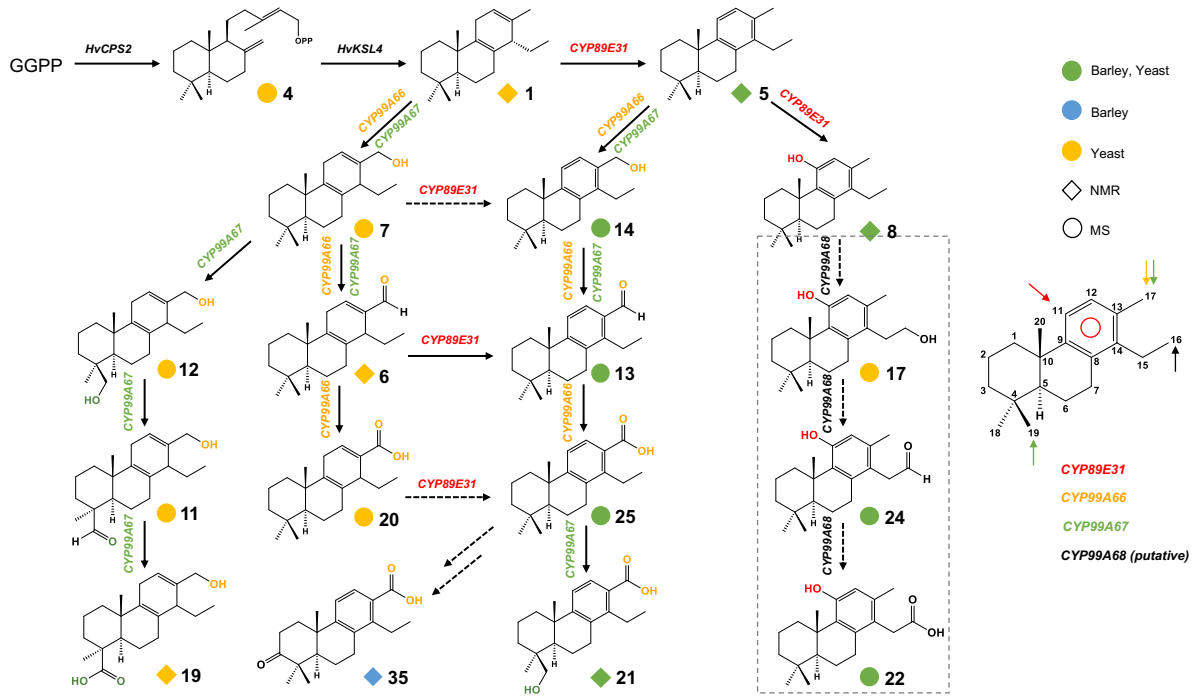

Figure 2.8 Elucidated biosynthesis pathway of pathogen induced barley diterpenoids by heterologous expression

Diterpenoids identified in barley are colored blue while diterpenoids identified by heterologous expression in yeast are colored orange. Diterpenoids that can be expressed in yeast and are present in barley are colored green. The oxidations introduced by CYP89E31, CYP99A66, CYP99A67, CYP99A68 to hordediene or hordetriene are colored in red, orange, green, and black respectively, except for the ketone group of **35**.

Hordediene and further oxidized hordedienes were well expressed in yeast and *N. benthamiana*. However, none of them accumulates in barley roots or root exudates (**Fig. 2.8**). The difference between diterpenoids **1**, **7**, **6**, **20** and diterpenoids **5**, **14**, **13**, **25** is only in ring C. Since CYP89E31 can catalyze the conversion of **1** to **5**, it is hypothesized that CYP89E31 can also catalyze the conversion of **7**, **6**, **20** to **14**, **13**, **25** respectively (**Fig. 2.8**). The conversion of **6** to **13** by CYP89E31 was confirmed by an *in vitro* assay. The enzyme for the assay was prepared by microsome isolation of transformed yeast strain expressing CYP89E31 and ATR1. **6** was almost completely converted to **13** when it was incubated with the microsomal preparation containing CYP89E31, although a partial conversion was also observed when the microsomal preparation containing empty vector was incubated (**Fig. S6**). This indicates that this conversion can also occur spontaneously. However, product **15** with an additional -

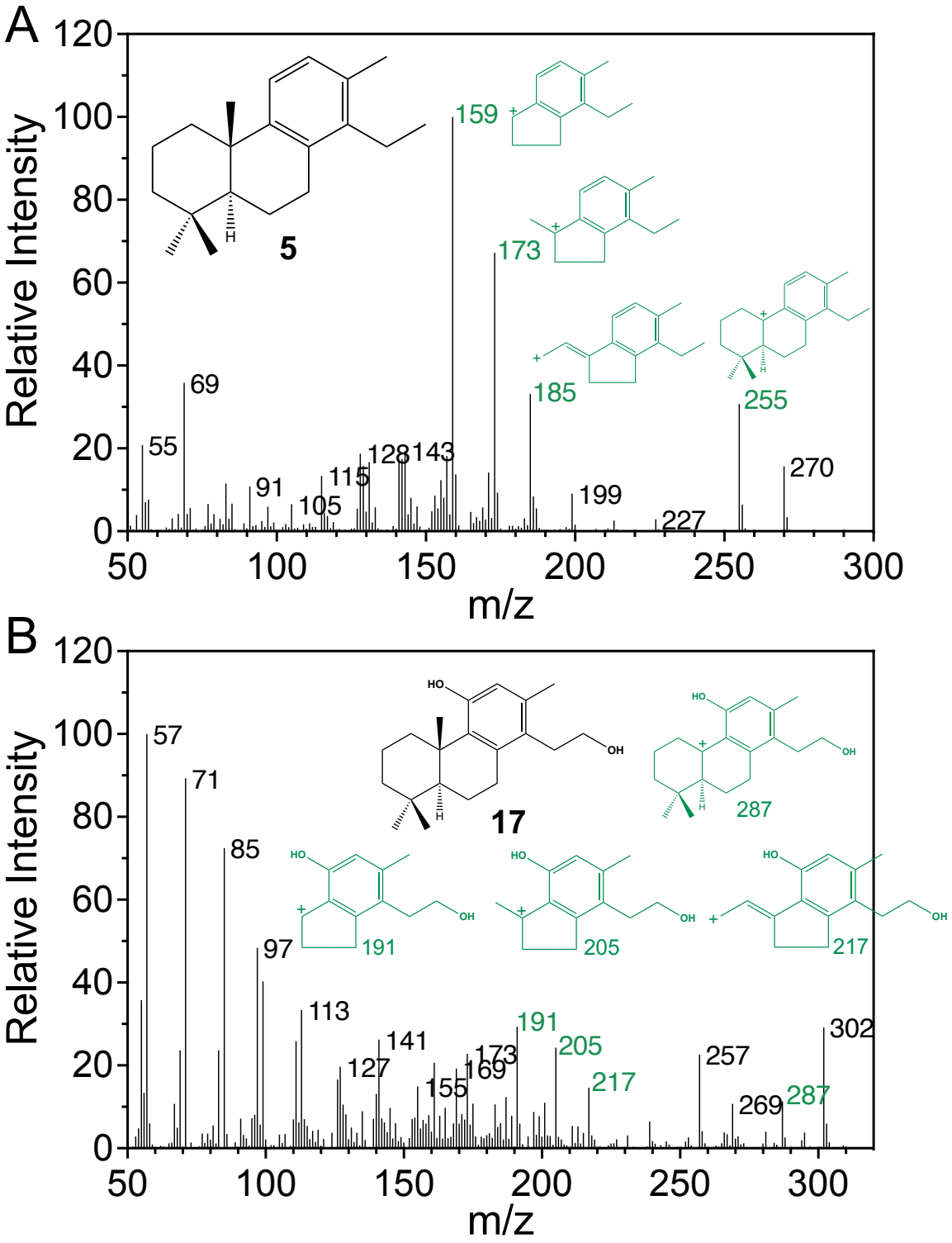

Figure 2.9 Fragment annotation of EI spectra of 5 and 17

(A) EI spectrum of **5**, the annotation of fragments was recreated from (Silva *et al.*, 2001).

OH group at C11 was observed only with CYP89E31 present in the reaction (**Fig. S6**). It suggests that CYP89E31 converted **6** to **13**, and **13** was further oxidized to **15** by

CYP89E31. The hypothesis that **7** and **20** can be converted to **14**, **25** by CYP89E31 respectively has not been tested yet.

Product **35** with an aldehyde group at C3 position was detected in barley while it could not be produced by yeast or *N. benthamiana* in this assay. The presence of an aldehyde group cannot be explained by the activities of the four CYPs from the cluster in chromosome 2. It suggests that it is introduced by enzymes outside of the cluster. A similar situation has also been reported in other biosynthesis gene clusters. For example, in the biosynthesis pathway of momilactones, CYP76M8, CYP76M14 and CYP701A8 are from chromosome 2, 1, 6 respectively, which are not in the major gene cluster located at chromosome 4 (De La Peña & Sattely, 2021).

2.5 Mutation of *HvCPS2* and *HvKSL4* by CRISPR/Cas9 gene editing

To confirm our hypothesis that the diterpenoids we detected in *Bs*-infected barley roots are products derived from the biosynthesis gene cluster in chromosome 2 and to functionally characterize of these secondary metabolites, we collaborated with Dr. Ivan Ascosta's group at the MPI of Plant Breeding Research, Cologne. They performed targeted mutation of *HvCPS2* and *HvKSL4* by CRISPR/Cas9 gene editing on the cultivar Golden Promise fast (GP-fast) (Gol *et al.*, 2020). The seeds and genome DNA of the CRISPR lines were sent to us, and the rest experiments including genotyping and infection assay were done in Prof. Dr. Tissier's lab.

Genotyping of CRISPR lines and Screening for Homozygous lines

The genotypes of CRISPR lines were determined by amplification of a fragment near the guide RNA followed by Sanger sequencing. Seeds from two independent mutant lines for each gene were grown. Plants homozygous for the mutation and transgene-free were selected for seed production, which were used for the following experiments.

The selected two *HvCPS2* mutants and two *HvKSL4* mutants were named *cps2-1* and *cps2-2*, *ksl4-1* and *ksl4-2*, respectively. The *cps2-1* mutant has two times 1 bp insertion while *cps2-2* has one time 1 bp insertion (**Tab. 2.1D and E**). Both mutants result in truncated HvCPS2 proteins (**Tab. 2.1A and B**). The *ksl4-1* and *ksl4-2* are both 1 bp insertion lines, exhibiting the mutation at the same position but different

nucleotide, which were inserted. The outcome of the two *ksl4* mutants at the protein level is the same, resulting in the same truncated HvKSL4 protein (**Tab. 2.1C**).

Table 2.1 Genotyping of *HvCPS2* and *HvKSL4* mutants

A

	180	190
WT	LEQEQDWMPCG	FEIN
cps2-1	LEQEQDWMPCG	LRD*

B

	230	240
WT	IPLNVLHAI	PTTLLFSLE
cps2-2	IPLNVLHAI	LNDPTLQP*

C

	130	140
WT	GNGYWGSGE	FD
ksl4-1	GNGYWGSGE	I*
ksl4-2	GNGYWGSGE	I*

D

	*HvCPS2*_sgRNA1
WT	CCATGT-GGCTTCGAGATTAACTTC
cps2-1	CCATGTGGGCTTCGAGATTAACTTC
cps2-2	CCATGT-GGCTTCGAGATTAACTTC

E

	*HvCPS2*_sgRNA2
WT	CCATAC-CAACGACCCTACTCTTCA
cps2-1	CCATACTCAACGACCCTACTCTTCA
cps2-2	CCATACTCAACGACCCTACTCTTCA

F

	*HvKSL4*_sgRNA1
WT	CCGGTG-AATTTGACTCACCAGCCA
ksl4-1	CCGGTGAAATTTGACTCACCAGCCA
ksl4-2	CCGGTGTAATTTGACTCACCAGCCA

Note: (A), (B), (C) Proteins sequences of HvCPS2 or HvKSL4 in wild-type or mutant plants. (D), (E), (F) DNA sequences of *HvCPS2* or *HvKSL4* in wild-type or mutant plants. Mutation in DNA sequences and the outcome in corresponding protein sequences are colored in red. PAM sequences recognized by Cas9 are colored in green.

Characterization of *HvCPS2* and *HvKSL4* mutants in *Bs* infection assay

An infection assay employing the pathogen *B. sorokiniana* was done on five genotypes of barley roots, including the wild-type barley cultivar, Golden Promise fast (GP-fast) (Gol *et al.*, 2020), *cps2-1*, *cps2-2*, *ksl4-1*, *ksl4-2*. Quantification of the gene expression after roots infection shows, as expected, the expression of *HvCPS2* or *HvKSL4* was significantly lower in its associated mutants, compared with the wild type (**Fig. 2.10**). *HvCPS2* was induced in *ksl4* mutants but not significantly compared to the wild type. Similarly, the expression of *HvKSL4* was also high in *cps2* mutants, although slightly reduced compared to the wild type (**Fig. 2.10**). At the metabolites level, the induced diterpenoids in the wild-type plants are entirely absent in all four mutants (**Fig. 2.10**). These results conclusively confirmed our hypothesis that these diterpenoids detected in barley roots derive from products of the two diTPSs encoded by *HvCPS2* and *HvKSL4* in the chromosome 2 gene cluster.

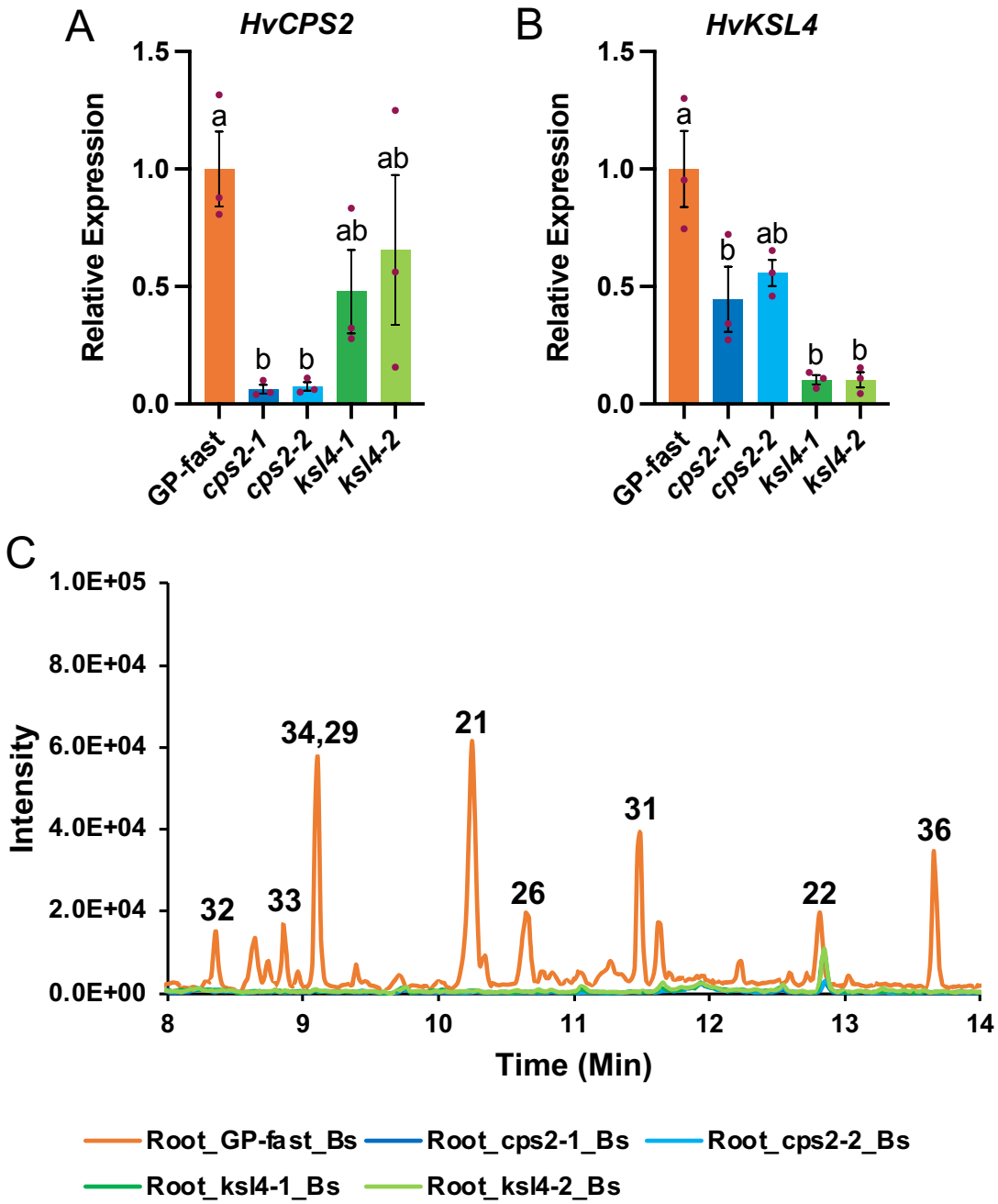

Figure 2.10 Gene expression of the barley diTPSs and chromatography profiles of diterpenoids in wild-type and mutant barley roots after 6 dpi with *B. sorokiniana*

(A), (B) Quantification of *HvCPS2* and *HvKSL4* in wild-type barley and mutants by qRT-PCR. Barley *ubiquitin* (*UBI*) was used as the reference gene. All expression data were normalized to that in GP-fast. Letters represent statistically significant differences using one-way ANOVA and Tukey's post-hoc test. Bars, Mean ± SEM (n=3). (C) Chromatograms (LC-MS/MS) of diterpenoids in wild-type barley and mutants after *Bs* infection (selected ions: m/z 313.2, 315.2, 317.2, 331.2; negative mode). Structures and MS/MS spectra of the diterpenoids are presented in **Fig. S2**.

Next, we sought to study the effect of pathogen infection on the growth of host plants and thereby evaluated the performance of barley with or without ability to produce diterpenoids. For this, wild type, *cps2* and *ksl4* plants were infected with *B. sorokiniana* (*Bs*). The fresh weight of roots after 6 dpi was weighed for infected and non-infected plants. It is well known that plants show a delay in growth when they are challenged by pathogens. This is because extra efforts are needed to produce many secondary metabolites, defense compounds for example, and molecules for other defense-related responses. It is called growth-defense balance. Different growth rates were observed for the five genotypes (**Fig. 2.11A**); therefore, percentage of root biomass reduction was calculated for a comparison of the five genotypes of barley in growth reduction after infection. Since we proposed that these diterpenoids are phytoalexins of barley, it is expected that four diterpenoid-defective mutants are more susceptible to *Bs*, thus it would result in a stronger reduction of growth compared with the wild-type plants. Compared with wild-type plants, stronger growth reduction was observed for *cps-ko2* and *ksl4-2* while slightly weaker was observed for *cps-ko1* and *ksl4-1* (**Fig. 2.11A**), but the two-way ANOVA test showed that the interaction of genotypes and *Bs* infection was not significant (P value = 0.1197). No clear conclusion can be drawn yet but these data suggests that there is no significant difference in growth reduction among the wild type, *cps2* and *ksl4* after challenge by *Bs*.

Then, we quantified the relative amount of the fungus *Bs* by qRT-PCR. Surprisingly, less amount of *Bs* was detected in the roots of all four mutants, compared with the wild type (**Fig. 2.11B**). Jointly, these results challenged our hypothesis, raising questions about the biological functions of the group of diterpenoids. It is known that *Bs* is an adaptive pathogen to the barley cultivar Golden Promise. It may have evolved a mechanism to detoxify the diterpenoid phytoalexins produced by barley. This would result in the absence of protective function of the phytoalexins. Even so, the same amount of *Bs* colonization in the mutants is expected compared with that in the wild-type plants. However, less colonization in the mutants was observed in the assay. It seems like these diterpenoids are facilitating the *Bs* infection of barley roots. Further studies are needed to understand the role of these diterpenoids in the interaction of barley and the pathogen *Bs*.

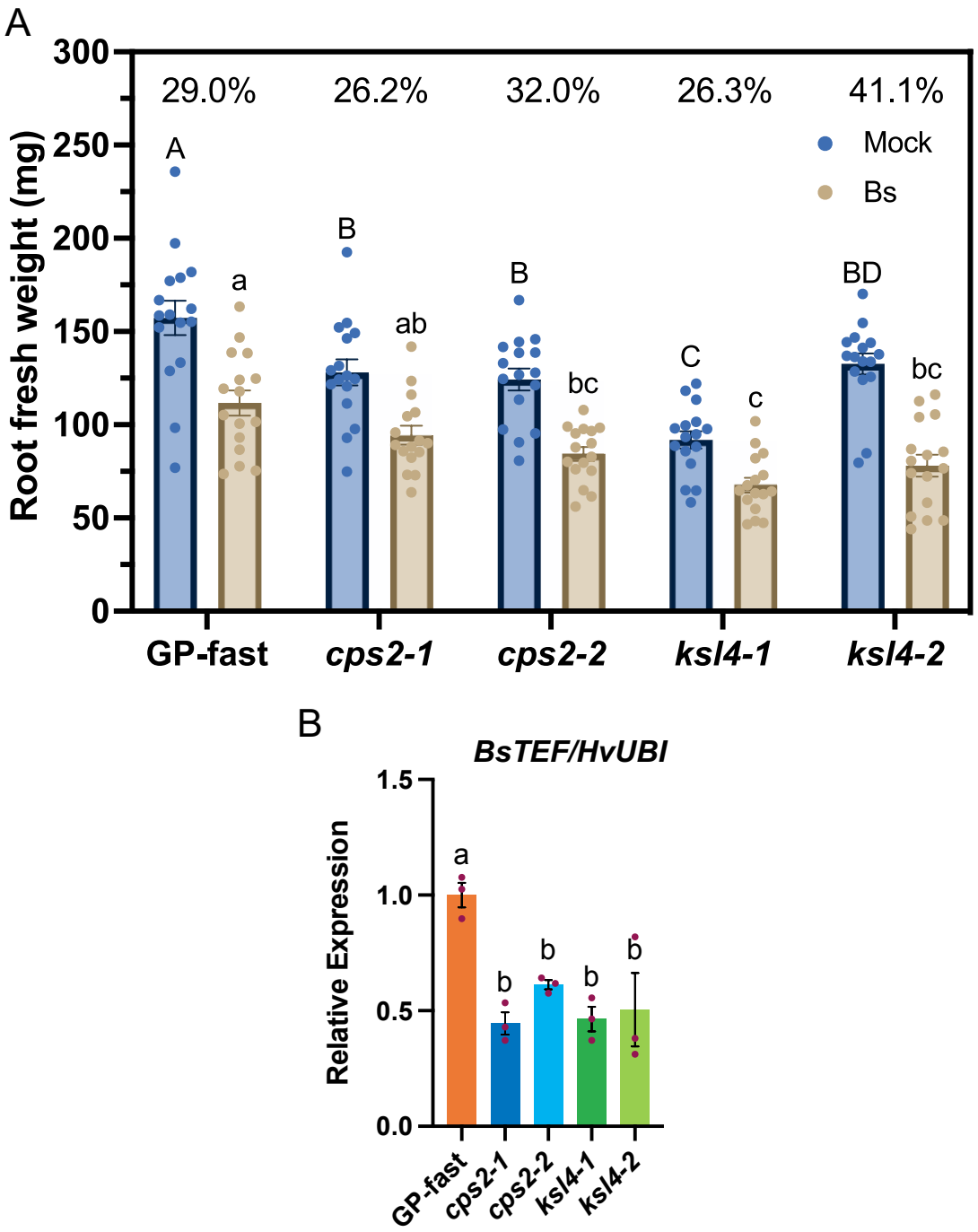

Figure 2.11 Quantification of fresh weight of barley roots and the relative amount of *Bs* in barley roots after 6 dpi with *Bs* or mock inoculation

(A) Fresh weight of roots was weighed. Bars, Mean ± SEM (n = 16). Number represents percentage of biomass reduction for each genotype of barley after *Bs* infection. It was calculated by the formular, the mean difference of root weight between mock and *Bs*-treatment divided by mean root weight of mock-treatment. Statistics: two-way ANOVA and Tukey's post-hoc test, p = 0.1197. Letters (uppercase letters for samples with mock-treatment, and lowercase letters for samples inoculated with Bs) represent statistically significant differences according to Tukey's post-hoc test ($p < 0.05$). Bars, Mean ± SEM (n = 16). (B) Quantification of *Bs* in the roots by qRT-PCR. The reference gene of barley is *Ubiquitin*. *BsTEF*: *Bipolaris sorokiniana* translation elongation factor. Statistics: one-way ANOVA and Tukey's post-hoc test, p = 0.0039. Bars, Mean ± SEM (n = 3).

2.6 Antifungal assay

The antifungal activity of diterpene **21** on *B. sorokiniana* (*Bs*), which was identified in barley roots and root exudates at a high abundant level, was tested by an *in vitro* assay. The growth curve of *Bs* was measured to evaluate the antifungal activity. A small level of inhibition activity on the growth of *Bs* was observed during the early stage (0-40 h, **Fig. 2.12**). However, after 40 h, *Bs* started growing faster in the medium with the diterpene **21** (100 or 200 µM, **Fig. 2.12**), compared with the control sample (0 µM). At the end of this assay (48 h), the mean OD of *Bs* culture with diterpene **21** at the concentration of 100 or 200 µM was slightly higher than that of the control sample, though it is not statistically significant (one-way ANOVA, P value = 0.3087). Larger differences are expected at later time points after 48 h. These data suggest that the fungus, *Bs*, may be able to metabolize the diterpene **21** to detoxify the plant phytoalexin. It may explain that the inhibition of **21** on the growth of *Bs* was not continuous but weakening as a function of time. Moreover, better growth after 40 h indicates that diterpene **21** or **21** derivatives may be able to promote or stimulate the growth of *Bs*.

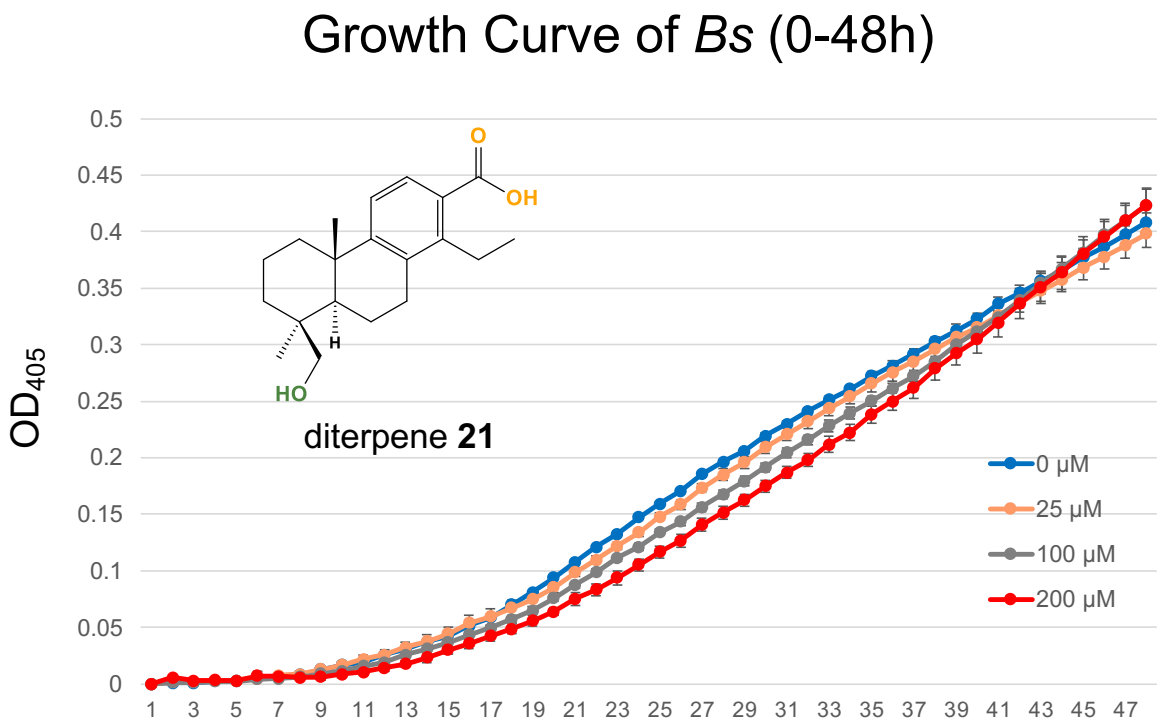

Figure 2.12 Growth curve of *B. sorokiniana*

The antifungal activity of diterpene **21**, one of the most abundant diterpenoids in both the roots and exudates of barley, was tested in different concentrations. Optical density at the wavelength of 405 nm was measured to evaluate the growth of *Bs*.

2.7 Metabolism of barley diterpenoids by *Bipolaris sorokiniana*

To further study the metabolism of barley diterpene **21** by *B. sorokiniana* (*Bs*), *Bs* was grown in axenic culture with or without diterpene **21**, whilst in parallel diterpene **21** was added into the medium without *Bs* present. After 3 days of growth, the whole culture was extracted, and the metabolites were analyzed by UPLC-QToF-MS/MS.

A modification of diterpene **21** was observed when *Bs* being present. Several diterpenoid-derived metabolites were identified from the culture. Two metabolites **37** and **38** (**Fig. 2.13A**), with the m/z of 331 and 329, were characterized as diterpenoids by their MS/MS fragments (**Fig. S2**). Their higher masses compared with **21** suggests they are oxidized derivatives of **21**. The mass difference of 16 and 14 respectively compared with **21** indicates that one more oxygen atom was added to diterpene **21**. Another group of metabolites with the same m/z of 549 including **39**, **40**, **41**, and **42**, were identified and characterized as conjugates of diterpene **21** and sesquiterpenes (**Fig. 2.13**). The formation of these conjugates is supposed to be a combination the diterpene acid **21** and a sesquiterpenoid with an alcohol group by an esterification to form an ester and water. The mass of the non-esterified sesquiterpene precursor should be 252, and it was used to extract peaks from the LC-MS/MS data. Several [M-H]- ion peaks with the m/z of 251, were found, and the one with the highest abundance was labeled as **43**. By searching of literatures (Phan *et al.*, 2019; Li *et al.*, 2020; Wang, Y-D *et al.*, 2022) and analysis of its MS/MS fragments (**Fig. 2.13C**), **43** is inferred as helminthosporic acid, a sesquiterpenoid metabolite isolated from *B. sorokiniana* (Phan *et al.*, 2019; Li *et al.*, 2020). The most abundant conjugates **42**, is inferred as diterpene **21** conjugated with helminthosporic acid (**Fig. 2.13D**). The other three conjugates are likely to be isomers of **42**. Since more than one sesquiterpene with the m/z of 251 was founded in the LC-MS/MS data of *Bs* culture, they may have also been conjugated to diterpene **21**. These conjugates and **37**, **38** can also be detected in the exudate of barley roots inoculated with *Bs*. A similar chromatographic profile of these conjugates was observed from the *in vitro* assay, compared with that from the extracts of medium

where infected barley roots were grown, providing evidence that the same modification of **21** by *Bs* occurs *in vivo* too (**Fig. 2.13A**).

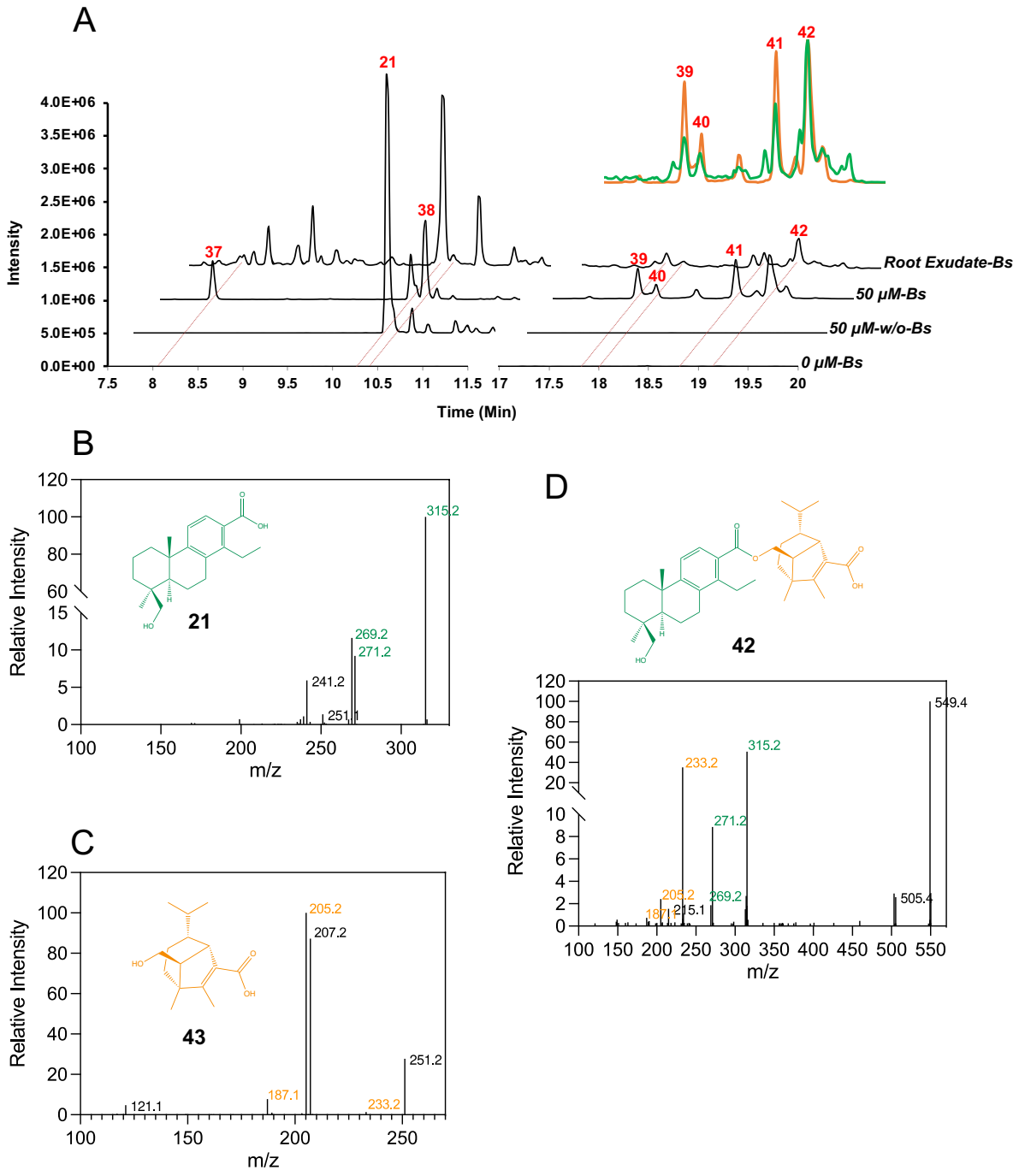

Figure 2.13 Metabolism of barley diterpene 21 by *Bipolaris sorokiniana*

(A) Selected ion chromatograms (m/z 315.2, 329.2, 331.2, 549.3; LC-MS/MS) of extracts of *Bs* culture or root exudates. Ion chromatograms (m/z 549.3) of extracts of *Bs* culture (in green) or root exudates (in orange) are superimposed while the intensity of ions were normalized to the largest peak. (B), (C), (D) MS/MS spectra of **21**, **43**, **42** respectively. For the spectrum of **42**, the fragments putatively derived from **21** are colored in green whilst that from **43** are colored in orange.

3. Discussion

3.1 Hordediene, a new diterpene backbone in the Poaceae

Seven types of diterpenoid phytoalexins were characterized from the Poaceae. They are pimarane-type diterpenoids including momilactones (*syn*-pimarane) and oryzalexins A-F (*ent*-sandaraco-pimarane), *ent*-cassane-type diterpenoids including phytocassanes, stemarane-type diterpenoids including oryzalide S, *ent*-kaurane-type diterpenoids including oryzalides and kauralexins, dolabrane-type diterpenoids including dolabralexins, and casbane-type diterpenoids including *ent*-10-oxodepressin (**Fig. 3.1 and Fig. 1.3**). Except *ent*-10-oxodepressin (Inoue *et al.*, 2013), which has a macrocyclic skeleton, all diterpenoid phytoalexins from the Poaceae identified so far are labdane-related diterpenoids.

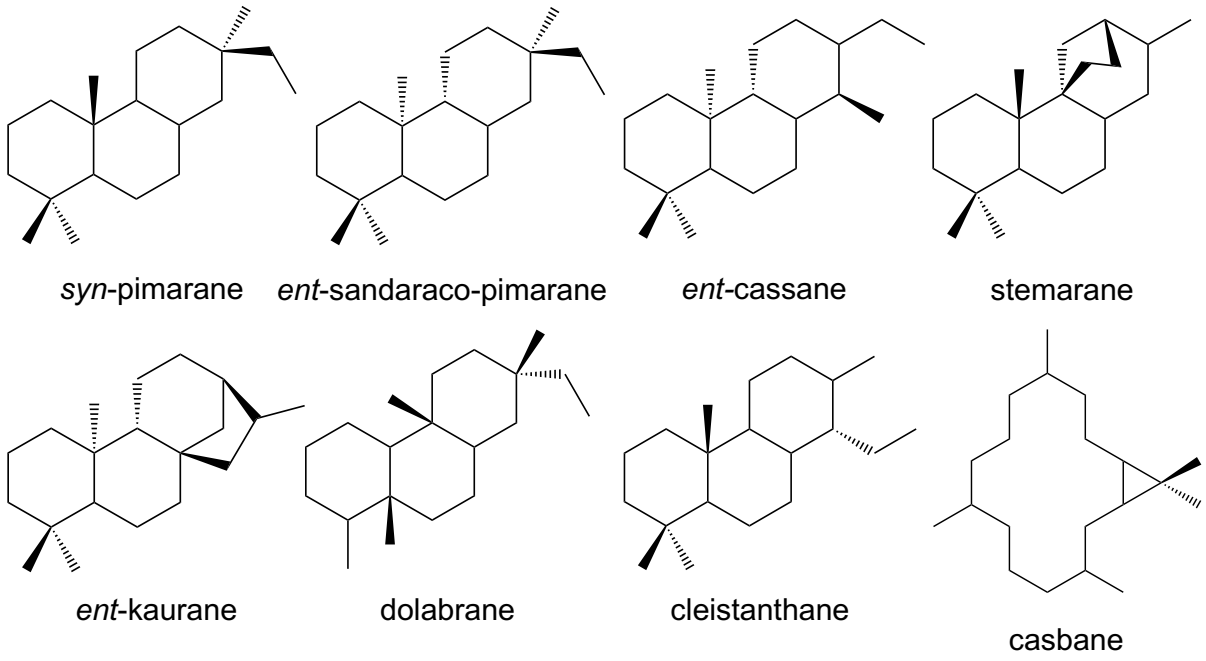

Figure 3.1 The type of diterpene backbones from the Poaceae

HvKSL4 catalyzes the cyclization of (+)-CPP to hordediene (Liu *et al.*, 2021). Two possible pathways of the cyclization reaction were studied recently (Liang *et al.*, 2022). Hordediene, is a new diterpene backbone in the Poaceae, belonging to cleistanthane-type diterpenoids (**Fig. 3.1**). Cleistanthane diterpenoids represent a small group of diterpenoids which is characterized by the presence of an ethyl group attached to C17, with occurrence in plants and fungi. Many of them are of the *ent*-configuration such as

phyllanembloids A–F from roots of *Phyllanthus emblica* (Lv et al., 2015), but some of the normal configuration, such as zythiostromic acids (Ayer & Khan, 1996). Intriguingly, several cleistanthane diterpenoids with some identical to that of barley were isolated from plants of the Vellozia, a representative genus of the Velloziaceae (Pinto *et al.*, 1984; Riehl & Pinto, 2000; dos Santos *et al.*, 2021). However, little information on the biological function of these diterpenoids is known, although some show phytotoxic and larvicidal activities (Ferreira *et al.*, 2017).

3.2 Biological roles of diterpenoids in the rhizosphere of barley

Terpenoid phytoalexins have long been studied in other monocot plants, rice, and maize. Most of them are diterpenoids including rice derived momilactones, oryzalexins, phytocassanes, and maize derived kauralexins. However, maize derived zealexins are sesquiterpenes. Among the maize and rice derived phytoalexins, many of them exhibit antimicrobial activities. Momilactone A and B exhibit potent inhibitory on germ tube elongation of *Magnaporthe oryza*, with a median effective dose (ED_{50}) around 15 and 3 μM respectively (Cartwright *et al.*, 1977). Phytocassanes and oryzalexins are active for the inhibition of spore germination of *Magnaporthe oryza*, with ED_{50} values ranging from 10 to 500 μM (Sekido *et al.*, 1987; Koga *et al.*, 1995; Koga *et al.*, 1997). *In vitro*, kauralexin B3 significantly inhibits the growth of the phytopathogens *Rhizopus microsporus* and *Colletotrichum graminicola* at the concentration of about 30 μM (Schmelz *et al.*, 2011). In a recent study, kauralexins deficiency mutants of maize exhibited increased disease susceptibility to *Fusarium graminearum*, which could cause stalk rot of maize (Ding *et al.*, 2019).

In this thesis, over 15 diterpenoids were detected in barley roots, of which individually the most part is secreted into the medium by the roots. The biosynthesis of these diterpenoids is only little induced by an endophytic fungus, *Serendipita vermifera*, but strongly by the pathogenic fungus *B. sorokiniana* (Liu *et al.*, 2021). A recent report on the metabolic profiling of barley spikelets upon *Fusarium graminearum* infection showed two diterpenoids with the masses of 302.2 and 318.2 that were the most strongly induced compounds (32 and 22 fold change respectively) (Karre *et al.*, 2017). Without firm identification, they were annotated as neoabietic and 7-hydroxykaurenoic acid respectively. We suspect that they also belong to the diterpenoid group we

identified here. This would suggest that they are not specifically induced by *B. sorokiniana* but can be induced by a wide range of phytopathogens. These barley derived diterpenoids are hypothesized to be phytoalexins, while in axenic culture, the diterpene acid **21** only exhibit a negligible inhibition on the growth of *B. sorokiniana* (**Fig. 2.12**). However, the highest concentration we tested in this assay was only 200 µM. It is worth to test higher concentrations because a greater concentration may be needed to inhibit mycelial growth than that to inhibit spore germination. For example, oryzalexin D showed an ED_{50} of 75 µM for the inhibition of *Magnaporthe oryzae* spore germination, but an ED_{50} of 750 µM were needed for the inhibition of mycelial growth (Sekido & Akatsuka, 1987). In addition, so far, only one out of more than 15 barley diterpenoids was tested towards its antimicrobial activity. Variation on the activities of phytoalexins was reported among zealexins. Zealexin A1 suppressed the growth of *Aspergillus flavus* and *Fusarium graminearum* at the concentration of around 100 µM while zealexin A2 showed no activity at any concentration (Huffaker *et al.*, 2011). Therefore, other candidates with potentially higher activities are waiting to be explored in follow up research.

In nature, like what we identified in barley roots, organisms usually produce complex mixtures of terpenes instead of just one or two compounds. For defense, one discussed advantage is that the individual component can act synergistically to provide greater toxicity or deterrence than the equivalent of a single substance (Gershenzon & Dudareva, 2007). For example, the antifungal activity of either one of two steroidal glycoalkaloids from potato was enhanced several-fold by the addition of as little as 10-20% of the second steroidal glycoalkaloid (Fewell & Roddick, 1993). For adapted enemies, such synergism may be attributed to the ability of some components to increase the persistence of others by inhibiting detoxification or excretion processes (Berenbaum & Neal, 1985; Stermitz *et al.*, 2000). Thus, it is highly interesting to test the activities of barley diterpenoids in a context of mixture. However, no matter whether to test these compounds individually or in combinations, one primary problem remains to have enough pure substances. It could be very challenging to achieve it due to their trace abundance in host plants or low productivity in a heterologous expression system. There are some other proposals regarding the possible value of mixtures. For example, for organisms with a wide range of enemies, a diverse

combination of defenses may help achieve simultaneous protection against numerous predators, pathogens, and parasites. Mixtures containing compounds with different physical and chemical properties have been suggested to impede the ability of enemies to evolve resistance (Pimentel & Bellotti, 1976).

Many terpenoid phytoalexins have been identified from a variety of plants so far, however, very little is known about their mode of action. Knowledge on how they work at the molecular level would help to understand their functions in plant defense. The highly lipophilic nature of many terpenes suggests that their principal targets are cell membranes, and their toxicity is caused by loss of chemiosmotic control (Cox *et al.*, 2000; Inoue *et al.*, 2004). The effect of oryzalexin D, a rice diterpenoid phytoalexin, on DNA, RNA, protein, lipid and chitin biosynthesis, respiration and cell membrane permeability was investigated in *Pyricularia oryzae*. At the ED_{50} of 750 µM, oryzalexin D caused leakage of potassium and inhibited the uptake of glutamate by mycelial cells of *P. oryzae*, suggesting that interference with the cell membrane function is the primary mechanism of action of oryzalexin D against *P. oryzae* (Sekido & Akatsuka, 1987). Hydroxylated 17-hydroxygeranyllinalool diterpene glycosides (17-HGL-DTGs) produced by the wild tobacco *Nicotiana attenuate* when ingested by hervivores, inhibit the biosynthesis of essential structural components of herbivore cell membranes to achieve defensive functions (Li *et al.*, 2021). In addition to cell membranes, there are also some other targets of terpenoids. A well-known anticancer diterpenoid Taxol, isolated from yew, kills tumor cells by binding to tubulin, which interferes with microtubule dynamics and arrests mitosis (Jordan & Wilson, 2004). However, little is known about the defense functions of Taxol in *planta*. Another hypothesis on the functions of terpenoids in plant defense is that terpenes synergize the effects of other toxins by acting as solvents to facilitate their passage through membranes. For example, the monoterpenes from the plant *Porophyllum gracile* were shown to increase the toxicity of a polyacetylene plant defense compound to the lepidopteran *Ostrinia nubilalis* (Guillet *et al.*, 1998).

Plants shape their environment by chemical communication. In recent years, more and more attention has been paid to the interaction of plants with the belowground environment, mainly focusing on the narrow zone of soil that surrounds the plant root,

the rhizosphere (Venturi & Keel, 2016). The rhizosphere is a highly complex ecosystem accommodating diverse microorganisms including fungi, bacteria, or nematodes. Plants roots secrete a group of primary metabolites and secondary metabolites, which can shape, signal, and interfere with the rhizosphere microflora. Vice versa, the rhizosphere microbiome has a direct effect on plant health and resistance to pathogens (Pieterse *et al.*, 2014). There are already evidences of specialized metabolites secreted by the roots, which impact on the composition of the microbiome (Massalha *et al.*, 2017; Huang *et al.*, 2019; Murphy *et al.*, 2021). Root triterpene metabolites in *Arabidopsis thaliana* were reported to be involved in mediating the establishment of an *Arabidopsis*-specific microbiota (Huang *et al.*, 2019). Employing a synthetic microbial community (SynCom) consisting of 19 taxonomically diverse bacterial strains isolated from the *A. thaliana* root microbiota, they demonstrated that these triterpenoids could selectively modulate the growth of these bacteria. Interestingly, some root bacteria were found to be able to selectively metabolize certain triterpenoids, such as thalianyl fatty acid esters (Huang *et al.*, 2019). A very recent study reported that the rhizosphere microbiome from the maize mutant *Zman2*, which is deficient in dolabralexin and kauralexin diterpenoids, differed significantly from that of the wild-type plant in *alpha*-proteobacteria of the order Sphingomonadales, suggesting a role of the maize diterpenoids in the assembly of the rhizosphere microbiome, in addition to chemical defenses (Murphy *et al.*, 2021). Besides of root microbiota, effects of root metabolites on nematode pests have also been studied. In rice, mutants which lack diterpenoid phytoalexins showed increased susceptibility to the rice root-knot nematode, *Meloidogyne graminicola*. A field experiment revealed that the mutant plants exhibited an altered composition of root nematode communities (Desmedt *et al.*, 2022). Additionally, benzoxazinoids from maize were reported to show differential and selective effects on soil nematodes (Sikder *et al.*, 2021). There are some reports studying the microbiota in barley rhizosphere but very few specifically on the interactions of plant specialized metabolites and the barley root microbiome (Bulgarelli *et al.*, 2015; Maver *et al.*, 2021; Escudero-Martinez *et al.*, 2022; Mahdi *et al.*, 2022). In this thesis study, we observed that without induction, the identified diterpenoids are present in barley roots and exudates at a low basal level, suggesting their potentially additional roles in the rhizosphere. In further research, the diterpenoid deficiency lines *cps2* and *ksl4*,

together with the wild type, can be used for a comparison study of the composition of root microbiota.

3.3 Detoxification of diterpenoid phytoalexins by the pathogen *B. sorokiniana*

The lifestyle of a pathogen often determines how they interact with the defense compounds of the host plant (Tiku, 2020). The lifestyles of pathogens are often divided into three categories, biotrophic, necrotrophic, and hemibiotrophic. Biotrophs derive nutrients and energy from living cells, while necrotrophs derive them from dead cells; they invade and kill plant tissue rapidly and live on the dead remains. Hemibiotrophs have an initial period of biotrophy, followed by necrotrophy. Biotrophic pathogens depend on the colonization of living tissue, and the maintenance of cellular integrity may prevent the release of defense compounds from their hosts. Additionally, biotrophs often with greater host-specialization tend to present greater basal tolerance of coevolved host antimicrobials and may be less dependent on specific detoxification (Westrick *et al.*, 2021). Contrarily, necrotrophic and hemibiotrophic fungi induce cell death and compromise the integrity of plant tissues during colonization. Thus, detoxifications of host antimicrobials are often reported in these two categories of pathogens. The detoxification is facilitated by a variety of mechanisms including metabolization of defense compounds to nontoxic derivatives, or transporter-mediated efflux to maintain the compounds at sublethal thresholds.

In this thesis study, after the inoculation of *B. sorokiniana* with **21**, two classes of compounds derived from the conversion of **21** (Mass, 316), were observed (**Fig. 2.13**). The first class consists of two compounds with the mass of 330 and 332. They are inferred to be **21** derivatives by further oxygenation. The enzyme which is responsible for the reaction remains unknown so far. Since a large number of sesquiterpenoids were identified in *B. sorokiniana* (Phan et al., 2019), it would not be surprising that one enzyme, e.g. a monooxygenase, from the biosynthesis pathway of these sesquiterpenoids is employed nonspecifically for the enzymatic detoxification of **21**. However, to date, the biosynthesis of the sesquiterpenoids of *B. sorokiniana* is still unknown. Despite the broad range of terpenoid phytoalexins known, and despite the number of phytopathogens known to metabolize terpenoids *in vitro*, according to the

literature (Westrick *et al.*, 2021), the only described enzymes in terpenoid detoxification are from the pine pathogen *Grosmannis clavigera*. Two Baeyer-Villiger monooxygenases were identified that were involved in the detoxification of the antifungal monoterpene, limonene (Wang *et al.*, 2014). The Baeyer-Villiger oxidation is an oxidation reaction in which ketones are converted to esters and cyclic ketones to lactones. The biochemical version of the reaction catalyzed by Baeyer-Villiger monooxygenases was reported later in several bacteria and fungi (Torres Pazmiño *et al.*, 2010). Baeyer-Villiger monooxygenases have a very broad range of substance diversity. They catalyze key steps in the degradation of acetone, bulky cyclic aliphatic ketone and linear ketones (Torres Pazmiño *et al.*, 2010). Highly complex compounds like steroids, sesquiterpenoids and aflatoxins can also act as the substrate of this enzyme family (Torres Pazmiño *et al.*, 2010). It is worth to mine the genome of *B. sorokiniana* for candidate genes of Baeyer-Villiger monooxygenase family and test their ability to metabolize the diterpenoids identified in barley. Momilactone A, a rice phytoalexin was degraded by the rice blast fungus into 3,6-dioxo-19-nor-9β-pimara-7,15-diene, which was proposed to be an intermediate of a detoxification pathway. However, the enzyme which dose the conversion remains unknown (Imai *et al.*, 2012).

The second class of metabolized compounds consists of a group of metabolites, which are proposed to be barley diterpene **21** conjugated with sesquiterpenes from *B. sorokiniana* (**Fig. 2.13**). They have not been described so far, to the best of our knowledge, in the context of plants and pathogen infection. Detailed literature search revealed four sesquiterpene conjugates (**Fig. 3.2**) isolated from the culture of the potato endophytic fungus *Bipolaris eleusines* were reported (Li *et al.*, 2018; He *et al.*, 2019; Ai *et al.*, 2022). They are very similar to the compounds we described in **Fig. 2.13D**. The common unit of the conjugates is a sesquiterpene, which can be helminthosporol or helminthosporic acid (**Fig. 3.2**), two natural products isolated from the Bipolaris genus, including *Bipolaris sorokiniana* (Phan *et al.*, 2019). The other moiety of these compounds is variable and can be 2-hydroxypropanoic acid, phenylthiazole, and xanthone so far (**Fig. 3.2**). Regarding their biological activities, bipolarithizole A, bipolenins I and J exhibit potent antifungal activity with minimal inhibitory concentration (MIC) of 14-40 μM (He *et al.*, 2019; Ai *et al.*, 2022). So far, no biosynthesis gene for these conjugates has been characterized, however, one high

possible hypothesis is that the synthesis enzyme for bipolenins conjugates or diterpene-sesquiterpene conjugates is the same or from the same family. Furthermore, this enzyme can be a very promising target for fungi control. Inhibition of this enzyme chemically or biologically in the phytopathogens from the genus Bipolaris may help to reduce their tolerance to the phytoalexins from the host plants, thus achieving an inhibited growth of the fungi.

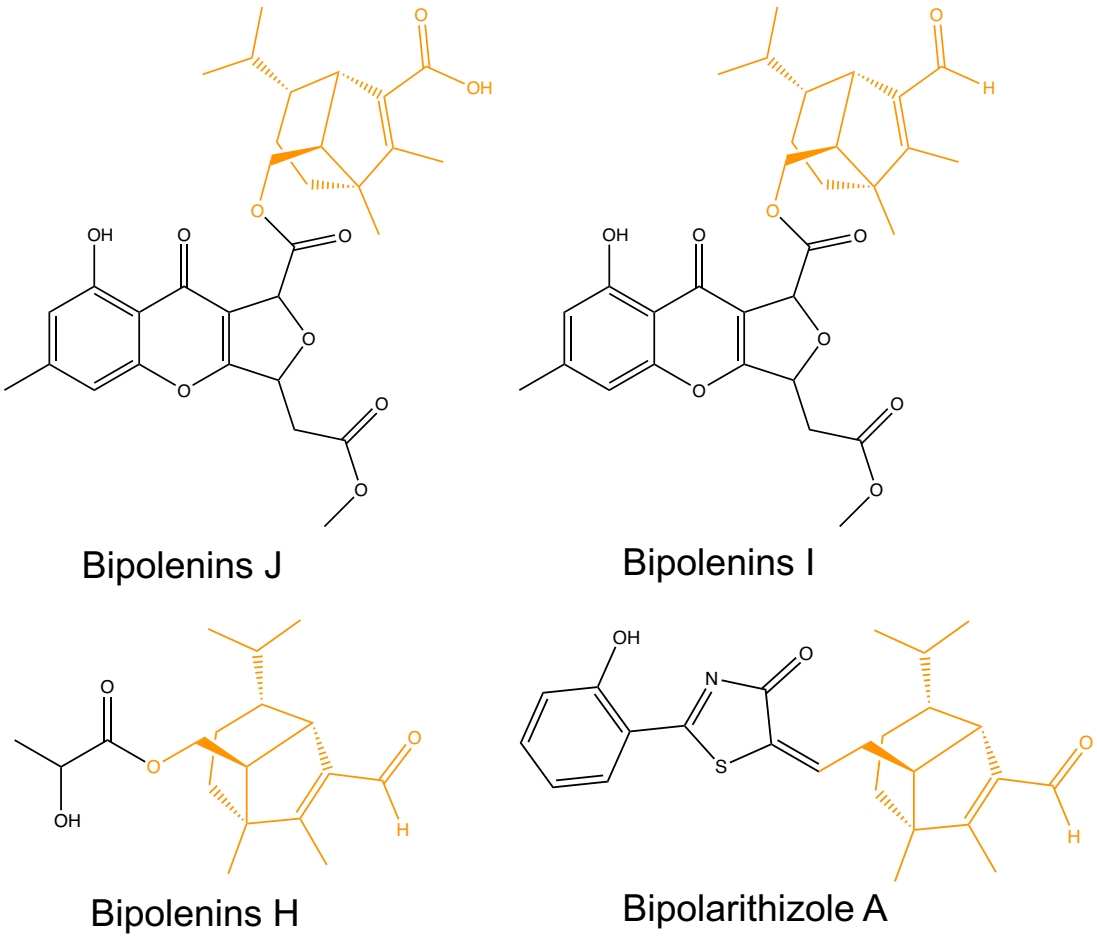

Figure 3.2 Sesquiterpenoid conjugates isolated from the culture of *Bipolaris eleusines*

The shared moiety of these compounds is helminthosporol or helminthosporic acid and is colored in orange.

As we described in section **2.5**, contrarily, we observed less colonization of *B. sorokiniana* in the diterpenoid deficiency mutants than in the wild-type plants. Therefore, we hypothesize that in addition to be phytoalexins, the barley diterpenoids may have extra functions in the interaction of barley roots and *B. sorokiniana*. Our proposal is that in certain ways, the roots infection by *B. sorokiniana* is facilitated by the diterpenoids from barley. Such a facilitation could be attributed to chemotaxis.

Fungal pathogens and symbionts have been known to orient hyphal growth towards chemical stimuli from the host plants (Zentmyer, 1961; Turrà & Di Pietro, 2015; Turrà *et al.*, 2015). Intriguingly, a study in 1988, reported that germ tubes of *Cochliobolus sativus* (anamorph: *Bipolaris sorokiniana*) grew chemotropically towards sterilized barley roots and root exudates (Jansson *et al.*, 1988). Chemotropism was confined to the zone approximately 0-2 mm from the root or the source of root exudate. Without knowing the exactly active molecules of the root exudates yet, the diterpenoids we identified could be one component of the stimuli molecules. Less colonization of *B. sorokiniana* in diterpenoid deficiency mutants than that in the wild-type barley (**Fig. 2.11**), could be explained by the lacking or reduction of such chemical stimuli. To verify this hypothesis, an assay could be designed to test the activity of stimulation to *B. sorokiniana*, employing the root exudates from wild type and mutant plants, or purified barley diterpenoids. Potentially, and taking the diterpenoid phytoalexins from other monocots into consideration, we suspect the diterpenoids of barley are toxic phytoalexins. Then one question could be that why the fungus would approach these toxic molecules. However, this can be explained by the ability of *B. sorokiniana* to further metabolize the diterpenoids to many derivatives, and it can be considered as a process of detoxification. Regarding to the chemotropism in fungus-plant interaction, a comprehensive study was performed using *Fusarium oxysporum* and the host *Solanum lycopersicum* (Turrà *et al.*, 2015). *F. oxysporum* can redirect hyphal growth rapidly and specifically towards gradients of different chemoattractants, including sugars, amino acids, peptide pheromones and plant root exudates. It was further shown that directed growth of the *F. oxysporum* towards the roots of the host tomato is triggered by the catalytic activity of secreted class III peroxidases, a family of haem-containing enzymes present in all land plants (Passardi *et al.*, 2004; Turrà *et al.*, 2015). The chemotropic response requires conserved elements of the fungal cell integrity mitogen-activated protein kinase (MAPK) cascade (Levin David, 2005) and the seven-pass transmembrane protein Ste2, a functional homologue of the *Saccharomyces cerevisiae* sex pheromone α receptor (Arkowitz, 2009). These results revealed a potentially conserved chemotropic mechanism of root-colonizing fungi and suggested a function for the fungal pheromone-sensing machinery in locating plant hosts in a complex environment (Turrà *et al.*, 2015). In fungal symbionts, it has been shown that strigolactones, a group of sesquiterpene lactones released by plant roots, induce

extensive hyphal branching in germinating spores of the arbuscular mycorrhizal fungus *Gigaspora margarita* thereby increasing the probability of the symbiont to contact to the root (Akiyama *et al.*, 2005). Exploring the roles of specialized metabolites of the plant host in the rhizosphere would help to understand the language of the chemical communication between host plants and other organisms.

3.4 The biosynthetic gene cluster in barley chromosome 2 is evolutionarily conserved within the monocots

Investigations of specialized diterpenoid metabolism have been conducted in several monocot species, including rice (*Oryza sativa*) (Shimura *et al.*, 2007), maize (*Zea mays*) (Schmelz *et al.*, 2011; Ding *et al.*, 2019), switchgrass (*Panicum virgatum*) (Pelot *et al.*, 2018; Muchlinski *et al.*, 2021), and wheat (*Triticum aestivum*) (Wu *et al.*, 2012; Zhou, K. *et al.*, 2012; Polturak *et al.*, 2022). Many of the diterpenoids, mainly from rice and maize, have been characterized as phytoalexins (Schmelz *et al.*, 2014). In this thesis, we showed that like maize and rice, barley (*Hordeum vulgare*) from the Triticeae, is also able to produce diterpenoid phytoalexins when challenged with a pathogen. To our best knowledge, they are the first class of diterpenoid phytoalexins which are characterized from the species. This, production of diterpenoid phytoalexins appears to be a common feature of monocots.

It is noteworthy that genes involved in the biosynthesis of these diterpenoids are frequently localized in clusters encoding diterpene synthases (diTPSs) and cytochrome P450s (CYPs) (Shimura *et al.*, 2007; Swaminathan *et al.*, 2009; Liang *et al.*, 2021). It is of interest to know whether the hordediene biosynthetic gene cluster is specific to *Hordeum vulgare* L., and to investigate if there are evolutionary relations with the diterpenoid biosynthetic gene clusters in other monocots. A search for regions in rice, maize, and wheat that are syntenic to the cluster on barley chromosome 2 was performed using MCScanX (Wang, Y *et al.*, 2012). Syntenic regions to the barley gene cluster were founded in the rice and wheat genomes but not in the maize genome (**Fig. 3.3A**). The syntenic region in rice contains one of the biosynthesis gene clusters for momilactones, which has been thoroughly studied. Very similar gene clusters to the one in barley were found in the syntenic regions of the wheat genome. Because *Triticum aestivum* is a hexaploid species, it was expected that clusters would be found

in the corresponding regions of the homeologous chromosomes (**Fig. 3.3A**). The function of the gene clusters in wheat still remains largely unknown despite that some *CPS* and *KSL* genes from these clusters were characterized (Polturak *et al.*, 2022). However, functions of the CYPs from the cluster, probably involved in the further oxidation of a diterpene backbone, are still unknown, and no associated diterpenoids from wheat plants have been identified yet. A micro-synteny analysis to identify orthologs among these gene clusters was performed. *CPS*, *KSL*, and multiple *CYPs* from the CYP99 family are conserved in all the clusters except that no *CYP* is present in the syntenic region of wheat chromosome 2B (**Fig. 3.3B**). Furthermore, our analysis and previous publications showed that large regions of rice chromosome 4 including the region of momilactone biosynthetic gene cluster (MBGC) are syntenic to regions of barley or wheat chromosome 2 (Ahn *et al.*, 1993; Thiel *et al.*, 2009). Therefore, probably these gene clusters share a common evolutionary origin. A similar hypothesis was also described recently in (Polturak *et al.*, 2022) by a synteny analysis between the MBGC of rice and the diterpenoid gene clusters of wheat. A more recent study investigated the birth and evolution of MBGCs in grass by comparative genomic analyses of 40 monocot plant genomes. They concluded that the MBGC in Oryzoideae originated from a MBGC-like cluster in Triticeae via two events of lateral gene transfer and was followed by loss or recruitment of genes (Wu *et al.*, 2022). However, the derived diterpenoid products are different among these clusters although they may share a common origin. The cluster of rice produces momilactones, while the one of barley produces hordediene derived diterpenoids, and one cluster of wheat produces isopimara-7,15-diene derived diterpenoids according to the literature (Polturak *et al.*, 2022). Additionally, of these clusters, each one contains a class of enzymes which are specific and not syntenic to genes in the other two species. In MBGC of rice, there are two short-chain dehydrogenase/reductase (SDR) genes, *OsMS1* and *OsMS2*, while in the barley cluster, it is a CYP from CYP89 family, and in the wheat clusters, there are multiple CYPs from the CYP71 family (**Fig. 3.3B**). They are supposed to be tailoring enzymes for the diterpene backbone from each cluster, which may also have contributed to the diversity of diterpenoid products of the clusters in different species.

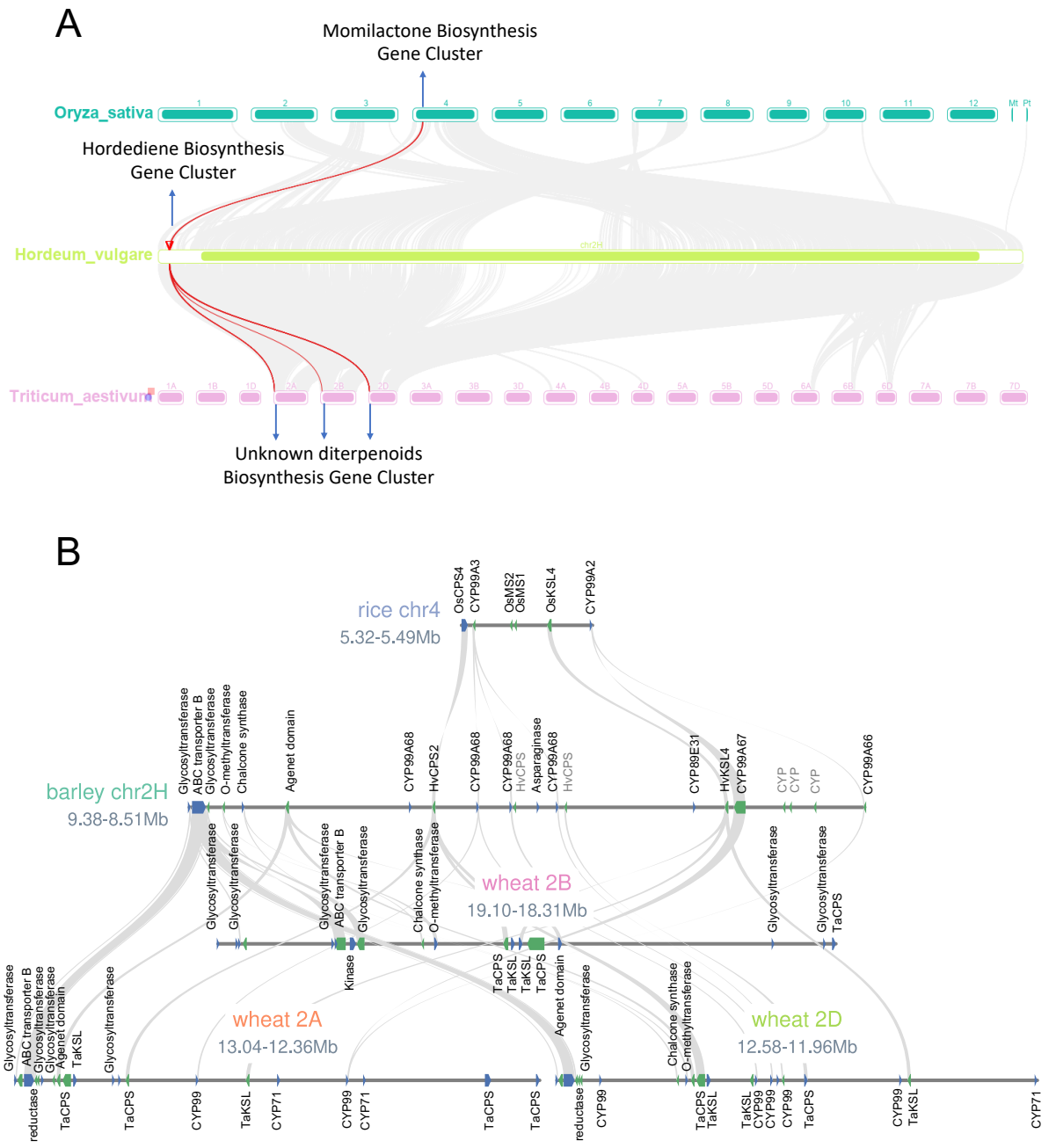

Figure 3.3 Synteny analysis of barley chromosome 2, rice and wheat genome

(A) Synteny analysis of barley chromosome 2, rice and wheat genome. Homolog pairs are connected by grey curved lines, and homolog pairs among the three analyzed gene clusters are colored red. (B) Micro-synteny analysis of genes in momilactone cluster of rice, hordediene cluster of barley, and the diterpenoid clusters of wheat. The annotation of genes in wheat clusters derives from the functional annotation of the best hit by a blastp search against the Swiss-Prot database (Consortium, 2020).

In addition to diterpenoids, biosynthetic gene clusters have also been reported for other classes of secondary metabolites including triterpenoids, cyanogenic glycosides, benzylisoquinoline alkaloids, and steroidal alkaloids et al. in both monocots and eudicots (Nützmann *et al.*, 2016). Why the genes are clustered is still enigmatic, but

the physical association and duplication of genes offer several potential advantages. First, genetic linkage of genes will reduce the risk of disruption of the favorable gene sets by recombination, and physical association may also reduce the risk of accumulation of possible toxic or unexpected functional intermediates due to mutation or loss of one gene in the cluster (Nützmann *et al.*, 2016). Second, the presence of multiple copies of highly similar genes provides opportunities for gene rearrangements and independent evolution, thereby providing the base for rapid chemical innovations. The capacity to evolve novel defenses rapidly constitutes a key evolutionary adaptation in the arms race against pests and pathogens (Liu *et al.*, 2021).

3.5 Model of current understanding

An established model to describe the molecular arms race between plants and pathogens is called the zig-zag model (Jones & Dangl, 2006). In this model, pathogen associated molecular pattern-triggered immunity (PTI) evolved initially to halt further colonization. Successful pathogens then developed effectors, which can interfere with PTI, resulting in effector-triggered susceptibility. In the next phase, some effectors were then recognized by nucleotide-binding site–leucine-rich repeat (NB-LRR) proteins, thus activating effector-triggered immunity (ETI). By natural selection and fast evolution, pathogens can avoid ETI by diversifying recognized effectors or acquiring new ones that suppress ETI. Similarly, newly evolved plant NB-LRR alleles can recognize the newly acquired effectors, activating ETI again.

In this thesis study, we observed a chemical arms race between the host plant and an adapted pathogen. When the host plant, barley is challenged by a pathogen, *B. sorokiniana*, it produces a class of diterpenoids. An antifungal bioassay showed that a highly abundant diterpenoid (**21**) inhibited spore germination and growth of *Fusarium culmorum*, and delayed spore germination of *Serendipita indica*, mycelium growth of *Serendipita vermifera* (recent data from the group of Prof. Zuccaro, not shown in this thesis). Thus, they function as defense compounds of barley against fungal pathogen. However, only a negligible effect of barley diterpenoid **21** on the growth of *B. sorokiniana* was observed. A metabolomic profiling of an axenic culture of *B. sorokiniana* supplied with the barley diterpenoid **21**, showed that the diterpenoid can be metabolized to two groups of modified compounds. This can be regarded as a

detoxification process of the diterpenoid by *B. sorokiniana*. I speculate that a mechanism to maintain the chemical defense by inhibiting the detoxification or diversifying defense compounds is expected to exist in certain barley varieties which show resistance to *B. sorokiniana*, though it is still unknown yet. Moreover, less colonization of *B. sorokiniana* in diterpenoid deficiency mutants compared with the wild-type plants suggests an additional function of this group of diterpenoids. Preliminary data from the group of Prof. Zuccaro showed that the spore gemination and growth of *B. sorokiniana* were stimulated by the diterpene **21**. In addition, an article reported germ-tubes of *B. sorokiniana* showed chemotropic growth towards barley roots and root exudates (Jansson *et al.*, 1988). We hypothesize that the group of barley diterpenoids are the or some of the effective molecules that trigger the chemotropism of *B. sorokiniana*. The chemotropism may have played a role in the infection process of barley. For example, these barley specialized metabolites may have been used as landmarks for localizing host plants in a complex environment such as the soil.

4. Summary and outlook

Phytoalexins are specialized metabolites that are induced upon pathogen infection and contribute to the chemical defense of plants. Upon infection by the fungal pathogen *B. sorokiniana*, several diterpenoids with molecular masses of 316, 318 and 332 were induced in barley roots and secreted into the medium. We identified a gene cluster in barley (*Hordeum vulgare* L.) localized on chromosome 2 that covers over 600 kb and comprises genes coding for a (+)-copalyl diphosphate synthase (HvCPS2), a kaurene synthase like (HvKSL4) and several cytochrome P450 oxygenases (CYPs) (Liu *et al.*, 2021). Most of the genes on the cluster are strongly induced and co-expressed upon infection by *B. sorokiniana*, indicating that these genes are responsible for the biosynthesis of barley diterpenoids induced by *B. sorokiniana* infection. Expression of HvCPS2 and HvKSL4 in yeast and *N. benthamiana* resulted in the production of a single major product, whose structure was determined to be of the cleistanthane type and was named hordediene (Liu *et al.*, 2021). Co-expression in yeast and *N. benthamiana* of HvCPS2, HvKSL4 and three CYPs from the cluster resulted in the production of several diterpenoids, including the most abundant product **21** with a molecular mass of 316, which is identified in barley roots as well, demonstrating that we were able to reconstitute the barley pathway in yeast and *N. benthamiana*. This compound and several intermediates in the pathway were isolated and their structures were determined by NMR. Mutants were generated by CRISPR/Cas9 gene editing in *HvCPS2* and *HvKSL4*. Plants with homozygous mutations in either of these two genes resulted in a complete loss of the identified diterpenoids in barley, showing that these diterpene synthases are responsible for the production of diterpenoids in barley roots during pathogen infection. Low antifungal activity of **21** on the growth of *B. sorokiniana* and the modification of **21** to two groups of derivatives by *B. sorokiniana* indicates the presence of detoxification mechanisms in the pathogen. Lower colonization in barley with mutations in *HvCPS2* or *HvKSL4* than that in wild-type plants suggests additional functions of this group of diterpenoids in barley.

The biological functions of the barley diterpenoids still remain to be elucidated. Regarding the role as phytoalexin, more bioassays with additional fungal species and

different diterpenoids of barley need to be performed. The activity of a mixture of two or more diterpenoids compared with that of the individual one is also worth investigating. However, these assays all rely on the producing of diterpenoid substances in yeast or *N. benthamiana*, which is quite time-consuming and labor-intensive to get enough. An alternative assay could be a comparison of the performance of the mutants and the wild-type barley challenged with different pathogens. Since these diterpenoids were also detected in the leaf and stem of barley, one question is whether they play a role in defense against pathogens in these organs. Several observations indicate that *B. sorokiniana* shows chemotropism to the diterpenoids of barley. Several robust methods have been developed to quantitatively measure the chemotropism (Jansson *et al.*, 1988; Turrà *et al.*, 2015). Assays could be designed to test the activity of purified barley diterpenoids or root exudates of wild-type and mutant plants.

The detoxification mechanism of *B. sorokiniana* is also worth further studies. It is probably a single enzymatic reaction for a broad range of substrates since many different sesquiterpene conjugates were detected in this study and were reported in other studies (**Fig 3.3**). Data mining of the transcriptome data in (Sarkar *et al.*, 2019), and of the genome sequence of *B. sorokiniana* could be an approach to identify candidates of the enzyme for the proposed reaction. Traditional biochemical approaches for identification of the enzyme can also be an alternative way. Mutation of the gene encoding the enzyme and test of virulence of the mutants as a pathogen could be planed after the identification. If these were successful, this gene could be used as a target for the control of *B. sorokiniana*, or even other pathogenic fungi if such a mechanism is conserved in a broad range of fungal species.

Since the diterpenoids are present at a low basal level in non-infected plants, one question that could be asked is do they play a role in the recruitment or shaping of root microbiota in barley? A comparison of the microbiota composition in the rhizosphere of wild-type barley and mutants would provide a first insight into this question.

5. Materials and Methods

5.1 Materials

Chemicals, solvents, and supplies

Chemicals, media components, and solvents were obtained from the following suppliers: Carl Roth, Duchefa Biochemie, Merck, J.T. Baker, Sigma-Aldrich, and Honeywell Riedel-de Haën™. Molecular biology supplies and kits were obtained from Bio & Sell, Biozym, highQu GmbH, Life Technologies (Thermo Fisher Scientific), Macherey-Nagel, Merck, New England Biolabs, and Promega. Primer synthesis and sequencing were performed by Eurofins Genomics.

Organisms

Escherichia coli

The bacteria strain *E. coli* (DH10B, Invitrogen) was used to propagate plasmid vectors. Genotype: F– *mcrA* Δ(*mrr-hsdRMS-mcrBC*) φ80*lacZ*ΔM15 Δ*lacX74 recA1 endA1 araD139* Δ (*ara-leu*)7697 *galU galK* λ– *rpsL*(Str^R) *nupG*

Agrobacterium tumefaciens

The *Agrobacterium tumefaciens* GV3101::pMP90 (Koncz & Schell, 1986) was used for transit expression in *Nicotiana benthamiana*.

Saccharomyces cerevisiae

The yeast strain (INV*Sc*1, Invitrogen) was used for the heterologous expression of plant proteins.

Genotype: *MATa his3D1 leu2 trp1-289 ura3-52 MA*T *his3D1 leu2 trp1-289 ura3-52*

Bipolaris sorokiniana

The plant pathogen, *B. sorokiniana* (ND90Pr) were used to study the defense response of barley roots under the challenge of pathogen infection.

Hordeum vulgare L.

Barley (*Hordeum vulgare* L.) was used as the host plant for the pathogen *B. sorokiniana*.

Two cultivars, Golden Promise and GP-fast (GoI *et al.*, 2020), were used as wild type. Four mutants, *cps2-1*, *cps2-2*, *ksl4-1*, and *ksl4-2* were generated from the cultivar GP-fast by CRISPR/Cas9 gene editing.

Nicotiana benthamiana

The wild type *N. benthamiana* was used for the transit expression of plant proteins.

Media

The media used to grow *E. coli*, yeast, Agrobacterium, and barley are listed with their composition and optional supplements in **Tab. 5.1**. All media were sterilized at 120 °C and 2 bar for 15 mins.

Table 5.1 Media composition and supplements

Medium type	Composition	Supplements	Reference
LB medium (*E. coli*, *A. tumefaciens*)	10 g/L Tryptone, 10 g/L NaCl, 5 g/L Yeast extract, pH 7.5	10 g/L Micro agar, 50 µg/mL Carbenicillin, 50 µg/mL Gentamycin, 50 µg/mL Kanamycin, 25 µg/mL Rifampicin, 100 µg/mL Spectinomycin, 50 µg/mL X-Gal	(Bertani, 1951)
SOC medium (*E. coli*)	20 g/L Tryptone, 5 g/L Yeast extract, 10 mM NaCl, 2.5 mM KCl, 10 mM $MgCl_2$, 10 mM $MgSO_4$, 20 mM Glucose		(Hanahan, 1983)
YPD (*S. cerevisiae*)	20 g/L Peptone, 10 g/L Yeast extract, pH 6.5	20 g/L Micro agar, 2% (w/v) D(+)-glucose or D(+)-galactose	Clontech Yeast Protocols (PT3024-1)
Synthetic Dropout medium (SCU) (*S. cerevisiae*)	6.7 g/L Yeast Nitrogen Base without amino acids, 0.8-1 g/L Dropout supplement without Uracil	20 g/L Micro agar, 2% (w/v) D(+)-glucose or D(+)-galactose	Clontech Yeast Protocols (PT3024-1)
CM medium (*B. sorokiniana*)	10 mL solution A (100 g $Ca(NO_3)2{\cdot}4H_2O$ per L ddH_2O; autoclaved), 10 mL solution B (20 g KH_2PO_4, 25 g $MgSO_4{\cdot}7H_2O$, 15 g NaCl per L ddH_2O, pH 5.3, filter-sterilized), 0.5 mL Srb's micronutrients (57.2 mg H_3BO_3, 393 mg $CuSO_4{\cdot}5H_2O$, 13.1 mg KI, 60.4 mg $MnSO_4{\cdot}H_2O$, 36.8 mg, $(NH_4)_6Mo_7O_{24}{\cdot}4H_2O$, 490 mg $ZnSO_4{\cdot}H_2O$ per L ddH_2O; autoclaved), 0.5 mL	15 g/L Plant Agar	(Sarkar *et al.*, 2019)

	iron solution (9.5 mg $FeCl_3 \cdot 6H_2O$ per L ddH_2O; filter-sterilized), 1 g yeast extract, 0.5 g peptone, 0.5 g tryptone, and 10 g glucose.		
1/10 PNM (*Hordeum vulgare* L.)	0.5 mM KNO_3, 0.367 mM KH_2PO_4, 0.144 mM K_2HPO_4, 2 mM $MgSO_4$ x H_2O, 0.2 mM $Ca(NO_3)_2$, 0.25% (v/v) Fe-EDTA (0.56% w/v $FeSO_4$ x $7H_2O$ and 0.8% w/v Na_2EDTA x $2H_2O$), 0.428 mM NaCl; pH-adjusted to 6.0 and buffered with 10 mM MES	For solid media, 0.4% (w/v) GELRITE (Duchefa) was added.	(Lahrmann *et al.*, 2013)

Plasmid vectors and primers

The plasmid vectors and primers used in this study are listed in **Tab. 5.2** and **Tab. 5.3** respectively.

Table 5.2 Plasmid vectors used in this thesis study

Plasmid	Purpose	Feature	Reference
pAGT564	Golden Gate Cloning	LacZ, empty vector	(Scheler *et al.*, 2016)
pAGT1020	Golden Gate Cloning	GGPPs	(Scheler *et al.*, 2016)
pAGT1023	Golden Gate Cloning	ATR1	(Scheler *et al.*, 2016)
pAGT7557	Protein expression in yeast	GGPPs:trHvCPS2	this thesis study
pAGT7558	Protein expression in yeast	GGPPs:trHvKSL4	this thesis study
pAGT7944	Protein expression in yeast	GGPPs:trHvCPS2:trHvKSL4:ATR1:HvCYP89E31	this thesis study
pAGT7945	Protein expression in yeast	GGPPs:trHvCPS2:trHvKSL4:ATR1:HvCYP99A66	this thesis study
pAGT7946	Protein expression in yeast	GGPPs:trHvCPS2:trHvKSL4:ATR1:HvCYP99A67	this thesis study
pAGT8835	Protein expression in yeast	GGPPs:trHvCPS2:trHvKSL4:ATR1:HvCYP99A68	this thesis study
pAGT7937	Protein expression in yeast	GGPPs:trHvCPS2:trHvKSL4:ATR1:HvCYP89E31: HvCYP99A66	this thesis study
pAGT8837	Protein expression in yeast	GGPPs:trHvCPS2:trHvKSL4:ATR1:HvCYP89E31: HvCYP99A68	this thesis study
pAGT8266	Protein expression in yeast	GGPPs:trHvCPS2:trHvKSL4:ATR1:HvCYP89E31: HvCYP99A66:HvCYP99A67	this thesis study
pAGT8768	Protein expression in yeast	ATR1:HvCYP89E31	this thesis study
pAGM19821	Golden Gate Cloning	trHMGR	AG Marillonnet
pAGT526	Golden Gate Cloning	cytGGPPs	AG Tissier
pAGM4731	transient expression in *N. benthamiana*	p35S:GFP:tOCS	AG Marillonnet
pAGT9112	transient expression in *N. benthamiana*	p35S:cytGGPPs:tOCS	this thesis study
pAGT9127	transient expression in *N. benthamiana*	p35S:trHvCPS2:tOCS	this thesis study
pAGT9128	transient expression in *N. benthamiana*	p35S:trHvKSL4:tOCS	this thesis study
pAGT9191	transient expression in *N. benthamiana*	p35S:trHvCYP89E31:tOCS	this thesis study
pAGT9192	transient expression in *N. benthamiana*	p35S:HvCYP99A66:tOCS	this thesis study

pAGT9193	transient expression in *N. benthamiana*	p35S:HvCYP99A67:tOCS	this thesis study
pAGT9194	transient expression in *N. benthamiana*	p35S:HvCYP99A68:tOCS	this thesis study
pAGT9110	transient expression in *N. benthamiana*	p35S:trHMGR:tOCS	this thesis study

Table 5.3 Primers used in this thesis study

Gene	Application	Direction	Sequence
GenBank accession no. M60175 (*HvUBIQUITIN*)	qPCR	Forward	ACCCTCGCCGACTACAACAT
		Reverse	CAGTAGTGGCGGTCGAAGTG
HORVU2Hr1G004540 (*HvKSL4*)	qPCR	Forward	GTTATCTCTGCGCTGCTGCC
		Reverse	GAGGATCCTCCCATTTCTCAGC
	genotyping	Forward	GATCGGGAGGCCAGGATAAG
		Reverse	CAGATCATAGTTGCGAATTAATGCAG
	truncate transit peptide	Forward	TTGGTCTCAACATAATGGCTTACGTTGAA TCTAGACC
		Reverse	TTGGTCTCAACAAACCAATTCGTTTTGAG ACAAAATG
HORVU2Hr1G004620 (*HvCPS2*)	qPCR	Forward	GCGTCTGCAGCCCATGAGA
		Reverse	GCGGTCTTCCTCCCTCTGC
	genotyping	Forward	GTTGCAGGTATGTTATTTATCAAAG
		Reverse	CAATTTTTTTCTGTTCAAATTTGGTATG
	truncate transit peptide	Forward	TTGGTCTCAACATAATGGTTTTGTCCTCTA AATCTCCA
		Reverse	TTGGTCTCAACAAGGGTTAACTTCGTAAC CATGTTG
HORVU2Hr1G004550 (*HvCYP89E31*)	qPCR	Forward	GCGTCTGCAGCCCATGAGA
		Reverse	GCGGTCTTCCTCCCTCTGC
HORVU2Hr1G004530 (*HvCYP99A67*)	qPCR	Forward	GCGATCATATCGGATATGTTCACG
		Reverse	TCTTGTTGTCAAAGGTACGACGC
HORVU2Hr1G004480 (*HvCYP99A66*)	qPCR	Forward	GTTCGTCGACGCCCTCACT
		Reverse	CCGTGAACATATCCAATATGATCG
BsTEF	qPCR	Forward	CGCCGTACCGGAAAGTCTG
		Reverse	GGCGAAACGACCAAGAGGA
hygromycin	genotyping	Forward	GCGATTGCTGATCCCCATGT
		Reverse	GGCGTCGGTTTCCACTATCG

5.2 Growth methods

Plant growth and fungal inoculation

Barley seeds were sterilized in 70% ethanol for 1 min, followed by washing with sterile distilled water and 1.5 h incubation in 12% sodium hypochlorite with 0.02% tween under continuous shaking. After 3 times 30 mins washing, the seeds were placed on wet filter paper in darkness and at room temperature for 4 days for germination. Four seedlings were transferred to 1/10 PNM (Plant Nutrition Medium, pH 6) in sterile glass jars (1 L, WECK) and grown in a day/night cycle of 16/8 h at 22/18 °C, 60% humidity

under 108 µmol m^{-2} s^{-1} light intensity. For seed propagation and screening for homozygous lines, plants were grown in a greenhouse under long-day conditions at 18-21 °C and 55-65% relative humidity.

For fungal inoculation assay, *B. sorokiniana* conidia were collected according to the procedures described in (Sarkar *et al.*, 2019). Briefly, Conidia of *Bs* were collected in distilled water from the 14-day-old agar plate. Spores were pellected by centrifugation at 4000 rpm for 10 mins, followed by 3 times of washing by sterile distilled water and diluted to a final concentration of 5000 spores/mL for inoculations on PNM medium. Barley roots were inoculated with 3 ml of *Bs* conidia (5000 spores/ml) per jar for 6 days. Sterile water was used as a mock treatment. Roots washed thoroughly and the corresponding medium were collected and snap-frozen in liquid nitrogen for other assays.

The wild-type *N. benthamiana*, plants were grown in a climate-controlled photo chamber under the following conditions, a day/night cycle of 16/8 h at 21/18 °C, 60% humidity under 100 µmol m^{-2} s^{-1} light intensity.

Bipolaris sorokiniana

Bipolaris sorokiniana (ND90Pr) were growth on CM medium with 1.5% agar in the dark at 28 °C.

Escherichia coli

For transformation assay, *E. coli* were cultured on LB agar medium at 37 °C for 16 h. In liquid medium, the culture was grown under continuous shaking at 200 rpm.

Agrobacterium rhizogenes

After transformation, Agrobacteria were cultured on LB plates at 28 °C for 3 days. In liquid medium, the culture was grown under continuous shaking at 180 rpm.

Saccharomyces cerevisiae

Yeast strains were cultured in YPD or SCU medium at 30 °C, with shaking at 250 rpm if liquid medium was used.

5.3 Bacteria and yeast transformation

Transformation of *E. coli*

100 or 200 ng of plasmid DNA or 15 µl ligation mix was added to the chemically competent cells and incubated on ice for 30 mins. The cells were then heat shocked for 90 s at 42 °C and them cooled on ice for 2 mins. The cells were revived for 1 h in SOC medium at 37 °C with shaking at 350 rpm. After revival, an aliquot of 50 µl was plated on LB agar plates containing suitable antibiotics and X-Gal for blue-white selection of constructs containing *LacZ* marker gene. Positive colonies were tested by restriction digestion of plasmid DNA.

Transformation of *A. rhizogenes*

An aliquot of electro-competent cells was thawed on ice for few mins and 200-500 ng (1 µl) of plasmid DNA was added to the thawed cells. The mixture was then added to a pre-chilled cuvette (VWR cuvette with 2 mm gap) and inserted into the cuvette arm of electroporator (Micropulser Electroporator, BioRad Laboratories GmbH, Munich, Germany). A pulse of 2.2 kV for approximately 5 ms was applied to cells, 250 µl LB was then added for the revival and then cultured in an Eppendorf tube at 28 °C for 2-3 h. After revival in LB, cells were plated on LB agar with appropriate antibiotics and grown for 2-3 days at 28 °C.

Transformation of *Saccharomyces cerevisiae*

Competent cells were prepared using monovalent cation lithium acetate method (LiAc). Yeast cells from a glycerol stock was streaked on YPD plate without antibiotic and grown for 2 days at 30 °C. A single colony was then used to inoculate 20 ml YPD medium and grown overnight with shaking at 30 °C. The primary culture with an OD_{600} of 4.5 was then used to inoculate 250 ml YPD medium and grown for 3-4 h until an OD_{600} of 0.9 was reached. The culture was then centrifuged at 4000 rpm for 10 min at 4 °C. The pelleted cells were resuspended in 50 ml sterile ddH_2O followed by centrifugation and resuspended in 1 ml transformation buffer (**Tab. 5.4**). For long-term storage, glycerol was added (15%) and aliquots of 25 µl were made. The aliquots were slowly frozen overnight in a Styrofoam box at –80 °C and later stored at –80 °C.

Lithium acetate (LiAc)-PEG method was used for yeast transformation. A 10 µl aliquot of salmon sperm DNA, which had been single stranded by heating at 95 °C for 10 mins, was briefly centrifuged and kept on ice. 300 ng plasmid DNA and 12 µl of competent cells were added and mixed. Next, 300 µl plating buffer (**Tab. 5.4**) was added and mixed carefully, followed by inoculation with vigorous shaking (600 rpm) at 30 °C for 30 mins. 5 µl of DMSO was add and mixed carefully, before the heat shock of 15 mins at 42 °C. After a brief span, the supernatant was removed as much as possible, and cells were resuspended in 100 µl sterile distill water and plated out on SCU agar plates. Plates were inoculated at 30 °C for 3-4 days.

Table 5.4 Components of yeast transformation buffer and plating buffer

Transformation buffer		**Plating buffer**	
Substances	Amount for 100 ml	Substances	Amount for 100 ml
Lithium Acetate (1 M), pH 7.5	10 ml	Lithium Acetate (1 M), pH 7.5	10 ml
TE (100 mM Tris, pH 7.5; 10 mM EDTA)	5 ml	TE (100 mM Tris, pH 7.5; 10 mM EDTA)	10 ml
ddH_2O	85 ml	50% PEG-3350	80 ml

Note: Solutions were filter sterilized and stored at room temperature.

5.4 Heterologous expression of diterpenoids

Heterologous expression of diterpenoids in yeast

Codon-optimized DNA sequences of *HvCPS2*, *HvKSL4* and four *HvCYPs* were synthesized by GeneArt Services (Invitrogen) for yeast expression. Each gene was further cloned into Golden Gate compatible yeast expression level 1 vector, together with a synthetic galactose-inducible promoter and a terminator. Different gene combinations were then assembled into a yeast expression level M vector by a 50-cycle restriction–ligation reaction with BpiI and T4-Ligase. Constructs were then transformed into *S. cerevisiae* strain INV*Sc*1 and plated out onto SCU selection medium. Three positive colonies were picked and inoculated into 5 ml SCU medium containing 2% of glucose and grown for 24 h at 30 °C with shaking. To induce protein expression, the cell pellet was resuspended in fresh SCU medium containing 2%

galactose. After another 24 h of growth, the whole culture was extracted with 2 ml n-hexane.

Transient expression in *Nicotiana benthamiana*

Transit peptides of protein HvCPS2 and HvKSL4 were predicted by the two online tools, ChloroP 1.1 (http://www.cbs.dtu.dk/services/ChloroP/) and LOCALIZER (http://localizer.csiro.au/). Truncated sequences without transit peptides of these two genes were generated by PCR reactions using designed primers and subsequently sequenced. The *HMG reductase*, *GGPPs*, *trHvCPS2*, *trHvKSL4* and four *HvCYPs* were cloned into T-DNA vectors (binary vector pL1F-1) driven by the 35S promoter and flanked by the Ocs terminator (Weber *et al.*, 2011b). The resulting T-DNA plasmids were transformed into *Agrobacterium tumefaciens* strain GV3101::pMP90 and plated out onto LB agar plates with appropriate antibiotics. Bacteria were harvested and resuspended in infiltration medium (10 mM $MgCl_2$, 10 mM MES, 20 µM acetosyringone, pH=5.6) after 48 h inoculation at 28 °C. To co-infiltrate several genes, each bacteria suspension was diluted to a final OD_{600} of 0.4, then all strains were mixed equally to an appropriate volume for infiltration. The suspension was infiltrated into the abaxial side of several leaves in three individual 4-week-old *N. benthamiana* plants using a syringe without needle. After treatment, the plants were cultivated in a climate controlled phytochamber for 4 days. Three leaf discs (9 mm diameter) per infiltrated spot were harvested and extracted by 2 ml n-hexane, followed by drying down under nitrogen flow and GC/LC-MS analysis.

5.5 Microsome isolation and *in vitro* enzyme assay

A protocol from the literature with modification was used for microsome isolation (Urban *et al.*, 1997; Scheler *et al.*, 2016). The construct carrying *HvCYP89E31* and *ATR1* were transformed into yeast strain INV*Sc*1. A single positive colony was picked to inoculate 5 ml of SCU medium with 2% glucose and grown for 24 h at 30 °C with shaking. The culture was then used to inoculate 100 ml of SCU medium with 2% glucose in a 500 ml flask at 30 °C for 24 h. The cells were then collected by centrifugation, resuspended in 100 ml fresh YPD medium with 2 % galactose to induce protein expression and inoculated under shaking for another 24 h at 30 °C. All the following steps were carried out at 4 °C. The cells were harvested by centrifugation

and resuspended in 30 ml of pre-chilled TEK buffer (50 mM Tris-HCl pH 7.5, 1 mM EDTA, 100 mM KCl), centrifuged again and resuspended in 2 ml TES buffer (50 mM Tris-HCl pH 7.5, 600 mM sorbitol, 10 g/L BSA, 1.5 mM β-mercaptoethanol) and transferred to a 50 ml tube. Acid-washed autoclaved 450–600 µm diameter glass beads were added into the tube until the surface of the cell suspension are reached. The suspension was shaken vigorously by hand for 1 min and returned back to ice for 1 min. This step was repeated four times. The glass beads were washed by 5 ml TES buffer three times, and the supernatant was collected and combined to a new tube, followed by centrifugation at 7,500 g for 10 min. The supernatant was transferred to ultracentrifugation tubes and centrifuged for 2 h at 100,000 g. The pellet was gently washed successively with 5 ml TES and 2.5 ml TEG buffer (50 mM Tris-HCl pH 7.5, 1 mM EDTA and 30% glycerol) after the supernatant was removed, then transferred to a Potter homogenizer with a spatula. 2 ml TEG buffer was added to the homogenizer and the pellet was carefully homogenized. 100 µl aliquots were transferred to 1.5 ml microtubes and stored at −80 °C until used.

In vitro CYP enzyme assays were performed in a 600 µl reaction volume, containing 40 µl of microsome preparation, 100 µM substrate, 1 mM NADPH, 50 mM sodium phosphate pH 7.4. The solution was incubated at 30 °C for 2 h with gentle shaking. Products were extracted with 1 ml n-hexane under strong agitation (vortex). After centrifugation, the organic phase was collected, then dried under a N2 stream and resuspended in 100 µl n-hexane for GC-MS analysis.

5.6 Purification of diterpenoids by silica gel chromatography or SPE

For the purification of hordediene, 1 L of yeast culture was grown and extracted with 1 L n-hexane. The raw extracts were dried in a rotary evaporator and resuspended in 4 ml n-hexane, then loaded into two properly conditioned SiOH SPE cartridges (500 mg, MACHEREY-NAGEL). The cartridges were then washed multiple times of 2 ml n-hexane. The breakthrough and washing fractions were collected. After drying down under nitrogen stream, an aliquot of each fraction was measured by GC-MS to check the purity of the product. Fractions with pure hordediene were combined (around 2 mg) and used for structure elucidation by NMR.

Hordetriene and more oxidized diterpenoids were first extracted from some liters of yeast culture. After concentration, the raw extracts were dissolved in 4 ml n-hexane and loaded into a pre-conditioned self-packed silica gel column (5 g, 15 mm X 100 mm). The column was then eluted by n-hexane and successively by 99:1, 98:2, 97:3, 96:4, 95:5 n-hexane: ethyl acetate solutions. For highly oxidized diterpenoids, **21**, for instance, up to 30% ethyl acetate in n-hexane was used for elution. The volume of each elution solution was 10 ml but the elution was separately collected into five 2 ml microtubes. An aliquot of each fraction was measured by GC/LC-MS and the fractions with pure product were combined and then used for NMR structure elucidation. The yield of hordetriene and other products was around 0.2 to 0.5 mg per liter culture.

Nuclear magnetic resonance (NMR) conditions

The following experiments and data analysis were performed by **Dr. Andrea Porzel** or **Dr. Pauline Stark**.

H, ^{13}C, 2D (^{1}H,^{1}H gDQCOSY; ^{1}H,^{1}H zTOCSY;^{1}H,^{1}H ROESYAD; ^{1}H,^{13}C gHSQCAD; 1H,^{13}C gHMBCAD), selective (^{1}H,^{1}H zTOCSY1D; ^{1}H,^{1}H ROESY1D), and band selective (^{1}H,^{13}C bsHMBC) NMR spectra were measured with an Agilent VNMRS 600 instrument at 599.83 MHz (^{1}H) and 150.84 MHz (^{13}C) using standard CHEMPACK 8.1 pulse sequences implemented in the VNMRJ 4.2A spectrometer software. TOCSY mixing time: 80 ms; ROESY mixing time: 300 ms; HSQC optimized for ^{1}JCH = 146 Hz; HMBC optimized for ^{n}JCH = 8 Hz. All spectra were obtained with C_6D_6 + 0.03% TMS as solvent at +25 °C. Chemical shifts were referenced to internal TMS (δ ^{1}H = 0 ppm) and internal C6D6 (δ ^{13}C = 128.0 ppm).

5.7 Metabolomics

Metabolites extraction from barley roots and PNM medium

100 mg (fresh weight) of frozen and cryo-ground root matter was extracted using 900 µl dichloromethane/ethanol (2:1, v/v) and 100 µl hydrochloric acid solution (pH 1.4). Extraction and duplicate removal of hydrophilic metabolites was achieved by 1 min FastPrep bead milling (FastPrep24, MP Biomedicals) followed by phase separation during centrifugation. For extraction 1.6 ml wall-reinforced cryo-tubes (Biozyme) each containing steel and glass beads were used. The upper aqueous phase was discarded

and replaced for a second round of bead mill extraction/centrifugation. Thereafter, the aqueous phase was removed and the lower organic phase was collected. Subsequently 600 ul tetrahydrofuran (THF) was used for exhaustive extraction (FastPrep). After centrifugation the organic THF extract was combined with the first extract and dried under a stream of N2.

Root exudates were extracted from 60 mL of gelrite media. For this, the gel was distributed into two 50 mL Falcon tubes. To each tube 5 ml ethyl acetate were added. The tubes were thoroughly shaken by hand and centrifuged. The upper phase (organic extract) was collected before fresh ethyl acetate was added for another two consecutive extractions. The combined extracts of three extraction rounds were combined and dried in a stream of N2.

GC-MS

Dried extracts were suspended in 200 µl n-hexane. The analysis of yeast and plant extracts was carried out using a Trace GC Ultra gas chromatograph (Thermo Scientific) coupled to an ATAS Optic 3 injector and an ISQ single quadrupole mass spectrometer (Thermo Scientific) with electron impact ionization. Chromatographic separation was performed on a ZB-5MS capillary column (30 m × 0.25 mm x 0.25 mm, Phenomenex) using splitless injection and an injection volume of 1 µl. The injection temperature rose from 60 °C to 250 °C with 7 °C s^{-1} and the flow rate of helium was 2 ml min^{-1}. The GC oven temperature ramp was as follows: 50 °C for 1 min, 50 to 300 °C with 7 °C min^{-1}, 300 to 330 °C with 20 °C min^{-1} and 330 °C for 5 min. Mass spectrometry was performed at 70 eV, in a full scan mode with m/z from 50 to 450. Data analysis was done with the device specific software Xcalibur (Thermo Scientific).

Some samples were analyzed on a ZB-5HT capillary column (30 m × 0.25 mm x 0.25 mm, Phenomenex) using splitless injection and an injection volume of 1 µl. The injection temperature rose from 130 °C to 280 °C with 5 °C s^{-1} and the flow rate of helium was 2 ml min^{-1}. The GC oven temperature ramp was as follows: 130 °C for 2 min, 130 to 250 °C with 8 °C min^{-1}, 250 to 310 °C with 10 °C min^{-1} and 310 °C for 5 min. MS spectra were acquired using the same parameters which are described above.

RP-UPLC-ESI-MS/MS

For UPLC-MS/MS analysis dried extracts were suspended in 180 µl 80% methanol/ 20% water. Separation of medium polar metabolites was performed on a Nucleoshell RP18 (2.1 × 150 mm, particle size 2.1 µm, Macherey & Nagel, GmbH, Düren, Germany) using a Waters ACQUITY UPLC System, equipped with a Binary Solvent Manager and Sample Manager (20 µl sample loop, partial loop injection mode, 5 µl injection volume, Waters GmbH Eschborn, Germany). Eluents A and B were aqueous 0.3 mmol/L NH4HCOO (adjusted to pH 3.5 with formic acid) and acetonitrile, respectively. Elution was performed isocratically for 2 min at 5% eluent B, from 2 to 19 min with a linear gradient to 95% B, from 19-21 min isocratically at 95% B, and from 21.01 min to 24 min at 5% B. The flow rate was set to 400 µl min^{-1} and the column temperature was maintained at 40 °C. Metabolites were detected by positive and negative electrospray ionization and mass spectrometry.

Mass spectrometric analysis of small molecules was performed by MS-TOF-SWATH-MS/MS (TripleToF 5600, AB Sciex GmbH, Darmstadt, Germany) operating in negative or positive ion mode and controlled by Analyst 1.7.1 software (AB Sciex GmbH, Darmstadt, Germany). The source operation parameters were as follows: ion spray voltage, −4500 V / +5500 V; nebulizing gas, 60 psi; source temperature 600 °C; drying gas, 70 psi; curtain gas, 35 psi. TripleToF instrument tuning and internal mass calibration were performed every 5 samples with the calibrant delivery system applying APCI negative or positive tuning solution (AB Sciex GmbH, Darmstadt, Germany), respectively.

TripleToF data acquisition was performed in MS^1-ToF mode and MS^2-SWATH mode. For MS^1 measurements, ToF masses were scanned between 65 and 1250 Dalton with an accumulation time of 50 ms and a collision energy of 10 V (−10 V). MS^2-SWATH experiments were divided into 26 Dalton segments of 20 ms accumulation time. Together the SWATH experiments covered the entire mass range from 65 to 1250 Dalton in 48 separate scan experiments, which allowed a cycle time of 1.1 s. Throughout all MS/MS scans a declustering potential of 35 V (or −35 V) was applied. Collision energies for all SWATH-MS/MS were set to 35 V (−35 V) and a collision energy spread of ±25 V, maximum sensitivity scanning, and elsewise default settings.

For some samples, mass spectrometric analysis of small molecules was performed by MS-TOF-IDA-MS/MS (ZenoTOF 7600, AB Sciex GmbH, Germany) operating in negative or positive ion mode and controlled by SCIEX OS software 2.1.6 (AB Sciex GmbH, Darmstadt, Germany). The source operation parameters were as follows: ion spray voltage, −4500 V / +5500 V; ion source gas 1, 60 psi; source temperature 600 °C; ion source gas 2, 70 psi; curtain gas, 35 psi; CAD gas 7. ZenoTOF instrument tuning and internal mass calibration were performed every 5 samples with the calibrant delivery system applying X500 ESI negative or positive calibration solution (AB Sciex GmbH, Germany), respectively.

ZenoTOF data acquisition was performed in MS^1-ToF mode and MS^2-IDA mode. For MS^1 measurements, ToF masses were scanned between 65 and 1500 Dalton with an accumulation time of 100 ms and a collision energy of 10 V (−10 V). MS^2-IDA experiments were performed using the following parameters: ToF mass range 65 to 1500; declustering potential of 80 (or −80 V) with a spread of 50; maximum candidate ions of 40 with an intensity threshold of 1000 cps; collision energy of 35 V (−35 V) with a spread of 25 V; Zeno threshold 20000 cps; accumulation time of 20 ms. Total scan time of one cycle for both MS^1 and MS^2 was 1.166 s.

5.8 Molecular biology methods

Golden gate modular cloning

Golden gate modular cloning (MoClo System) (Engler *et al.*, 2008; Weber *et al.*, 2011a) can assemble many DNA fragments in a single step with high efficiency. Golden gate system takes the ability of type IIs restriction endonucleases that cut outside of their recognition site sequence, allowing DNA fragments flanked by compatible restriction sites and overhangs to be digested and ligated easily. Since the ligated products lack the original type IIs restriction site it will not be re-digested in a second restriction ligation reaction. Four base pairs are placed distal to the cleavage site such that recognition sites are removed after digestion and only 4 base pair overhang remains, these overhangs are used to assemble multiple DNA fragments in a specific unidirectional manner.

Polymerase chain reaction (PCR)

PCR is used to synthesize new strand complementary to the template employing DNA polymerase and designed primers. A normal PCR cycle involves three basic steps: denaturation of template DNA fragment, annealing of complementary primers and elongation of DNA strand. The PCR reaction was performed in a thermocycler with heated lid (C1000 Touch™ Thermal Cycler, BioRad Laboratories GmbH, Germany). Different DNA polymerases were used depending on the downstream requirement of the PCR product. All PCR reactions were performed according to manufacturer's guidelines (**Tab. 5.5**, **Tab. 5.6**).

Table 5.5 Components of PCR reactions

KOD hot start polymerase		**highQu ALLin™ Taq DNA polymerase**	
Components	Amount	Components	Amount
10X Buffer	2.5 µl	MasterMix, 2X	12.5 µl
dNTPs (2 mM each)	2.5 µl	Forward primer (10 µM)	1 µl
Forward primer (10 µM)	0.75 µl	Reverse primer (10 µM)	1 µl
Reverse primer (10 µM)	0.75 µl	Template DNA	10-30 ng
Template DNA	10-30 ng	ddH_2O	Up to 25 µl
$MgSO_4$ (25 mM)	1.5 µl		
DNA polymerase (1U/µl)	1 µl		
ddH_2O	Up to 25 µl		

Table 5.6 Thermal programs of PCR reactions

Phase	**KOD hot start polymerase**		**highQu ALLinTM Taq DNA polymerase**		**No. of cycles**
Polymerase activation	95 °C	2 mins	95 °C	3 min	1
Denaturation	95 °C	20 s	95 °C	30 s	35
Annealing	Lowest primer Tm	20 s	55-65 °C	30 s	35
Extension	70 °C	20 s/Kb	72 °C	15 s/Kb	35
Final Extension	70 °C	2 mins	72 °C	5 mins	1

Agarose gel electrophoresis

PCR products were analyzed by electrophoretic separation in a 1% Agarose Gel which was prepared by dissolving Agarose (Roth, Karlsruhe, Germany) in 1x TAE buffer (40 mM Tris-HCl pH 7.6, 20 mM acetic acid, and 1 mM EDTA), followed by brief boiling.

Before casting the gel, one drop of ethidium bromide (EB, Roth) per 30 ml TAE buffer was added for DNA staining. Electrophoretic separation was performed at 100 V for 20-30 min depending on the size of the product. A gel documentation system (FUSION FX7, Germany) was used to visualize the DNA fragments in the gel. Depending on the purity of PCR products, either PCR purification or gel extraction were performed using kit Monarch® PCR & DNA Cleanup (New England BioLabs) or Monarch® DNA Gel Extraction (New England BioLabs) according to manufacturer's instructions.

Isolation of plasmid DNA

Plasmid DNA was isolated from a 5 ml overnight culture of *E. coli* using NucleoSpin® Plasmid EasyPure Kit (Macherey Nagel, Germany) according to manufacturer's instructions, the concentration was measured using Nanodrop and stored at -20 °C.

Isolation of genomic DNA

For genomic DNA isolation, 30-100 mg of frozen plant materials were homogenized to a fine powder using Retsch Beadmill (Retsch MM 400) and a steel bead of 7 mm at a frequency of 30 Hz for 1 min. Genomic DNA from frozen fine powder was extracted using NucleoSpin® Plant II kit (Macherey Nagel, Germany) according to manufacturer's guidelines and the concentration of DNA was measured using NanoDrop and stored at -20 °C.

Isolation of RNA

RNA was isolated from 30-100 mg of frozen plant material, grounded in liquid nitrogen by mortar and pestle. RNA isolation was performed using Spectrum™ Plant Total RNA-Kit (Sigma-Aldrich) according to manufacturer's instructions followed by DNase digestion using Ambion DNA-*free*™ DNA Removal kit (Invitrogen, Thermo Scientific, Germany). RNA concentration was determined using NanoDrop Spectrophotometer. RNA integrity and quality were analyzed either using agarose gel electrophoresis (1% Agarose). RNA was stored at - 80 °C.

cDNA synthesis of mRNA

Complementary DNA (cDNA) was synthesized from RNA templates using Protoscript II First-strand cDNA synthesis kit. 0.5 µg to 1 µg RNA in 10 µl reaction solution was

used as a template and mixed with 2 µl of $d(T)_{23}$ VN, 10 µl Proscript II Reaction Mix (2X) and 2 µl Proscript II Enzyme Mix (10X). Total 24 µl cDNA synthesis reaction mix was incubated at 42 °C for one hour and the reaction was inactivated by incubating at 80 °C for 5 min. For further usage, cDNA was stored at -20 °C.

Quantitative polymerase chain reaction (qPCR)

Gene expression analysis was performed using qPCR. The qPCR was performed using an instrument from CFX Connect Real-Time PCR System (Biorad Laboratories, Munich, Germany). EvaGreen qPCR Mix II (Bio&Sell, Germany) was used in combination with gene-specific primers. The PCR conditions were 95 °C for 15 min; 40 cycles of 95 °C for 15 s, 60 °C for 30 s; 95 °C for 10 s. The melting curve was measured from 65 °C to 95 °C with a step of 0.1 °C per second. Relative expression of targeted genes was calculated using delta Ct method (Livak & Schmittgen, 2001).

5.9 Hygromycin resistance test for barley leaves

Since hygromycin was used to select successful transformants, a biochemical assay to test the resistance to hygromycin using the leaf disc was performed to select transgene free plants from the CRISPR lines. Selected plants were further tested of the presence of T-DNA by PCR using primers binding to the DNA sequence of hygromycin.

Table 5.7 Solutions for hygromycin resistance test

Stock solutions	**Working solutions (amount for 20 ml)** (0.01% Tween 20 + 50 mg/l Hygromycin B in 1X MS)
1X MS liquid medium, pH 5.8 (4.3 g/l Murashige & Skoog Basal Salt Mixture/Duchafa)	20 ml
10% Tween 20	20 µl
50 mg/ml Hygromycin B (SIGMA)	20 µl

The assay was done using the protocol as follows. Microplate wells were filled with 200 µl of working solution. Leaf discs of young barley leaves (9 mm diameter) were cut and floated on the working solution. Two wells were reserved for wild-type leaf samples. The plate was sealed with the adhesive PCR film, and then was incubated at 24 °C in light cabinet (16 h light/8 h dark) for three to four days until the selection

pattern is clear. Hygromycin-sensitive leaves get bleached or brownish, while hygromycin-resistant leaves stay green.

5.10 Antifungal assay

To measure the growth curve of *Bs* in different concentrations of **21**, the following assay was performed. Microplate wells were filled with 200 µl of working solution with different concentration of **21** (**Tab. 5.8**). Each concentration was tested in five replications. After pipetting, the plate was inoculated at 28 °C in either an incubator or TECAN device (Tecan Group Ltd., Switzerland). The value of OD_{405} was measured by TECAN every half hour for 48 h.

Table 5.8 Working solution for antifungal assay

21 in Concontration (Final)	**21 stock** (20 mM in DMSO)	**DMSO**	**CM medium**	***Bs* Spores** ($3x10^5$/ml)
200 µM	10 µl	10 µl	880 µl	100 µl
100 µM	5 µl	15 µl	880 µl	100 µl
25 µM	1.25 µl	18.75 µl	880 µl	100 µl
0 µM	0	20 µl	880 µl	100 µl
Blank	0	20 µl	980 µl	0

Note: final concentrations of **21**: 0, 25, 100, 200 µM in CM medium with 2% DMSO.

To measure degraded metabolites, the following extraction protocol was used. The *Bs* culture was transferred from the wells to 2 ml Eppendorf tubes. Each sample was extracted by two times of 500 µl ethyl acetate, and the extractions were combined in the end. During extraction, the ultrasonic bath and vertex device were used to improve extraction efficiency. The extracts were then analyzed by LC-MS/MS.

5.11 Synteny analysis

The synteny analysis was performed by MCScanX (Wang, Y *et al.*, 2012), employing the parameters '-s 5 -w 0 -m 15'. The orthologs were identified by blastp program, using the parameters 'E-value 1e-10; num of best hits 5'. The plot for synteny and microsynteny was generated by TBtools (Chen *et al.*, 2020) or MCScan (Python version) (Tang *et al.*, 2008) respectively. The version of genomes used for the analysis

is IRGSP-1.0 of rice, MorexV1 and MorexV2 of barley, and IWGSC RefSeq v1.0 of wheat.

6. References

Ahn S, Anderson JA, Sorrells ME, Tanksley SD. 1993. Homoeologous relationships of rice, wheat and maize chromosomes. *Molecular and General Genetics MGG* **241**(5): 483-490.

Ahuja I, Kissen R, Bones AM. 2012. Phytoalexins in defense against pathogens. *Trends in Plant Science* **17**(2): 73-90.

Ai H-L, Shi B-B, Li W, He J, Li Z-H, Feng T, Liu J-K. 2022. Bipolarithizole A, an antifungal phenylthiazole-sativene merosesquiterpenoid from the potato endophytic fungus Bipolaris eleusines. *Organic Chemistry Frontiers* **9**(7): 1814-1819.

Akiyama K, Matsuzaki K-i, Hayashi H. 2005. Plant sesquiterpenes induce hyphal branching in arbuscular mycorrhizal fungi. *Nature* **435**(7043): 824-827.

Al-Sadi AM. 2016. Variation in resistance to spot blotch and the aggressiveness of Bipolaris sorokiniana on barley and wheat cultivars. *Journal of Plant Pathology* **98**(1): 97-103.

Al-Sadi AM. 2021. Bipolaris sorokiniana-Induced Black Point, Common Root Rot, and Spot Blotch Diseases of Wheat: A Review. *Frontiers in Cellular and Infection Microbiology* **11**.

Anderson JP, Badruzsaufari E, Schenk PM, Manners JM, Desmond OJ, Ehlert C, Maclean DJ, Ebert PR, Kazan K. 2004. Antagonistic Interaction between Abscisic Acid and Jasmonate-Ethylene Signaling Pathways Modulates Defense Gene Expression and Disease Resistance in Arabidopsis. *The Plant Cell* **16**(12): 3460-3479.

Arkowitz RA. 2009. Chemical gradients and chemotropism in yeast. *Cold Spring Harbor perspectives in biology* **1**(2): a001958.

Armero J, Requejo R, Jorrín J, López-Valbuena R, Tena M. 2001. Release of phytoalexins and related isoflavonoids from intact chickpea seedlings elicited with reduced glutathione at root level. *Plant Physiology and Biochemistry* **39**(9): 785-795.

Ashour M, Wink M, Gershenzon J 2010. Biochemistry of Terpenoids: Monoterpenes, Sesquiterpenes and Diterpenes. *Annual Plant Reviews Volume 40: Biochemistry of Plant Secondary Metabolism*, 258-303.

Asselbergh B, De Vleesschauwer D, Höfte M. 2008. Global Switches and Fine-Tuning—ABA Modulates Plant Pathogen Defense. *Molecular Plant-Microbe Interactions* **21**(6): 709-719.

Atkinson NJ, Urwin PE. 2012. The interaction of plant biotic and abiotic stresses: from genes to the field. *Journal of Experimental Botany* **63**(10): 3523-3543.

Ayer WA, Khan AQ. 1996. Zythiostromic acids, diterpenoids from an antifungal Zythiostroma species associated with aspen. *Phytochemistry* **42**(6): 1647-1652.

Bamji SF, Corbitt C. 2017. Glyceollins: Soybean phytoalexins that exhibit a wide range of health-promoting effects. *Journal of Functional Foods* **34**: 98-105.

Banerjee A, Hamberger B. 2018. P450s controlling metabolic bifurcations in plant terpene specialized metabolism. *Phytochemistry Reviews* **17**(1): 81-111.

Bathe U, Tissier A. 2019. Cytochrome P450 enzymes: a driving force of plant diterpene diversity. *Phytochemistry* **161**: 149-162.

Bednarek P, Piślewska-Bednarek M, Ver Loren van Themaat E, Maddula RK, Svatoš A, Schulze-Lefert P. 2011. Conservation and clade-specific

diversification of pathogen-inducible tryptophan and indole glucosinolate metabolism in Arabidopsis thaliana relatives. *New Phytol* **192**(3): 713-726.

Beier S, Himmelbach A, Colmsee C, Zhang X-Q, Barrero RA, Zhang Q, Li L, Bayer M, Bolser D, Taudien S, et al. 2017. Construction of a map-based reference genome sequence for barley, Hordeum vulgare L. *Scientific Data* **4**(1): 170044.

Beier S, Himmelbach A, Colmsee C, Zhang XQ, Barrero RA, Zhang Q, Li L, Bayer M, Bolser D, Taudien S, et al. 2017. Construction of a map-based reference genome sequence for barley, Hordeum vulgare L. *Sci Data* **4**: 170044.

Berenbaum M, Neal JJ. 1985. Synergism between myristicin and xanthotoxin, a naturally cooccurring plant toxicant. *Journal of Chemical Ecology* **11**(10): 1349-1358.

Bertani G. 1951. Studies on lysogenesis. I. The mode of phage liberation by lysogenic Escherichia coli. *J Bacteriol* **62**(3): 293-300.

Bouizgarne B, El-Maarouf-Bouteau H, Frankart C, Reboutier D, Madiona K, Pennarun AM, Monestiez M, Trouverie J, Amiar Z, Briand J, et al. 2006. Early physiological responses of Arabidopsis thaliana cells to fusaric acid: toxic and signalling effects. *New Phytol* **169**(1): 209-218.

Browne LM, Conn KL, Ayert WA, Tewari JP. 1991. The camalexins: New phytoalexins produced in the leaves of camelina sativa (cruciferae). *Tetrahedron* **47**(24): 3909-3914.

Brückner K, Božić D, Manzano D, Papaefthimiou D, Pateraki I, Scheler U, Ferrer A, de Vos RCH, Kanellis AK, Tissier A. 2014. Characterization of two genes for the biosynthesis of abietane-type diterpenes in rosemary (Rosmarinus officinalis) glandular trichomes. *Phytochemistry* **101**: 52-64.

Bulgarelli D, Garrido-Oter R, Münch PC, Weiman A, Dröge J, Pan Y, McHardy AC, Schulze-Lefert P. 2015. Structure and function of the bacterial root microbiota in wild and domesticated barley. *Cell Host Microbe* **17**(3): 392-403.

Buscaill P, Chandrasekar B, Sanguankiattichai N, Kourelis J, Kaschani F, Thomas EL, Morimoto K, Kaiser M, Preston GM, Ichinose Y, et al. 2019. Glycosidase and glycan polymorphism control hydrolytic release of immunogenic flagellin peptides. *Science* **364**(6436).

C. Pinto A, L. Patitucci M, H.T. Zocher D, Kelecom A. 1985. Absolute configuration of four cleistanthane diterpenes from velloziaceae. *Phytochemistry* **24**(10): 2345-2347.

Camagna M, Ojika M, Takemoto D. 2020. Detoxification of the solanaceous phytoalexins rishitin, lubimin, oxylubimin and solavetivone via a cytochrome P450 oxygenase. *Plant Signaling & Behavior* **15**(2): 1707348.

Cao MJ, Zhang YL, Liu X, Huang H, Zhou XE, Wang WL, Zeng A, Zhao CZ, Si T, Du J, et al. 2017. Combining chemical and genetic approaches to increase drought resistance in plants. *Nat Commun* **8**(1): 1183.

Cartwright D, Langcake P, Pryce RJ, Leworthy DP, Ride JP. 1977. Chemical activation of host defence mechanisms as a basis for crop protection. *Nature* **267**(5611): 511-513.

Chen C, Chen H, Zhang Y, Thomas HR, Frank MH, He Y, Xia R. 2020. TBtools: An Integrative Toolkit Developed for Interactive Analyses of Big Biological Data. *Molecular Plant* **13**(8): 1194-1202.

Chen F, Tholl D, Bohlmann J, Pichersky E. 2011. The family of terpene synthases in plants: a mid-size family of genes for specialized metabolism that is highly diversified throughout the kingdom. *The Plant Journal* **66**(1): 212-229.

Cho M-H, Lee S-W. 2015. Phenolic Phytoalexins in Rice: Biological Functions and Biosynthesis. *International Journal of Molecular Sciences* **16**(12): 29120-29133.

Chomel M, Guittonny-Larchevêque M, Fernandez C, Gallet C, DesRochers A, Paré D, Jackson BG, Baldy V. 2016. Plant secondary metabolites: a key driver of litter decomposition and soil nutrient cycling. *Journal of Ecology* **104**(6): 1527-1541.

Chripkova M, Drutovic D, Pilatova M, Mikes J, Budovska M, Vaskova J, Broggini M, Mirossay L, Mojzis J. 2014. Brassinin and its derivatives as potential anticancer agents. *Toxicol In Vitro* **28**(5): 909-915.

Christenhusz MJ, Byng JW. 2016. The number of known plants species in the world and its annual increase. *Phytotaxa* **261**(3): 201–217-201–217.

Ciuffetti LM, VanEtten HD 1996. Virulence of a Pisatin Demethylase-Deficient: Nectria.

Consortium TU. 2020. UniProt: the universal protein knowledgebase in 2021. *Nucleic Acids Research* **49**(D1): D480-D489.

Cox SD, Mann CM, Markham JL, Bell HC, Gustafson JE, Warmington JR, Wyllie SG. 2000. The mode of antimicrobial action of the essential oil of Melaleuca alternifolia (tea tree oil). *Journal of Applied Microbiology* **88**(1): 170-175.

Cruickshank IAM, Perrin DR. 1960. Isolation of a Phytoalexin from Pisum sativum L. *Nature* **187**(4739): 799-800.

Dangl JL, Jones JDG. 2001. Plant pathogens and integrated defence responses to infection. *Nature* **411**(6839): 826-833.

Dawson IK, Russell J, Powell W, Steffenson B, Thomas WTB, Waugh R. 2015. Barley: a translational model for adaptation to climate change. *New Phytologist* **206**(3): 913-931.

De La Peña R, Sattely ES. 2021. Rerouting plant terpene biosynthesis enables momilactone pathway elucidation. *Nature Chemical Biology* **17**(2): 205-212.

Desjardins AE, Matthews DE, Vanetten HD. 1984. Solubilization and Reconstitution of Pisatin Demethylase, a Cytochrome P-450 from the Pathogenic Fungus Nectria haematococca 1. *Plant Physiology* **75**(3): 611-616.

Desmedt W, Kudjordjie EN, Chavan SN, Zhang J, Li R, Yang B, Nicolaisen M, Mori M, Peters RJ, Vanholme B, et al. 2022. Rice diterpenoid phytoalexins are involved in defence against parasitic nematodes and shape rhizosphere nematode communities. *New Phytol* **235**(3): 1231-1245.

Ding Y, Murphy KM, Poretsky E, Mafu S, Yang B, Char SN, Christensen SA, Saldivar E, Wu M, Wang Q, et al. 2019. Multiple genes recruited from hormone pathways partition maize diterpenoid defences. *Nature Plants* **5**(10): 1043-1056.

dos Santos IBF, Ribeiro LAF, Araújo FM, Ribeiro PR. 2021. Cleistanthane diterpenoids from the resin of Vellozia pyrantha A.A.Conc and their chemotaxonomic significance. *Biochemical Systematics and Ecology* **94**: 104216.

Dudareva N, Klempien A, Muhlemann JK, Kaplan I. 2013. Biosynthesis, function and metabolic engineering of plant volatile organic compounds. *New Phytologist* **198**(1): 16-32.

Ejike CECC, Gong M, Udenigwe CC. 2013. Phytoalexins from the Poaceae: Biosynthesis, function and prospects in food preservation. *Food Research International* **52**(1): 167-177.

Engler C, Kandzia R, Marillonnet S. 2008. A one pot, one step, precision cloning method with high throughput capability. *PLoS One* **3**(11): e3647.

Escudero-Martinez C, Coulter M, Alegria Terrazas R, Foito A, Kapadia R, Pietrangelo L, Maver M, Sharma R, Aprile A, Morris J, et al. 2022. Identifying plant genes shaping microbiota composition in the barley rhizosphere. *Nature Communications* **13**(1): 3443.

Estévez JM, Cantero A, Reindl A, Reichler S, León P. 2001. 1-Deoxy-d-xylulose-5-phosphate Synthase, a Limiting Enzyme for Plastidic Isoprenoid Biosynthesis in Plants. *Journal of Biological Chemistry* **276**(25): 22901-22909.

Estévez JM, Cantero A, Romero C, Kawaide H, Jiménez LF, Kuzuyama T, Seto H, Kamiya Y, León P. 2000. Analysis of the Expression of CLA1, a Gene That Encodes the 1-Deoxyxylulose 5-Phosphate Synthase of the 2-C-Methyl-d-Erythritol-4-Phosphate Pathway in Arabidopsis1. *Plant Physiology* **124**(1): 95-104.

Falara V, Pichersky E, Kanellis AK. 2010. A Copal-8-ol Diphosphate Synthase from the Angiosperm Cistus creticus subsp. creticus Is a Putative Key Enzyme for the Formation of Pharmacologically Active, Oxygen-Containing Labdane-Type Diterpenes. *Plant Physiology* **154**(1): 301-310.

Farrow SC, Facchini PJ. 2014. Functional diversity of 2-oxoglutarate/Fe (II)-dependent dioxygenases in plant metabolism. *Frontiers in Plant Science* **5**: 524.

Fedoroff NV, Battisti DS, Beachy RN, Cooper PJ, Fischhoff DA, Hodges CN, Knauf VC, Lobell D, Mazur BJ, Molden D, et al. 2010. Radically rethinking agriculture for the 21st century. *Science* **327**(5967): 833-834.

Ferreira MC, Cantrell CL, Duke SO, Ali A, Rosa LH. 2017. New Pesticidal Diterpenoids from Vellozia gigantea (Velloziaceae), an Endemic Neotropical Plant Living in the Endangered Brazilian Biome Rupestrian Grasslands. *Molecules* **22**(1): 175.

Fewell AM, Roddick JG. 1993. Interactive antifungal activity of the glycoalkaloids α-solanine and α-chaconine. *Phytochemistry* **33**(2): 323-328.

Finn RD, Coggill P, Eberhardt RY, Eddy SR, Mistry J, Mitchell AL, Potter SC, Punta M, Qureshi M, Sangrador-Vegas A. 2016. The Pfam protein families database: towards a more sustainable future. *Nucleic acids research* **44**(D1): D279-D285.

Fuchs A, de Vries FW, Landheer CA, van Veldhuizen A. 1980. 3-Hydroxymaackiainisoflavan, a pisatin metabolite produced by Fusarium oxysporum f. sp. pisi. *Phytochemistry* **19**(5): 917-919.

Gao Y, Honzatko RB, Peters RJ. 2012. Terpenoid synthase structures: a so far incomplete view of complex catalysis. *Natural product reports* **29**(10): 1153-1175.

Gershenzon J, Dudareva N. 2007. The function of terpene natural products in the natural world. *Nature Chemical Biology* **3**(7): 408-414.

Goh YX, Jalil J, Lam KW, Husain K, Premakumar CM. 2022. Genistein: a review on its anti-inflammatory properties. *Frontiers in Pharmacology* **13**: 820969.

Gol L, Haraldsson EB, von Korff M. 2020. Ppd-H1 integrates drought stress signals to control spike development and flowering time in barley. *Journal of Experimental Botany* **72**(1): 122-136.

Guillet G, Bélanger A, Arnason JT. 1998. Volatile monoterpenes in porophyllum gracile and p. ruderale (asteraceae): identification, localization and insecticidal synergism with α-terthienyl. *Phytochemistry* **49**(2): 423-429.

Gull A, Lone AA, Wani NUI. 2019. Biotic and abiotic stresses in plants. *Abiotic and biotic stress in plants*: 1-19.

Guo J, Ma X, Cai Y, Ma Y, Zhan Z, Zhou YJ, Liu W, Guan M, Yang J, Cui G, et al. 2016. Cytochrome P450 promiscuity leads to a bifurcating biosynthetic pathway for tanshinones. *New Phytologist* **210**(2): 525-534.

Gupta BK, Sahoo KK, Ghosh A, Tripathi AK, Anwar K, Das P, Singh AK, Pareek A, Sopory SK, Singla-Pareek SL. 2018. Manipulation of glyoxalase pathway confers tolerance to multiple stresses in rice. *Plant Cell Environ* **41**(5): 1186-1200.

Hadwiger LA, Schwochau ME. 1971. Ultraviolet Light-induced Formation of Pisatin and Phenylalanine Ammonia Lyase. *Plant Physiol* **47**(4): 588-590.

Han G-Z. 2019. Origin and evolution of the plant immune system. *New Phytologist* **222**(1): 70-83.

Hanahan D. 1983. Studies on transformation of Escherichia coli with plasmids. *J Mol Biol* **166**(4): 557-580.

Hartmann T 1996. Diversity and variability of plant secondary metabolism: a mechanistic view. In: Städler E, Rowell-Rahier M, Bauer R eds. *Proceedings of the 9th International Symposium on Insect-Plant Relationships*. Dordrecht: Springer Netherlands, 177-188.

Hartmann T. 2007. From waste products to ecochemicals: Fifty years research of plant secondary metabolism. *Phytochemistry* **68**(22): 2831-2846.

Hayashi K-i, Kawaide H, Notomi M, Sakigi Y, Matsuo A, Nozaki H. 2006. Identification and functional analysis of bifunctional ent-kaurene synthase from the moss Physcomitrella patens. *FEBS Letters* **580**(26): 6175-6181.

He J, Yang M-S, Wang W-X, Li Z-H, Elkhateeb WAM, Wen T-C, Ai H-L, Feng T. 2019. Anti-phytopathogenic sesquiterpenoid-xanthone adducts from potato endophytic fungus Bipolaris eleusines. *RSC Advances* **9**(1): 128-131.

Hedden P, Kamiya Y. 1997. Gibberellin biosynthesis: enzymes, genes and their regulation. *Annual review of plant biology* **48**(1): 431-460.

Herde M, Gärtner K, Köllner TG, Fode B, Boland W, Gershenzon J, Gatz C, Tholl D. 2008. Identification and Regulation of TPS04/GES, an Arabidopsis Geranyllinalool Synthase Catalyzing the First Step in the Formation of the Insect-Induced Volatile C16-Homoterpene TMTT. *The Plant Cell* **20**(4): 1152-1168.

Hou S, Wolinska KW, Hacquard S. 2021. Microbiota-root-shoot-environment axis and stress tolerance in plants. *Curr Opin Plant Biol* **62**: 102028.

Huang AC, Jiang T, Liu Y-X, Bai Y-C, Reed J, Qu B, Goossens A, Nützmann H-W, Bai Y, Osbourn A. 2019. A specialized metabolic network selectively modulates Arabidopsis root microbiota. *Science* **364**(6440): eaau6389.

Huffaker A, Kaplan F, Vaughan MM, Dafoe NJ, Ni X, Rocca JR, Alborn HT, Teal PEA, Schmelz EA. 2011. Novel Acidic Sesquiterpenoids Constitute a Dominant Class of Pathogen-Induced Phytoalexins in Maize. *Plant Physiology* **156**(4): 2082-2097.

Imai T, Ohashi Y, Mitsuhara I, Seo S, Toshima H, Hasegawa M. 2012. Identification of a Degradation Intermediate of the Momilactone A Rice Phytoalexin by the Rice Blast Fungus. *Bioscience, Biotechnology, and Biochemistry* **76**(2): 414-416.

Inoue Y, Sakai M, Yao Q, Tanimoto Y, Toshima H, Hasegawa M. 2013. Identification of a novel casbane-type diterpene phytoalexin, ent-10-oxodepressin, from rice leaves. *Biosci Biotechnol Biochem* **77**(4): 760-765.

Inoue Y, Shiraishi A, Hada T, Hirose K, Hamashima H, Shimada J. 2004. The antibacterial effects of terpene alcohols on Staphylococcus aureus and their mode of action. *FEMS Microbiology Letters* **237**(2): 325-331.

Ishihara A, Hashimoto Y, Tanaka C, Dubouzet JG, Nakao T, Matsuda F, Nishioka T, Miyagawa H, Wakasa K. 2008. The tryptophan pathway is involved in the defense responses of rice against pathogenic infection via serotonin production. *The Plant Journal* **54**(3): 481-495.

Jansson H-B, Johansson T, Nordbring-Hertz B, Tunlid A, Odham G. 1988. Chemotropic growth of germ-tubes of Cochliobolus sativus to barley roots or root exudates. *Transactions of the British Mycological Society* **90**(4): 647-650.

Jeandet P, Clément C, Courot E, Cordelier S. 2013. Modulation of phytoalexin biosynthesis in engineered plants for disease resistance. *Int J Mol Sci* **14**(7): 14136-14170.

Jh D. 2015. An Overview of Plant Immunity. *Journal of Plant Pathology & Microbiology* **6**(11).

Jiang S-Y, Jin J, Sarojam R, Ramachandran S. 2019. A Comprehensive Survey on the Terpene Synthase Gene Family Provides New Insight into Its Evolutionary Patterns. *Genome Biology and Evolution* **11**(8): 2078-2098.

Jones JDG, Dangl JL. 2006. The plant immune system. *Nature* **444**(7117): 323-329.

Jordan MA, Wilson L. 2004. Microtubules as a target for anticancer drugs. *Nature Reviews Cancer* **4**(4): 253-265.

Karre S, Kumar A, Dhokane D, Kushalappa AC. 2017. Metabolo-transcriptome profiling of barley reveals induction of chitin elicitor receptor kinase gene (HvCERK1) conferring resistance against Fusarium graminearum. *Plant Molecular Biology* **93**(3): 247-267.

Karunanithi PS, Zerbe P. 2019. Terpene synthases as metabolic gatekeepers in the evolution of plant terpenoid chemical diversity. *Frontiers in plant science* **10**: 1166.

Kasahara H, Hanada A, Kuzuyama T, Takagi M, Kamiya Y, Yamaguchi S. 2002. Contribution of the Mevalonate and Methylerythritol Phosphate Pathways to the Biosynthesis of Gibberellins in Arabidopsis. *Journal of Biological Chemistry* **277**(47): 45188-45194.

Kaufman TS, Mischne MP, Gonzalez-Sierra M, Ruveda EA. 1987. Synthesis and 13C nuclear magnetic resonance spectral analysis of some diterpenoids related to the cleistanthane type hydrocarbon isolated from Amphibolis antarctica. *Canadian journal of chemistry* **65**(9): 2024-2026.

Kitaoka N, Wu Y, Xu M, Peters RJ. 2015. Optimization of recombinant expression enables discovery of novel cytochrome P450 activity in rice diterpenoid biosynthesis. *Appl Microbiol Biotechnol* **99**(18): 7549-7558.

Kitaoka N, Wu Y, Zi J, Peters RJ. 2016. Investigating inducible short-chain alcohol dehydrogenases/reductases clarifies rice oryzalexin biosynthesis. *The plant journal* **88**(2): 271-279.

Kodama O, Miyakawa J, Akatsuka T, Kiyosawa S. 1992. Sakuranetin, a flavanone phytoalexin from ultraviolet-irradiated rice leaves. *Phytochemistry* **31**(11): 3807-3809.

Koga J, Kubota H, Gomi S, Umemura K, Ohnishi M, Kono T. 2006. Cholic Acid, a Bile Acid Elicitor of Hypersensitive Cell Death, Pathogenesis-Related Protein Synthesis, and Phytoalexin Accumulation in Rice. *Plant Physiology* **140**(4): 1475-1483.

Koga J, Ogawa N, Yamauchi T, Kikuchi M, Ogasawara N, Shimura M. 1997. Functional moiety for the antifungal activity of phytocassane E, a diterpene phytoalexin from rice. *Phytochemistry* **44**(2): 249-253.

Koga J, Shimura M, Oshima K, Ogawa N, Yamauchi T, Ogasawara N. 1995. Phytocassanes A, B, C and D, novel diterpene phytoalexins from rice, Oryza sativa L. *Tetrahedron* **51**(29): 7907-7918.

Koncz C, Schell J. 1986. The promoter of TL-DNA gene 5 controls the tissue-specific expression of chimaeric genes carried by a novel type of Agrobacterium binary vector. *Molecular and General Genetics MGG* **204**(3): 383-396.

Kumar J, Schäfer P, Hückelhoven R, Langen G, Baltruschat H, Stein E, Nagarajan S, Kogel K-H. 2002. Bipolaris sorokiniana, a cereal pathogen of global concern: cytological and molecular approaches towards better control. *Molecular Plant Pathology* **3**(4): 185-195.

Kumar S, Stecher G, Li M, Knyaz C, Tamura K. 2018. MEGA X: Molecular Evolutionary Genetics Analysis across Computing Platforms. *Mol Biol Evol* **35**(6): 1547-1549.

Lahrmann U, Ding Y, Banhara A, Rath M, Hajirezaei MR, Döhlemann S, von Wirén N, Parniske M, Zuccaro A. 2013. Host-related metabolic cues affect colonization strategies of a root endophyte. *Proceedings of the National Academy of Sciences* **110**(34): 13965-13970.

Laule O, Fürholz A, Chang H-S, Zhu T, Wang X, Heifetz PB, Gruissem W, Lange M. 2003. Crosstalk between cytosolic and plastidial pathways of isoprenoid biosynthesis in Arabidopsis thaliana. *Proceedings of the National Academy of Sciences* **100**(11): 6866-6871.

Levin David E. 2005. Cell Wall Integrity Signaling in Saccharomyces cerevisiae. *Microbiology and Molecular Biology Reviews* **69**(2): 262-291.

Li J, Halitschke R, Li D, Paetz C, Su H, Heiling S, Xu S, Baldwin IT. 2021. Controlled hydroxylations of diterpenoids allow for plant chemical defense without autotoxicity. *Science* **371**(6526): 255-260.

Li L, Chen X, Ma C, Wu H, Qi S. 2016. Piriformospora indica requires kaurene synthase activity for successful plant colonization. *Plant Physiology and Biochemistry* **102**: 151-160.

Li Y-Y, Tan X-M, Wang Y-D, Yang J, Zhang Y-G, Sun B-D, Gong T, Guo L-P, Ding G. 2020. Bioactive seco-Sativene Sesquiterpenoids from an Artemisia desertorum Endophytic Fungus, Cochliobolus sativus. *Journal of Natural Products* **83**(5): 1488-1494.

Li Z-H, Ai H-L, Yang M-S, He J, Feng T. 2018. Bioactive sativene sesquiterpenoids from cultures of the endophytic fungus Bipolaris eleusines. *Phytochemistry Letters* **27**: 87-89.

Liang J, Merrill AT, Laconsay CJ, Hou A, Pu Q, Dickschat JS, Tantillo DJ, Wang Q, Peters RJ. 2022. Deceptive Complexity in Formation of Cleistantha-8,12-diene. *Organic Letters* **24**(14): 2646-2649.

Liang J, Shen Q, Wang L, Liu J, Fu J, Zhao L, Xu M, Peters RJ, Wang Q. 2021. Rice contains a biosynthetic gene cluster associated with production of the casbane-type diterpenoid phytoalexin ent-10-oxodepressin. *New Phytologist* **231**(1): 85-93.

Liu H, Du Y, Chu H, Shih CH, Wong YW, Wang M, Chu IK, Tao Y, Lo C. 2010. Molecular Dissection of the Pathogen-Inducible 3-Deoxyanthocyanidin Biosynthesis Pathway in Sorghum. *Plant and Cell Physiology* **51**(7): 1173-1185.

Liu X, Grabherr HM, Willmann R, Kolb D, Brunner F, Bertsche U, Kuhner D, Franz-Wachtel M, Amin B, Felix G, et al. 2014. Host-induced bacterial cell wall decomposition mediates pattern-triggered immunity in Arabidopsis. *Elife* **3**.

Liu Y, Balcke GU, Porzel A, Mahdi L, Scherr-Henning A, Bathe U, Zuccaro A, Tissier A. 2021. A barley gene cluster for the biosynthesis of diterpenoid phytoalexins. *bioRxiv*: 2021.2005.2021.445084.

Livak KJ, Schmittgen TD. 2001. Analysis of Relative Gene Expression Data Using Real-Time Quantitative PCR and the 2−ΔΔCT Method. *Methods* **25**(4): 402-408.

Lo S-CC, De Verdier K, Nicholson RL. 1999. Accumulation of 3-deoxyanthocyanidin phytoalexins and resistance to Colletotrichum sublineolum in sorghum. *Physiological and Molecular Plant Pathology* **55**(5): 263-273.

Lo SC, Weiergang I, Bonham C, Hipskind J, Wood K, Nicholson RL. 1996. Phytoalexin accumulation in sorghum: Identification of a methyl ether of luteolinidin. *Physiological and Molecular Plant Pathology* **49**(1): 21-31.

Long RM, Lagisetti C, Coates RM, Croteau RB. 2008. Specificity of the N-benzoyl transferase responsible for the last step of Taxol biosynthesis. *Archives of Biochemistry and Biophysics* **477**(2): 384-389.

Lugtenberg B, Kamilova F. 2009. Plant-growth-promoting rhizobacteria. *Annu Rev Microbiol* **63**: 541-556.

Luna E, Pastor V, Robert J, Flors V, Mauch-Mani B, Ton J. 2011. Callose Deposition: A Multifaceted Plant Defense Response. *Molecular Plant-Microbe Interactions* **24**(2): 183-193.

Lv J-J, Yu S, Xin Y, Zhu H-T, Wang D, Cheng R-R, Yang C-R, Xu M, Zhang Y-J. 2015. Stereochemistry of cleistanthane diterpenoid glucosides from Phyllanthus emblica. *RSC Advances* **5**(37): 29098-29107.

Mahdi LK, Miyauchi S, Uhlmann C, Garrido-Oter R, Langen G, Wawra S, Niu Y, Guan R, Robertson-Albertyn S, Bulgarelli D, et al. 2022. The fungal root endophyte Serendipita vermifera displays inter-kingdom synergistic beneficial effects with the microbiota in Arabidopsis thaliana and barley. *The ISME Journal* **16**(3): 876-889.

Mahmoud SS, Croteau RB. 2001. Metabolic engineering of essential oil yield and composition in mint by altering expression of deoxyxylulose phosphate reductoisomerase and menthofuran synthase. *Proceedings of the National Academy of Sciences* **98**(15): 8915-8920.

Mascher M, Wicker T, Jenkins J, Plott C, Lux T, Koh CS, Ens J, Gundlach H, Boston LB, Tulpová Z, et al. 2021. Long-read sequence assembly: a technical evaluation in barley. *The Plant Cell* **33**(6): 1888-1906.

Massalha H, Korenblum E, Tholl D, Aharoni A. 2017. Small molecules below-ground: the role of specialized metabolites in the rhizosphere. *The Plant Journal* **90**(4): 788-807.

Maver M, Escudero-Martinez C, Abbott J, Morris J, Hedley PE, Mimmo T, Bulgarelli D. 2021. Applications of the indole-alkaloid gramine modulate the assembly of individual members of the barley rhizosphere microbiota. *PeerJ* **9**: e12498.

Meihls LN, Handrick V, Glauser G, Barbier H, Kaur H, Haribal MM, Lipka AE, Gershenzon J, Buckler ES, Erb M, et al. 2013. Natural variation in maize aphid resistance is associated with 2,4-dihydroxy-7-methoxy-1,4-benzoxazin-3-one glucoside methyltransferase activity. *Plant Cell* **25**(6): 2341-2355.

Meng X, Zhang S. 2013. MAPK cascades in plant disease resistance signaling. *Annu Rev Phytopathol* **51**: 245-266.

Misawa N. 2011. Pathway engineering for functional isoprenoids. *Current Opinion in Biotechnology* **22**(5): 627-633.

Mizutani M, Sato F. 2011. Unusual P450 reactions in plant secondary metabolism. *Archives of Biochemistry and Biophysics* **507**(1): 194-203.

Monat C, Padmarasu S, Lux T, Wicker T, Gundlach H, Himmelbach A, Ens J, Li C, Muehlbauer GJ, Schulman AH, et al. 2019. TRITEX: chromosome-scale sequence assembly of Triticeae genomes with open-source tools. *Genome Biology* **20**(1): 284.

Morran S, Eini O, Pyvovarenko T, Parent B, Singh R, Ismagul A, Eliby S, Shirley N, Langridge P, Lopato S. 2011. Improvement of stress tolerance of wheat and barley by modulation of expression of DREB/CBF factors. *Plant Biotechnol J* **9**(2): 230-249.

Mothes K. 1980. Nebenwege des stoffwechsels bei pflanze, tier und mikrobe. *Mitt. Chem. Ges. DDR* **27**: 2-10.

Muchlinski A, Jia M, Tiedge K, Fell JS, Pelot KA, Chew L, Davisson D, Chen Y, Siegel J, Lovell JT, et al. 2021. Furanoditerpenoid biosynthesis in the bioenergy crop switchgrass is catalyzed by an alternate metabolic pathway. *bioRxiv*: 2021.2003.2030.437764.

Mueller KO, Börger H. 1939. *Experimentelle Untersuchungen über die Phytophthora - Resistenz der Kartoffel*.

Murphy KM, Edwards J, Louie KB, Bowen BP, Sundaresan V, Northen TR, Zerbe P. 2021. Bioactive diterpenoids impact the composition of the root-associated microbiome in maize (Zea mays). *Scientific Reports* **11**(1): 333.

Nakano C, Okamura T, Sato T, Dairi T, Hoshino T. 2005. Mycobacterium tuberculosis H37Rv3377c encodes the diterpene cyclase for producing the halimane skeleton. *Chemical communications*(8): 1016-1018.

Navathe S, Yadav PS, Chand R, Mishra VK, Vasistha NK, Meher PK, Joshi AK, Gupta PK. 2020. ToxA–Tsn1 Interaction for Spot Blotch Susceptibility in Indian Wheat: An Example of Inverse Gene-for-Gene Relationship. *Plant Disease* **104**(1): 71-81.

Newton AC, Flavell AJ, George TS, Leat P, Mullholland B, Ramsay L, Revoredo-Giha C, Russell J, Steffenson BJ, Swanston JS, et al. 2011. Crops that feed the world 4. Barley: a resilient crop? Strengths and weaknesses in the context of food security. *Food Security* **3**(2): 141-178.

Nicholson RL, Kollipara SS, Vincent JR, Lyons PC, Cadena-Gomez G. 1987. Phytoalexin synthesis by the sorghum mesocotyl in response to infection by pathogenic and nonpathogenic fungi. *Proc Natl Acad Sci U S A* **84**(16): 5520-5524.

Nützmann H-W, Huang A, Osbourn A. 2016. Plant metabolic clusters – from genetics to genomics. *New Phytologist* **211**(3): 771-789.

Oikawa A, Ishihara A, Tanaka C, Mori N, Tsuda M, Iwamura H. 2004. Accumulation of HDMBOA-Glc is induced by biotic stresses prior to the release of MBOA in maize leaves. *Phytochemistry* **65**(22): 2995-3001.

Okada K. 2011. The Biosynthesis of Isoprenoids and the Mechanisms Regulating It in Plants. *Bioscience, Biotechnology, and Biochemistry* **75**(7): 1219-1225.

Otomo K, Kanno Y, Motegi A, Kenmoku H, Yamane H, Mitsuhashi W, Oikawa H, Toshima H, Itoh H, Matsuoka M. 2004. Diterpene cyclases responsible for the

biosynthesis of phytoalexins, momilactones A, B, and oryzalexins A–F in rice. *Bioscience, biotechnology, and biochemistry* **68**(9): 2001-2006.

Paech K. 2013. *Biochemie und Physiologie der sekundären Pflanzenstoffe*: Springer-Verlag.

Park HL, Yoo Y, Hahn T-R, Bhoo SH, Lee S-W, Cho M-H. 2014. Antimicrobial Activity of UV-Induced Phenylamides from Rice Leaves. *Molecules* **19**(11): 18139-18151.

Passardi F, Penel C, Dunand C. 2004. Performing the paradoxical: how plant peroxidases modify the cell wall. *Trends in Plant Science* **9**(11): 534-540.

Peck S, Mittler R. 2020. Plant signaling in biotic and abiotic stress. *J Exp Bot* **71**(5): 1649-1651.

Pedras MS, Minic Z, Jha M. 2008. Brassinin oxidase, a fungal detoxifying enzyme to overcome a plant defense -- purification, characterization and inhibition. *Febs j* **275**(14): 3691-3705.

Pedras MS, Yaya EE, Glawischnig E. 2011. The phytoalexins from cultivated and wild crucifers: chemistry and biology. *Nat Prod Rep* **28**(8): 1381-1405.

Pedras MSC, Ahiahonu PWK, Hossain M. 2004a. Detoxification of the cruciferous phytoalexin brassinin in Sclerotinia sclerotiorum requires an inducible glucosyltransferase. *Phytochemistry* **65**(19): 2685-2694.

Pedras MSC, Hossain M. 2006. Metabolism of crucifer phytoalexins in Sclerotinia sclerotiorum: detoxification of strongly antifungal compounds involves glucosylation. *Organic & Biomolecular Chemistry* **4**(13): 2581-2590.

Pedras MSC, Khan AQ. 2000. Biotransformation of the phytoalexin camalexin by the phytopathogen Rhizoctonia solani. *Phytochemistry* **53**(1): 59-69.

Pedras MSC, Montaut S, Suchy M. 2004b. Phytoalexins from the Crucifer Rutabaga: Structures, Syntheses, Biosyntheses, and Antifungal Activity. *The Journal of Organic Chemistry* **69**(13): 4471-4476.

Pedras MSC, Suchy M. 2005. Detoxification pathways of the phytoalexins brassilexin and sinalexin in Leptosphaeria maculans: isolation and synthesis of the elusive intermediate 3-formylindolyl-2-sulfonic acid. *Organic & Biomolecular Chemistry* **3**(10): 2002-2007.

Pedras MSC, Taylor JL. 1991. Metabolic transformation of the phytoalexin brassinin by the" blackleg" fungus. *The Journal of Organic Chemistry* **56**(8): 2619-2621.

Pedras MSC, Yaya EE. 2010. Phytoalexins from Brassicaceae: News from the front. *Phytochemistry* **71**(11): 1191-1197.

Pelot KA, Chen R, Hagelthorn DM, Young CA, Addison JB, Muchlinski A, Tholl D, Zerbe P. 2018. Functional Diversity of Diterpene Synthases in the Biofuel Crop Switchgrass. *Plant Physiology* **178**(1): 54-71.

Pelot KA, Mitchell R, Kwon M, Hagelthorn LM, Wardman JF, Chiang A, Bohlmann J, Ro D-K, Zerbe P. 2017. Biosynthesis of the psychotropic plant diterpene salvinorin A: Discovery and characterization of the Salvia divinorum clerodienyl diphosphate synthase. *The Plant Journal* **89**(5): 885-897.

Peters RJ. 2010. Two rings in them all: The labdane-related diterpenoids. *Natural Product Reports* **27**(11): 1521-1530.

Pham A-T, Maurer A, Pillen K, Brien C, Dowling K, Berger B, Eglinton JK, March TJ. 2019. Genome-wide association of barley plant growth under drought stress using a nested association mapping population. *BMC Plant Biology* **19**(1): 134.

Phan CS, Li H, Kessler S, Solomon PS, Piggott AM, Chooi YH. 2019. Bipolenins K-N: New sesquiterpenoids from the fungal plant pathogen Bipolaris sorokiniana. *Beilstein J Org Chem* **15**: 2020-2028.

Pieterse CMJ, Zamioudis C, Berendsen RL, Weller DM, Van Wees SCM, Bakker PAHM. 2014. Induced Systemic Resistance by Beneficial Microbes. *Annual Review of Phytopathology* **52**(1): 347-375.

Pimentel D, Bellotti AC. 1976. Parasite-Host Population Systems and Genetic Stability. *The American Naturalist* **110**(975): 877-888.

Pinto AC, Peixoto EM, Fiorani NGM. 1984. Diterpenes with pimarane and cleistanthane skeletons from Vellozia piresiana. *Phytochemistry* **23**(6): 1293-1296.

Polturak G, Dippe M, Stephenson MJ, Chandra Misra R, Owen C, Ramirez-Gonzalez RH, Haidoulis JF, Schoonbeek H-J, Chartrain L, Borrill P, et al. 2022. Pathogen-induced biosynthetic pathways encode defense-related molecules in bread wheat. *Proceedings of the National Academy of Sciences* **119**(16): e2123299119.

Preisig CL, Bell JN, Sun Y, Hrazdina G, Matthews DE, VanEtten HD. 1990. Biosynthesis of the Phytoalexin Pisatin 1: Isoflavone Reduction and Further Metabolism of the Product Sophorol by Extracts of Pisum sativum. *Plant Physiology* **94**(3): 1444-1448.

Pueppke SG, VanEtten HD. 1976. Accumulation of pisatin and three additional antifungal pterocarpans in Fusarium solani-infected tissues of Pisum sativum. *Physiological Plant Pathology* **8**(1): 51-61.

Reinhold-Hurek B, Bunger W, Burbano CS, Sabale M, Hurek T. 2015. Roots shaping their microbiome: global hotspots for microbial activity. *Annu Rev Phytopathol* **53**: 403-424.

Reznik H 1960. Vergleichende Biochemie der Phenylpropane. Berlin, Heidelberg: Springer Berlin Heidelberg. 14-46.

Riehl CAS, Pinto AC. 2000. A cleistanthane diterpene lactone from Vellozia compacta. *Phytochemistry* **53**(8): 917-919.

Rodríguez-Concepción M. 2004. The MEP pathway: a new target for the development of herbicides, antibiotics and antimalarial drugs. *Curr Pharm Des* **10**(19): 2391-2400.

Rodríguez-Concepción M. 2006. Early Steps in Isoprenoid Biosynthesis: Multilevel Regulation of the Supply of Common Precursors in Plant Cells. *Phytochemistry Reviews* **5**(1): 1-15.

Rohdich F, Bacher A, Eisenreich W. 2005. Isoprenoid biosynthetic pathways as anti-infective drug targets. *Biochem Soc Trans* **33**(Pt 4): 785-791.

Rohmer M, Seemann M, Horbach S, Bringer-Meyer S, Sahm H. 1996. Glyceraldehyde 3-Phosphate and Pyruvate as Precursors of Isoprenic Units in an Alternative Non-mevalonate Pathway for Terpenoid Biosynthesis. *Journal of the American Chemical Society* **118**(11): 2564-2566.

Rontein D, Onillon S, Herbette G, Lesot A, Werck-Reichhart D, Sallaud C, Tissier A. 2008. CYP725A4 from Yew Catalyzes Complex Structural Rearrangement of Taxa-4(5),11(12)-diene into the Cyclic Ether 5(12)-Oxa-3(11)-cyclotaxane. *Journal of Biological Chemistry* **283**(10): 6067-6075.

Rotasperti L, Sansoni F, Mizzotti C, Tadini L, Pesaresi P. 2020. Barley's Second Spring as a Model Organism for Chloroplast Research. *Plants* **9**(7): 803.

Rynkiewicz MJ, Cane DE, Christianson DW. 2001. Structure of trichodiene synthase from Fusarium sporotrichioides provides mechanistic inferences on the terpene cyclization cascade. *Proceedings of the National Academy of Sciences* **98**(24): 13543-13548.

Sachs J. 1874. *Lehrbuch der Botanik: nach dem gegenwärtigen Stand der Wissenschaft*: Engelmann.

Sallaud C, Giacalone C, Töpfer R, Goepfert S, Bakaher N, Rösti S, Tissier A. 2012. Characterization of two genes for the biosynthesis of the labdane diterpene Z-abienol in tobacco (Nicotiana tabacum) glandular trichomes. *The Plant Journal* **72**(1): 1-17.

Sang Y, Macho AP 2017. Analysis of PAMP-Triggered ROS Burst in Plant Immunity. In: Shan L, He P eds. *Plant Pattern Recognition Receptors: Methods and Protocols*. New York, NY: Springer New York, 143-153.

Sarkar D, Rovenich H, Jeena G, Nizam S, Tissier A, Balcke GU, Mahdi LK, Bonkowski M, Langen G, Zuccaro A. 2019. The inconspicuous gatekeeper: endophytic Serendipita vermifera acts as extended plant protection barrier in the rhizosphere. *New Phytologist* **224**(2): 886-901.

Savary S, Willocquet L, Pethybridge SJ, Esker P, McRoberts N, Nelson A. 2019. The global burden of pathogens and pests on major food crops. *Nat Ecol Evol* **3**(3): 430-439.

Schäfer W, Straney D, Ciuffetti L, Van Etten HD, Yoder OC. 1989. One Enzyme Makes a Fungal Pathogen, But Not a Saprophyte, Virulent on a New Host Plant. *Science* **246**(4927): 247-249.

Scheler U, Brandt W, Porzel A, Rothe K, Manzano D, Božić D, Papaefthimiou D, Balcke GU, Henning A, Lohse S, et al. 2016. Elucidation of the biosynthesis of carnosic acid and its reconstitution in yeast. *Nature Communications* **7**(1): 12942.

Schmelz EA, Huffaker A, Sims JW, Christensen SA, Lu X, Okada K, Peters RJ. 2014. Biosynthesis, elicitation and roles of monocot terpenoid phytoalexins. *The Plant Journal* **79**(4): 659-678.

Schmelz EA, Kaplan F, Huffaker A, Dafoe NJ, Vaughan MM, Ni X, Rocca JR, Alborn HT, Teal PE. 2011. Identity, regulation, and activity of inducible diterpenoid phytoalexins in maize. *Proceedings of the National Academy of Sciences* **108**(13): 5455-5460.

Schutt C, Netzly D. 1991. Effect of apiforol and apigeninidin on growth of selected fungi. *J Chem Ecol* **17**(11): 2261-2266.

Schwochau ME, Hadwiger LA. 1968. Stimulation of pisatin production in Pisum sativum by actinomycin D and other compounds. *Archives of Biochemistry and Biophysics* **126**(2): 731-733.

Seigler DS. 1998. *Plant secondary metabolism*: Springer Science & Business Media.

Seki H, Sawai S, Ohyama K, Mizutani M, Ohnishi T, Sudo H, Fukushima EO, Akashi T, Aoki T, Saito K. 2011. Triterpene functional genomics in licorice for identification of CYP72A154 involved in the biosynthesis of glycyrrhizin. *The Plant Cell* **23**(11): 4112-4123.

Sekido H, Akatsuka T. 1987. Mode of Action of Oryzalexin D against *Pyricularia oryzae*. *Agricultural and Biological Chemistry* **51**(7): 1967-1971.

Sekido H, Kamada K, Kodama O, Akatsuka T. 1987. Antifungal Activity of Enantiomers of Oryzalexins against *Pyricularia oryzae*. *Agricultural and Biological Chemistry* **51**(7): 2017-2018.

Shimizu T, Lin F, Hasegawa M, Okada K, Nojiri H, Yamane H. 2012. Purification and Identification of Naringenin 7-O-Methyltransferase, a Key Enzyme in Biosynthesis of Flavonoid Phytoalexin Sakuranetin in Rice. *Journal of Biological Chemistry* **287**(23): 19315-19325.

Shimura K, Okada A, Okada K, Jikumaru Y, Ko K-W, Toyomasu T, Sassa T, Hasegawa M, Kodama O, Shibuya N, et al. 2007. Identification of a Biosynthetic Gene Cluster in Rice for Momilactones. *Journal of Biological Chemistry* **282**(47): 34013-34018.

Shiono Y, Ogata K, Koseki T, Murayama T, Funakoshi T. 2010. A Cleistanthane Diterpene From a Marine-derived Fusarium Species Under Submerged Fermentation. **65**(6): 753-756.

SHIRAISHI T, OKU H, YAMASHITA M, OUCHI S. 1978. Elicitor and suppressor of pisatin induction in spore germination fluid of pea pathogen, Mycosphaerella pinodes. *Japanese Journal of Phytopathology* **44**(5): 659-665.

Sikder MM, Vestergård M, Kyndt T, Fomsgaard IS, Kudjordjie EN, Nicolaisen M. 2021. Benzoxazinoids selectively affect maize root-associated nematode taxa. *Journal of Experimental Botany* **72**(10): 3835-3845.

Silva GCd, Valente LMM, Patitucci ML, Pinto AdC, Menezes NLd. 2001. Diterpenóides com esqueleto cleistantano de Vellozia aff. carunculares Martius ex Seubert (Velloziaceae). *Química Nova* **24**: 619-625.

Simmonds P, Sallans B, Ledingham R. 1950. The occurrence of Helminthosporium sativum in relation to primary infections in common rootrot of wheat. *Scientific Agriculture* **30**(10): 407-417.

Sobolev VS. 2008. Localized Production of Phytoalexins by Peanut (Arachis hypogaea) Kernels in Response to Invasion by Aspergillus Species. *Journal of Agricultural and Food Chemistry* **56**(6): 1949-1954.

Sobolev VS, Khan SI, Tabanca N, Wedge DE, Manly SP, Cutler SJ, Coy MR, Becnel JJ, Neff SA, Gloer JB. 2011. Biological Activity of Peanut (Arachis hypogaea) Phytoalexins and Selected Natural and Synthetic Stilbenoids. *Journal of Agricultural and Food Chemistry* **59**(5): 1673-1682.

Sobolev VS, Neff SA, Gloer JB. 2009. New Stilbenoids from Peanut (Arachis hypogaea) Seeds Challenged by an Aspergillus caelatus Strain. *Journal of Agricultural and Food Chemistry* **57**(1): 62-68.

Sobolev VS, Neff SA, Gloer JB. 2010. New Dimeric Stilbenoids from Fungal-Challenged Peanut (Arachis hypogaea) Seeds. *Journal of Agricultural and Food Chemistry* **58**(2): 875-881.

Sobolev VS, Neff SA, Gloer JB, Khan SI, Tabanca N, De Lucca AJ, Wedge DE. 2010. Pterocarpenes elicited by Aspergillus caelatus in peanut (Arachis hypogaea) seeds. *Phytochemistry* **71**(17-18): 2099-2107.

Spielmeyer W, Ellis M, Robertson M, Ali S, Lenton JR, Chandler PM. 2004. Isolation of gibberellin metabolic pathway genes from barley and comparative mapping in barley, wheat and rice. *Theor Appl Genet* **109**(4): 847-855.

Sprague R, ed. 1950. *Diseases of Cereals and Grasses in North America: Fungi, Except Smuts and Rusts*. New York: The Ronald Press Company.

Starks CM, Back K, Chappell J, Noel JP. 1997. Structural Basis for Cyclic Terpene Biosynthesis by Tobacco 5-Epi-Aristolochene Synthase. *Science* **277**(5333): 1815-1820.

Stermitz FR, Lorenz P, Tawara JN, Zenewicz LA, Lewis K. 2000. Synergy in a medicinal plant: Antimicrobial action of berberine potentiated by 5′-methoxyhydnocarpin, a multidrug pump inhibitor. *Proceedings of the National Academy of Sciences* **97**(4): 1433-1437.

Stonecipher LL, Hurley PS, Netzly DH. 1993. Effect of apigeninidin on the growth of selected bacteria. *J Chem Ecol* **19**(5): 1021-1027.

Stott P. 2016. How climate change affects extreme weather events. *Science* **352**(6293): 1517-1518.

Sun M-Y, Ye Y, Xiao L, Rahman K, Xia W, Zhang H. 2016. Daidzein: A review of pharmacological effects. *African journal of traditional, complementary and alternative medicines* **13**(3): 117-132.

Sun TP, Kamiya Y. 1994. The Arabidopsis GA1 locus encodes the cyclase ent-kaurene synthetase A of gibberellin biosynthesis. *Plant Cell* **6**(10): 1509-1518.

Suzuki N, Rivero RM, Shulaev V, Blumwald E, Mittler R. 2014. Abiotic and biotic stress combinations. *New Phytol* **203**(1): 32-43.

Swaminathan S, Morrone D, Wang Q, Fulton DB, Peters RJ. 2009. CYP76M7 Is an ent-Cassadiene C11α-Hydroxylase Defining a Second Multifunctional Diterpenoid Biosynthetic Gene Cluster in Rice *The Plant Cell* **21**(10): 3315-3325.

Takasugi M, Katsui N, Shirata A. 1986. Isolation of three novel sulphur-containing phytoalexins from the chinese cabbage Brassica campestris L. ssp. pekinensis(cruciferae). *Journal of the Chemical Society, Chemical Communications*(14): 1077-1078.

Tang H, Wang X, Bowers JE, Ming R, Alam M, Paterson AH. 2008. Unraveling ancient hexaploidy through multiply-aligned angiosperm gene maps. *Genome research* **18**(12): 1944-1954.

Thiel T, Graner A, Waugh R, Grosse I, Close TJ, Stein N. 2009. Evidence and evolutionary analysis of ancient whole-genome duplication in barley predating the divergence from rice. *BMC Evolutionary Biology* **9**(1): 209.

Thomas SG, Rieu I, Steber CM. 2005. Gibberellin metabolism and signaling. *Vitam Horm* **72**: 289-338.

Tiku AR 2020. Antimicrobial Compounds (Phytoanticipins and Phytoalexins) and Their Role in Plant Defense. In: Mérillon J-M, Ramawat KG eds. *Co-Evolution of Secondary Metabolites*. Cham: Springer International Publishing, 845-868.

Torres Pazmiño DE, Dudek HM, Fraaije MW. 2010. Baeyer–Villiger monooxygenases: recent advances and future challenges. *Current Opinion in Chemical Biology* **14**(2): 138-144.

Turrà D, Di Pietro A. 2015. Chemotropic sensing in fungus–plant interactions. *Current Opinion in Plant Biology* **26**: 135-140.

Turrà D, El Ghalid M, Rossi F, Di Pietro A. 2015. Fungal pathogen uses sex pheromone receptor for chemotropic sensing of host plant signals. *Nature* **527**(7579): 521-524.

Ube N, Harada D, Katsuyama Y, Osaki-Oka K, Tonooka T, Ueno K, Taketa S, Ishihara A. 2019. Identification of phenylamide phytoalexins and characterization of inducible phenylamide metabolism in wheat. *Phytochemistry* **167**: 112098.

Ube N, Katsuyama Y, Kariya K, Tebayashi S-i, Sue M, Tohnooka T, Ueno K, Taketa S, Ishihara A. 2021. Identification of methoxylchalcones produced in response to CuCl2 treatment and pathogen infection in barley. *Phytochemistry* **184**: 112650.

Ube N, Yabuta Y, Tohnooka T, Ueno K, Taketa S, Ishihara A. 2019. Biosynthesis of Phenylamide Phytoalexins in Pathogen-Infected Barley. *Int J Mol Sci* **20**(22).

UEHARA K. 1958. On the production of phytoalexin by the host plant as a result of interaction between rice plant and the blast fungus (Piricularia oryzae Cav.). *Japanese Journal of Phytopathology* **23**(3): 127-130.

Ullrich SE. 2010. *Barley: production, improvement, and uses*: John Wiley & Sons.

Urban P, Mignotte C, Kazmaier M, Delorme F, Pompon D. 1997. Cloning, Yeast Expression, and Characterization of the Coupling of Two Distantly Related *Arabidopsis thaliana* NADPH-Cytochrome P450 Reductases with P450 CYP73A5. *Journal of Biological Chemistry* **272**(31): 19176-19186.

Vaidya AS, Helander JDM, Peterson FC, Elzinga D, Dejonghe W, Kaundal A, Park SY, Xing Z, Mega R, Takeuchi J, et al. 2019. Dynamic control of plant water use using designed ABA receptor agonists. *Science* **366**(6464).

van Dijk M, Morley T, Rau ML, Saghai Y. 2021. A meta-analysis of projected global food demand and population at risk of hunger for the period 2010–2050. *Nature Food* **2**(7): 494-501.

VanEtten H, Temporini E, Wasmann C. 2001. Phytoalexin (and phytoanticipin) tolerance as a virulence trait: why is it not required by all pathogens? *Physiological and Molecular Plant Pathology* **59**(2): 83-93.

VanEtten HD, Matthews DE, Smith D. 1982. Metabolism of phytoalexins. *Phytoalexins/general editors, JA Bailey and JW Mansfield*.

VanEtten HD, Matthews PS, Tegtmeier KJ, Dietert MF, Stein JI. 1980. The association of pisatin tolerance and demethylation with virulence on pea in Nectria haematococca. *Physiological Plant Pathology* **16**(2): 257-268.

Vaughan MM, Wang Q, Webster FX, Kiemle D, Hong YJ, Tantillo DJ, Coates RM, Wray AT, Askew W, O'Donnell C, et al. 2013. Formation of the Unusual Semivolatile Diterpene Rhizathalene by the Arabidopsis Class I Terpene Synthase TPS08 in the Root Stele Is Involved in Defense against Belowground Herbivory. *The Plant Cell* **25**(3): 1108-1125.

Venturi V, Keel C. 2016. Signaling in the Rhizosphere. *Trends in Plant Science* **21**(3): 187-198.

Verma S, Nizam S, Verma PK 2013. Biotic and Abiotic Stress Signaling in Plants. In: Sarwat M, Ahmad A, Abdin MZ eds. *Stress Signaling in Plants: Genomics and Proteomics Perspective, Volume 1*. New York, NY: Springer New York, 25-49.

Wang P, Zhao Y, Li Z, Hsu CC, Liu X, Fu L, Hou YJ, Du Y, Xie S, Zhang C, et al. 2018. Reciprocal Regulation of the TOR Kinase and ABA Receptor Balances Plant Growth and Stress Response. *Mol Cell* **69**(1): 100-112 e106.

Wang Q, Hillwig ML, Okada K, Yamazaki K, Wu Y, Swaminathan S, Yamane H, Peters RJ. 2012. Characterization of CYP76M5–8 indicates metabolic plasticity within a plant biosynthetic gene cluster. *Journal of Biological Chemistry* **287**(9): 6159-6168.

Wang Q, Hillwig ML, Peters RJ. 2011. CYP99A3: functional identification of a diterpene oxidase from the momilactone biosynthetic gene cluster in rice. *Plant J* **65**(1): 87-95.

Wang Y, Lim L, Madilao L, Lah L, Bohlmann J, Breuil C. 2014. Gene discovery for enzymes involved in limonene modification or utilization by the mountain pine beetle-associated pathogen Grosmannia clavigera. *Appl Environ Microbiol* **80**(15): 4566-4576.

Wang Y, Pruitt RN, Nurnberger T, Wang Y. 2022. Evasion of plant immunity by microbial pathogens. *Nat Rev Microbiol* **20**(8): 449-464.

Wang Y, Tang H, Debarry JD, Tan X, Li J, Wang X, Lee TH, Jin H, Marler B, Guo H, et al. 2012. MCScanX: a toolkit for detection and evolutionary analysis of gene synteny and collinearity. *Nucleic Acids Res* **40**(7): e49.

Wang Y-D, Yang J, Li Q, Li Y-Y, Tan X-M, Yao S-Y, Niu S-B, Deng H, Guo L-P, Ding G. 2022. UPLC-Q-TOF-MS/MS Analysis of Seco-Sativene

Sesquiterpenoids to Detect New and Bioactive Analogues From Plant Pathogen Bipolaris sorokiniana. *Frontiers in Microbiology* **13**.

Weber E, Engler C, Gruetzner R, Werner S, Marillonnet S. 2011a. A Modular Cloning System for Standardized Assembly of Multigene Constructs. *PLOS ONE* **6**(2): e16765.

Weber E, Gruetzner R, Werner S, Engler C, Marillonnet S. 2011b. Assembly of Designer TAL Effectors by Golden Gate Cloning. *PLOS ONE* **6**(5): e19722.

Weiergang I, Hipskind JD, Nicholson RL. 1996. Synthesis of 3-deoxyanthocyanidin phytoalexins in sorghum occurs independent of light. *Physiological and Molecular Plant Pathology* **49**(6): 377-388.

Wendt KU, Schulz GE. 1998. Isoprenoid biosynthesis: manifold chemistry catalyzed by similar enzymes. *Structure* **6**(2): 127-133.

Westrick NM, Smith DL, Kabbage M. 2021. Disarming the Host: Detoxification of Plant Defense Compounds During Fungal Necrotrophy. *Frontiers in Plant Science* **12**.

Whittington DA, Wise ML, Urbansky M, Coates RM, Croteau RB, Christianson DW. 2002. Bornyl diphosphate synthase: structure and strategy for carbocation manipulation by a terpenoid cyclase. *Proceedings of the National Academy of Sciences* **99**(24): 15375-15380.

Wink M, Van Wyk B-E. 2008. *Mind-altering and poisonous plants of the world*: Timber Press Portland.

Wu D, Hu Y, Akashi S, Nojiri H, Guo L, Ye C-Y, Zhu Q-H, Okada K, Fan L. 2022. Lateral transfers lead to the birth of momilactone biosynthetic gene clusters in grass. *The Plant Journal* **111**(5): 1354-1367.

Wu Y, Wang Q, Hillwig ML, Peters RJ. 2013. Picking sides: distinct roles for CYP76M6 and CYP76M8 in rice oryzalexin biosynthesis. *Biochemical Journal* **454**(2): 209-216.

Wu Y, Zhou K, Toyomasu T, Sugawara C, Oku M, Abe S, Usui M, Mitsuhashi W, Chono M, Chandler PM, et al. 2012. Functional characterization of wheat copalyl diphosphate synthases sheds light on the early evolution of labdane-related diterpenoid metabolism in the cereals. *Phytochemistry* **84**: 40-46.

Wu Z, Song L, Huang D. 2011. Food Grade Fungal Stress on Germinating Peanut Seeds Induced Phytoalexins and Enhanced Polyphenolic Antioxidants. *Journal of Agricultural and Food Chemistry* **59**(11): 5993-6003.

Xu M, Wilderman PR, Morrone D, Xu J, Roy A, Margis-Pinheiro M, Upadhyaya NM, Coates RM, Peters RJ. 2007. Functional characterization of the rice kaurene synthase-like gene family. *Phytochemistry* **68**(3): 312-326.

Zentmyer GA. 1961. Chemotaxis of Zoospores for Root Exudates. *Science* **133**(3464): 1595-1596.

Zerbe P, Bohlmann J. 2015. Plant diterpene synthases: exploring modularity and metabolic diversity for bioengineering. *Trends in Biotechnology* **33**(7): 419-428.

Zerbe P, Chiang A, Dullat H, O'Neil-Johnson M, Starks C, Hamberger B, Bohlmann J. 2014. Diterpene synthases of the biosynthetic system of medicinally active diterpenoids in Marrubium vulgare. *The Plant Journal* **79**(6): 914-927.

Zhang H, Zhu J, Gong Z, Zhu JK. 2022. Abiotic stress responses in plants. *Nat Rev Genet* **23**(2): 104-119.

Zheng X-H, Yang J, Lv J-J, Zhu H-T, Wang D, Xu M, Yang C-R, Zhang Y-J. 2018. Phyllaciduloids A–D: Four new cleistanthane diterpenoids from Phyllanthus acidus (L.) Skeels. *Fitoterapia* **125**: 89-93.

Zhou K, Gao Y, Hoy JA, Mann FM, Honzatko RB, Peters RJ. 2012. Insights into Diterpene Cyclization from Structure of Bifunctional Abietadiene Synthase from Abies grandis. *Journal of Biological Chemistry* **287**(9): 6840-6850.

Zhou K, Xu M, Tiernan M, Xie Q, Toyomasu T, Sugawara C, Oku M, Usui M, Mitsuhashi W, Chono M, et al. 2012. Functional characterization of wheat ent-kaurene(-like) synthases indicates continuing evolution of labdane-related diterpenoid metabolism in the cereals. *Phytochemistry* **84**: 47-55.

Zhu JK. 2016. Abiotic Stress Signaling and Responses in Plants. *Cell* **167**(2): 313-324.

Zi J, Matsuba Y, Hong YJ, Jackson AJ, Tantillo DJ, Pichersky E, Peters RJ. 2014. Biosynthesis of Lycosantalonol, a cis-Prenyl Derived Diterpenoid. *Journal of the American Chemical Society* **136**(49): 16951-16953.

7. Appendix

7.1 Supplementary figures

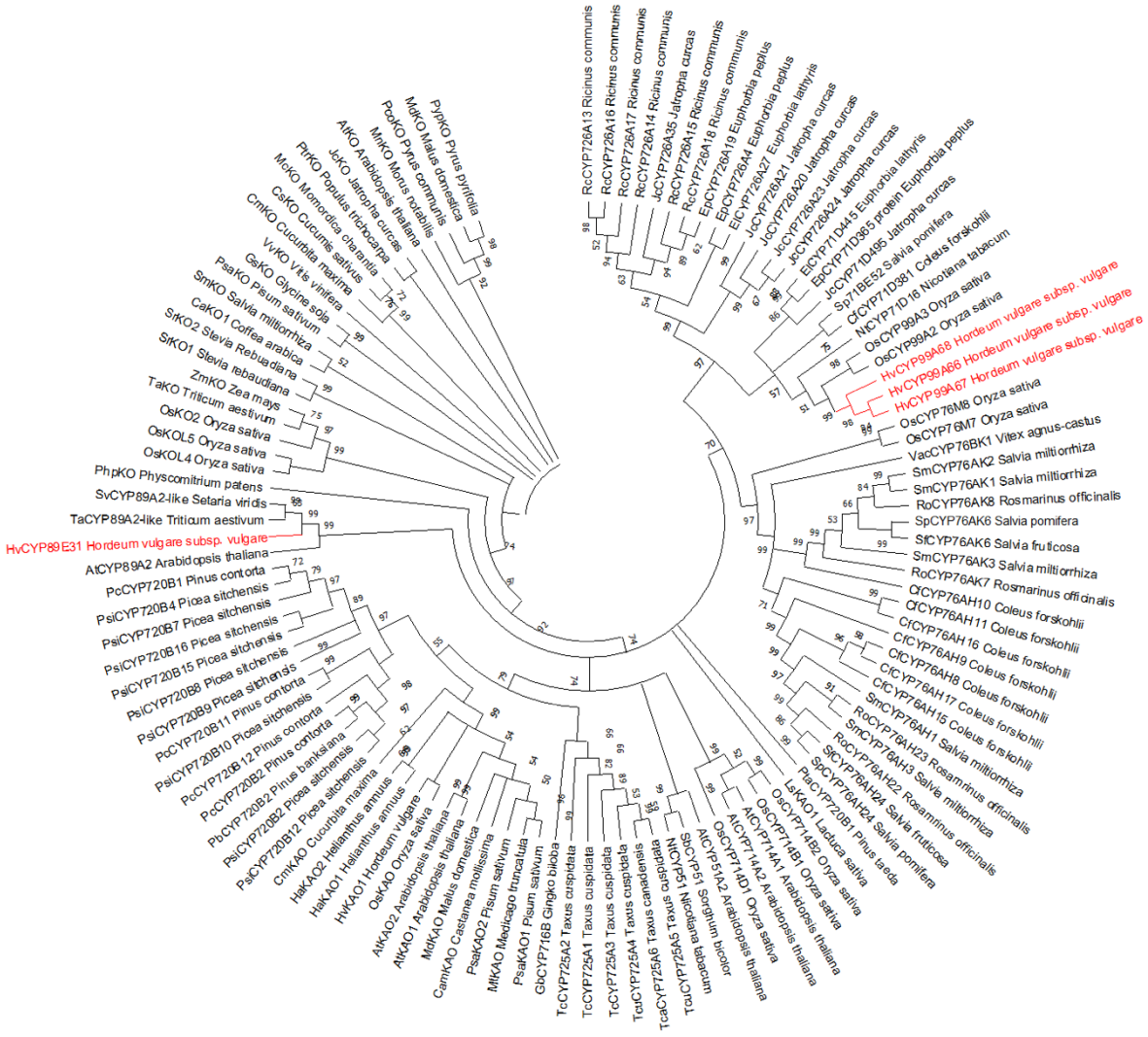

Figure S1 Phylogenetic analysis of CYP sequences from barley chromosome 2 diterpenoid cluster

The evolutionary history was inferred using the Maximum Likelihood method and Poisson correction model. The bootstrap consensus tree inferred from 1000 replicates is taken to represent the evolutionary history of the taxa analyzed. Branches corresponding to partitions reproduced in less than 50% of bootstrap replicates are collapsed. Evolutionary analyses were conducted in MEGA X (Kumar *et al.*, 2018). The list of sequences used is provided in **Table S4**. The CYPs from barley are in red.

1

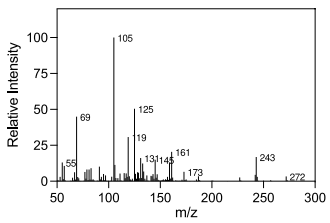

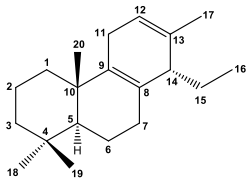

4

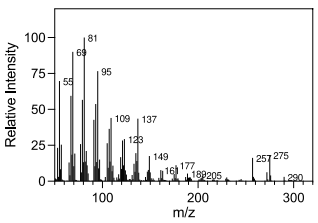

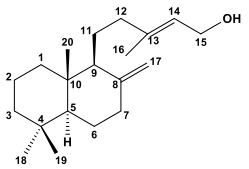

2

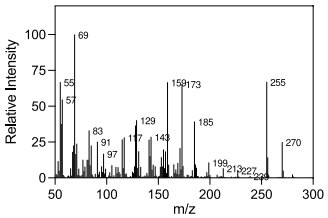

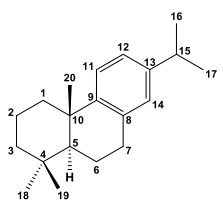

5

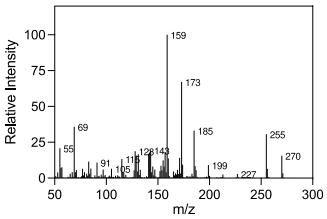

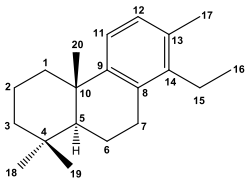

3

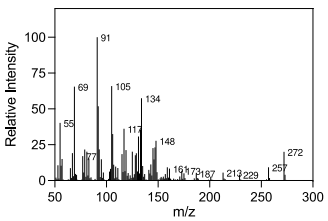

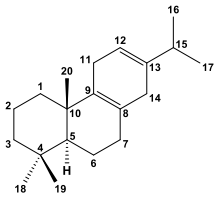

6

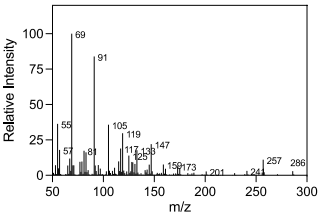

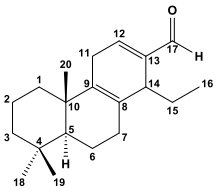

7

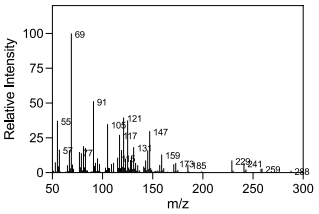

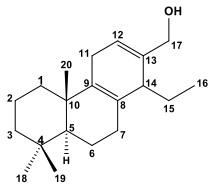

Putative, NO NMR

10

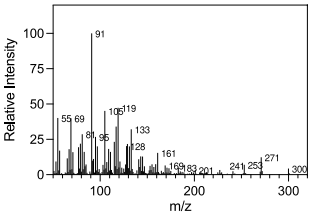

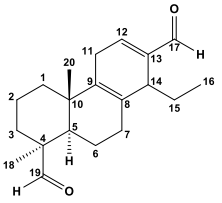

Putative, NO NMR

8

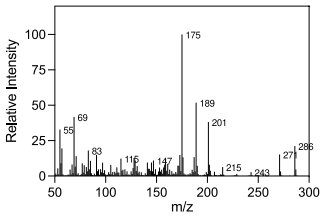

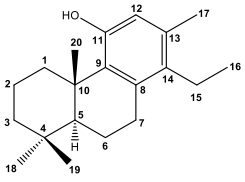

11

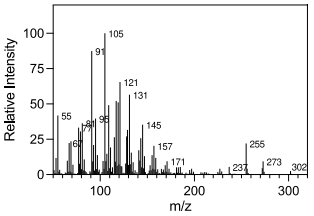

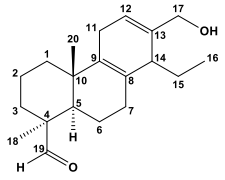

Putative, NO NMR

9

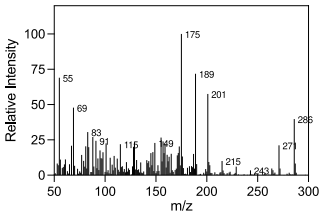

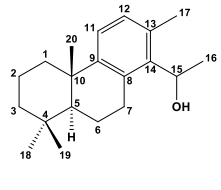

Putative, NO NMR

12

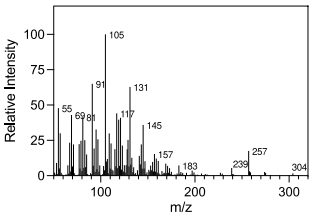

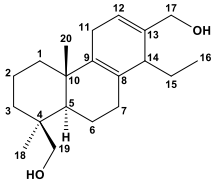

Putative, NO NMR

13

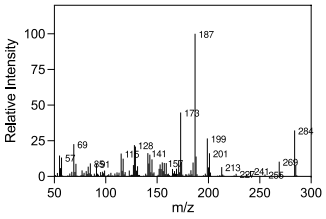

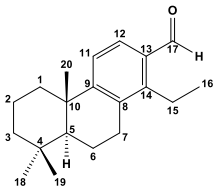

Putative, NO NMR

16

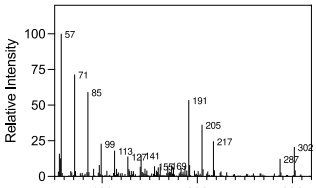

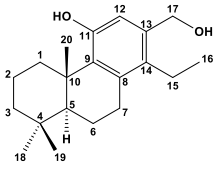

Putative, NO NMR

14

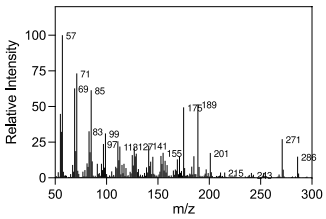

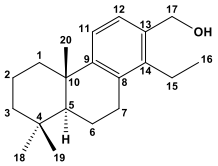

Putative, NO NMR

17

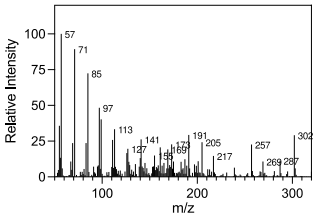

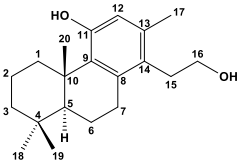

Putative, NO NMR

15

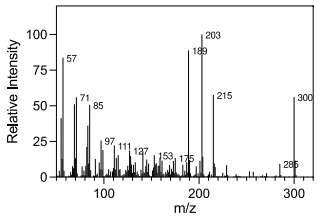

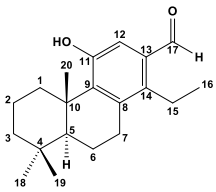

Putative, NO NMR

18

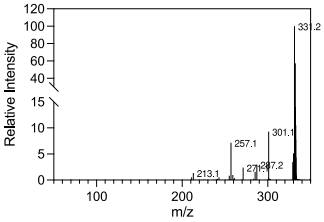

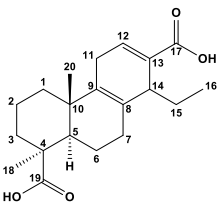

Putative, NO NMR

19

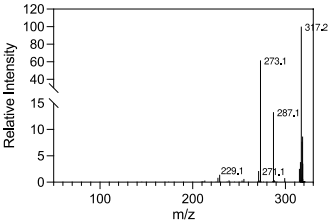

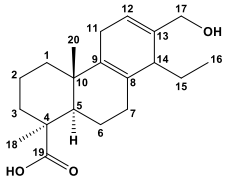

Putative, NO NMR

22

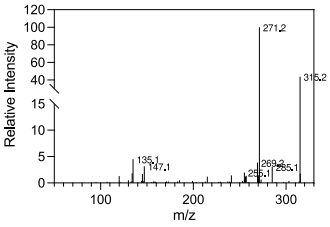

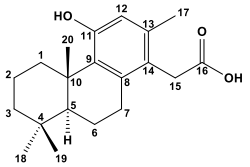

Putative, NO NMR

20

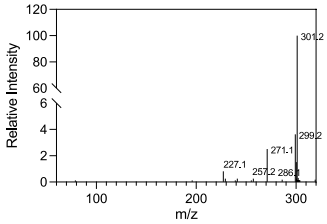

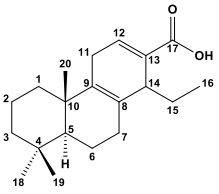

Putative, NO NMR

23

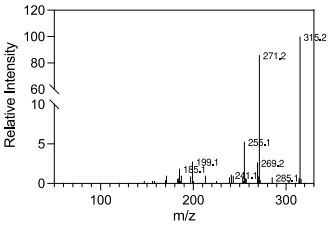

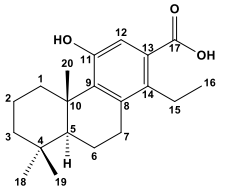

Putative, NO NMR

21

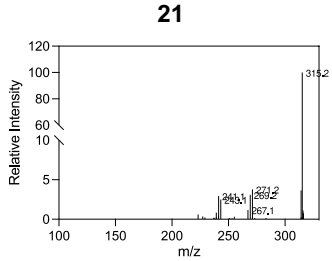

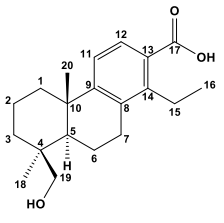

Putative, NO NMR

24

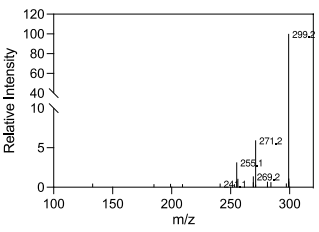

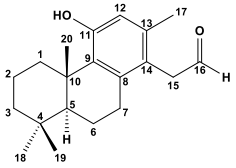

Putative, NO NMR

25

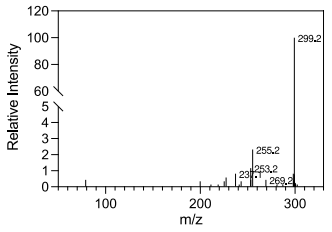

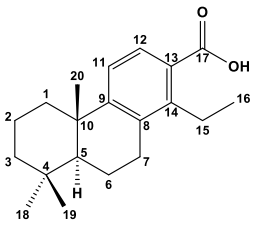

Putative, NO NMR

26

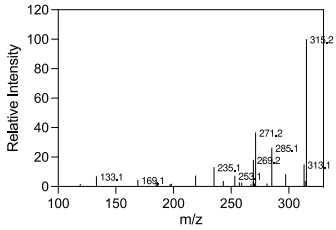

27

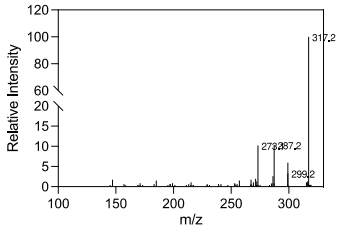

31

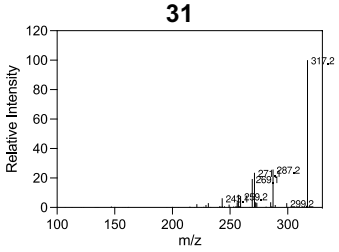

32

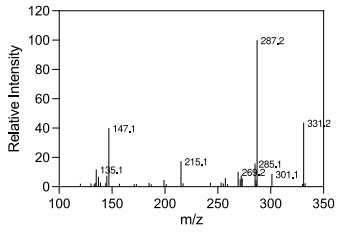

33

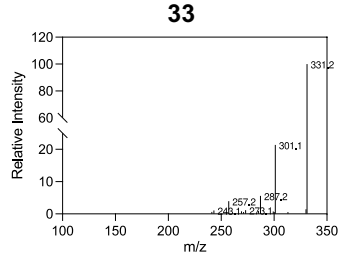

28

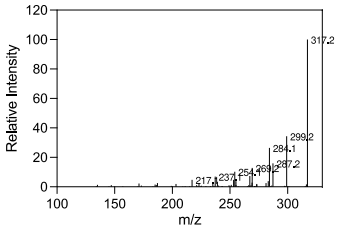

29

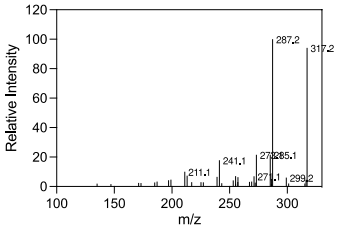

30

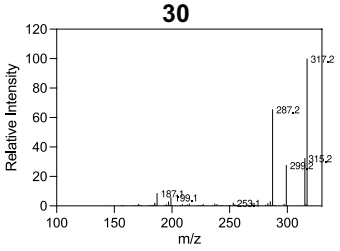

34

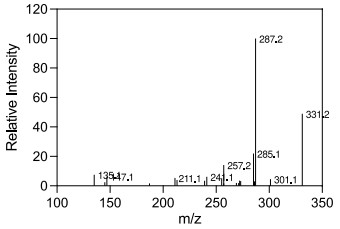

35

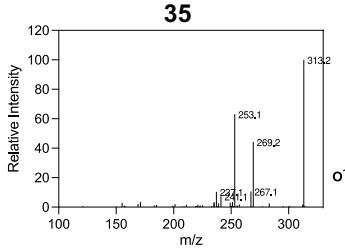

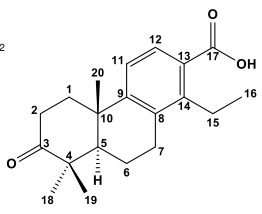

36

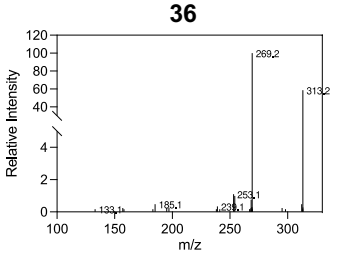

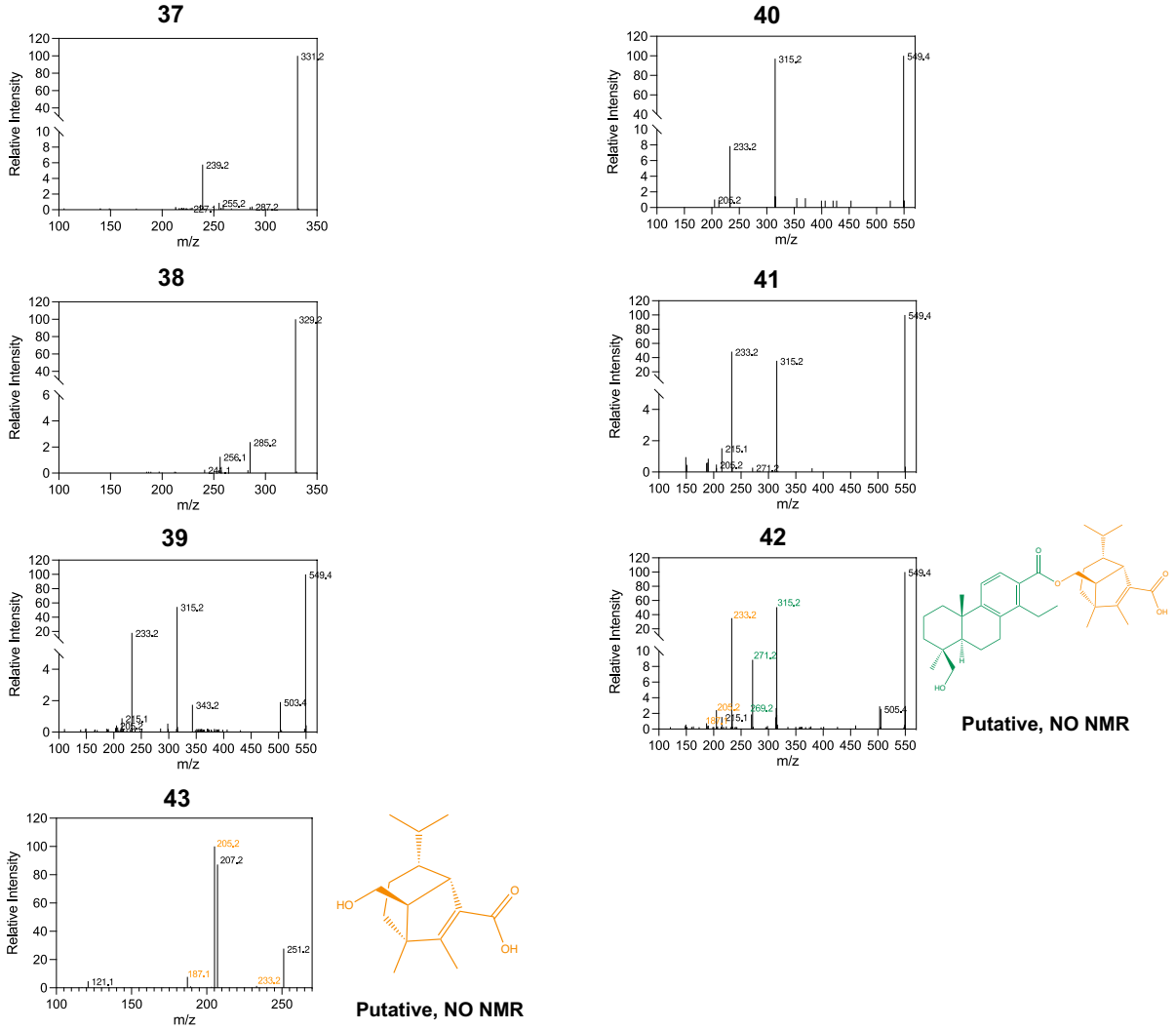

Figure S2 MS or MS/MS spectra of terpenoids shown in this thesis and their structures or putative structures

The structure of compound 35 was kindly shared by Dr. Gerd Balcke and Simon Isfort.

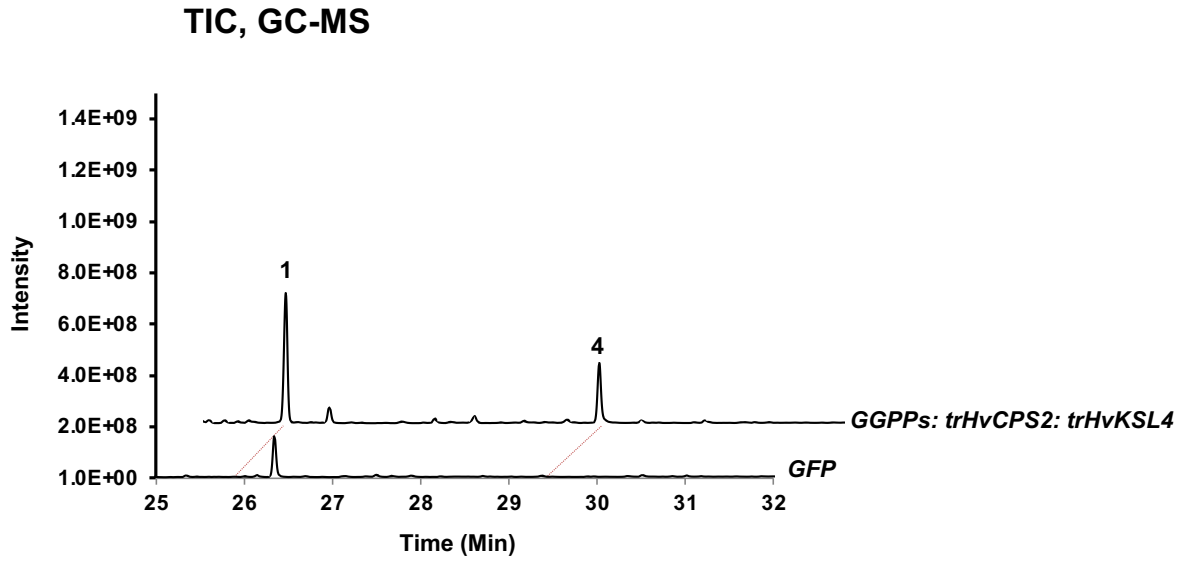

Figure S3 GC-MS analysis of transient expression in *N. Benthamiana*

The genes that were expressed are indicated on the right side of the chromatogram. A truncated version of HvCPS2 and HvKSL4, of which the transit peptides were removed, was used in this assay. Total ion chromatograms (TIC) are shown. Products are indicated by numbers. 1: hordediene; 4: (+)-copalol. MS Spectra of products are presented in **Fig. S2**.

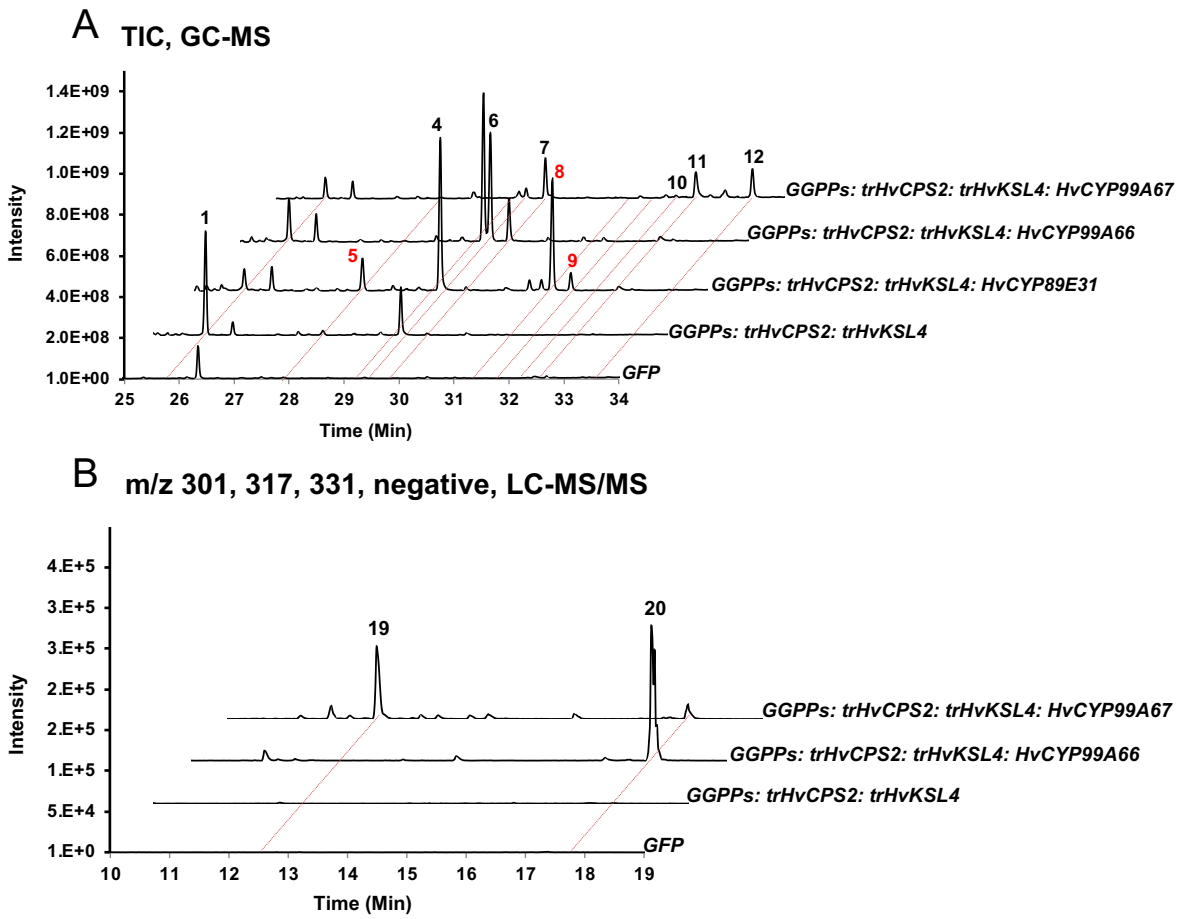

Figure S4 Characterization of HvCYP89E31, HvCYP99A66, HvCYP99A67, and HvCYP99A68 in *N. benthamiana*

(A) Total ion chromatograms (GC-MS) of extracts of leaf discs expressing the gene combinations indicated on the right. (B) Selected ion (m/z 301.2, 317.2, 331.2, negative mode) chromatograms (LC-MS/MS) of extracts of leaf discs expressing the gene combinations indicated on the right. Products that were detected in barley roots are colored red. MS or MS/MS spectra of products are presented in **Fig. S2**.

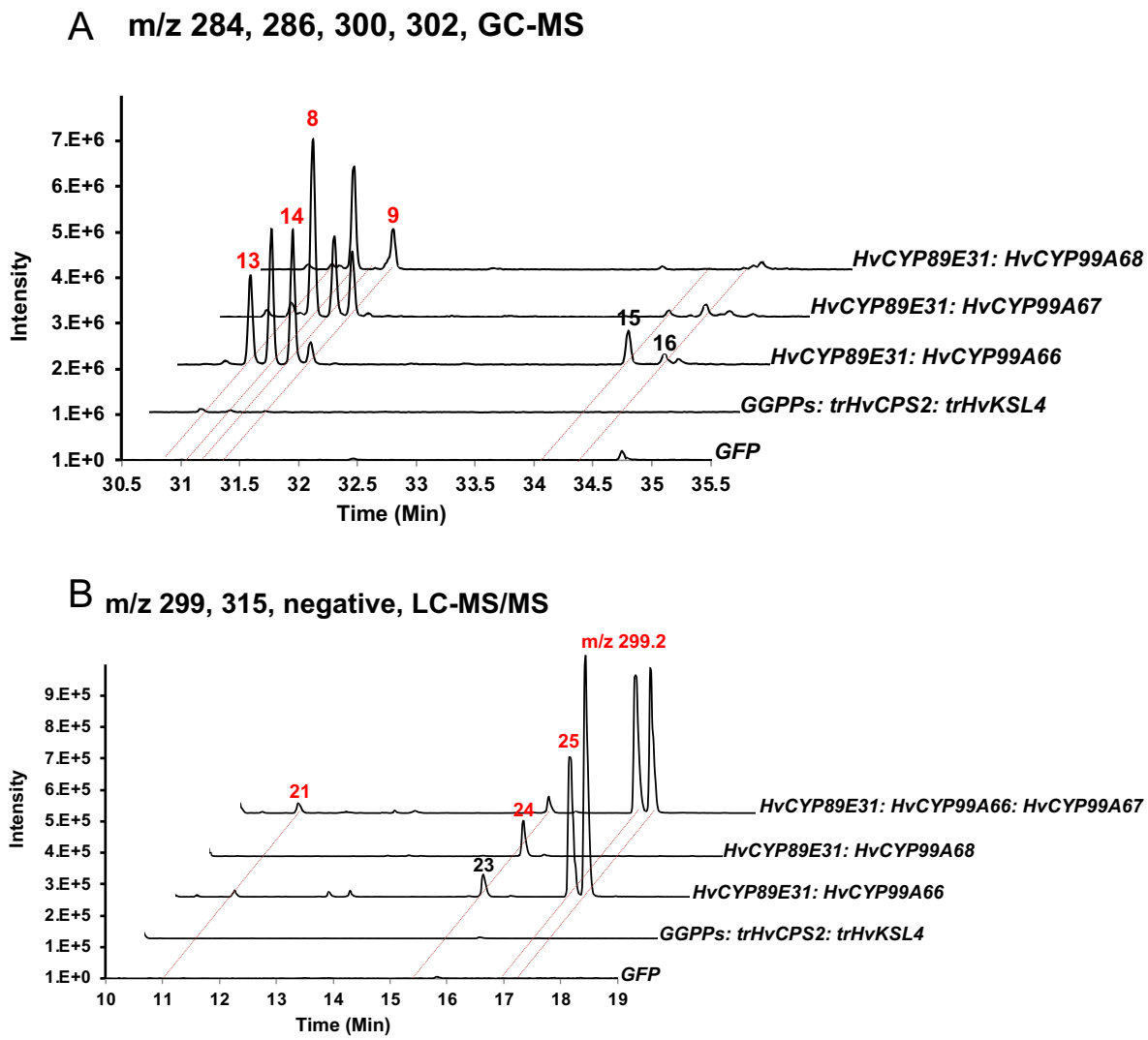

Figure S5 Co-expression of two or three CYPs in *N. benthamiana*

(A) Selected ion (m/z 284, 286, 300, 302) chromatograms (GC-MS) of extracts of leaf discs expressing the gene combinations indicated on the right. (B) Selected ion (m/z 299.2, 315.2, negative mode) chromatograms (LC-MS/MS) of extracts of leaf discs expressing the gene combinations indicated on the right. When *CYPs* were expressed, they were always co-expressed together with *trHvCPS2* and *trHvKSL4*, though it was not written in the figure. Products that were detected in barley roots are colored red. MS or MS/MS spectra of products are presented in **Fig. S2**.

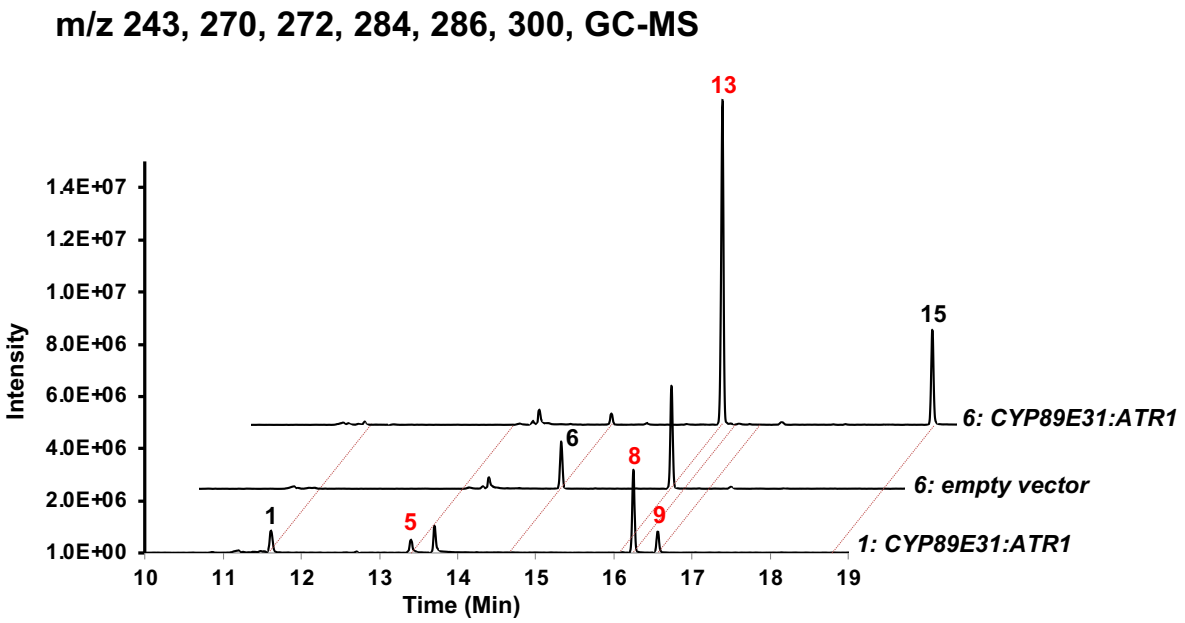

Figure S6 *In vitro* enzyme assays using microsomal preparation expressing CYP89E31 and ATR1

Microsomes expressing CYP89E31 and ATR1 and empty vector were incubated with **1** or **6.** Products were extracted and analyzed by GC-MS. Selected ion (m/z 243, 270, 272, 284, 286, 300) chromatograms are presented.

7.2 Supplementary tables

Table S1 List of genes from the chromosome 2 diterpenoid phytoalexin cluster

Genome version			Gene status	Name
MorexV1 (2017)	**MorexV2 (2019)**	**MorexV3 (2021)**		
2Hr1G004480	2HG0081780	2HG0099280	FL	CYP99A66
2Hr1G004510	2HG0081840	2HG0099340	FL	
2Hr1G004520	2HG0081840	NP	Pseudo	
2Hr1G004530	2HG0081840	2HG0099350	FL	CYP99A67
2Hr1G004540	2HG0081850	2HG0099360	FL	HvKSL4
2Hr1G004550	2HG0081860 UnG0627890 UnG0631950	2HG0099370[a] 2HG0099420[a] 2HG0099430[a]	FL	CYP89E31
NP	2HG0081880	2HG0099470	Pseudo	ψCPS
NP	2HG0081920	2HG0099500	Pseudo	ψCPS
2Hr1G004600	2HG0081930	2HG0099550	FL	CYP99A68[b]
2Hr1G004610	2HG0081980	2HG0099550	FL	CYP99A68[b]
2Hr1G004620	2HG0082000	2HG0099570	FL	HvCPS2
2Hr1G004640 2Hr1G004650	2HG0081890 2HG0082010 2HG0081930 UnG0636400	2HG0099480	FL	CYP99A68[b]

Notes: (a) the amino acid sequences of these two genes are identical. The sequences only differ in the 5'-UTR. (b) the amino acid sequences are identical except for one amino acid change in 2Hr1G004600. NP: not present, FL: full length. (ψ) pseudogene.

Table S2 CPS sequences used for phylogenetic analysis in Figure 2.2

Protein name	Species	Protein ID
AtCPS	*Arabidopsis thaliana*	NP_192187
CmCPS1	*Cucurbita maxima*	AAD04292
OsCPS1	*Orzya sativa*	BAF08464
OsCPS2	*Orzya sativa*	BAH91759
OsCPS4	*Orzya sativa*	NP_001052171
TaCPS1	*Triticum aestivum*	BAH56558
TaCPS2	*Triticum aestivum*	BAH56559
TaCPS3	*Triticum aestivum*	BAH56560
TaCPS4	*Triticum aestivum*	BAP01383
HvCPS1	*Hordeum vulgare*	AAT49065
ZmCPS1	*Zea mays*	NP_001105329
ZmCPS2	*Zea mays*	NP_001105257
ZmCPS3	*Zea mays*	AFW57228
ZmCPS4	*Zea mays*	AFW60403
HvCPS2	*Hordeum vulgare*	BAJ95441

Table S3 KS and KSL sequences used for phylogenetic analysis in Figure 2.2

Protein name	Species	Protein ID
AtKS	*Arabidopsis thaliana*	AAC39443
CmKS	*Cucurbita maxima*	Q39548
OsKS	*Orzya sativa*	NP_001053841
OsKSL4	*Orzya sativa*	NP_001052175
OsKSL5	*Orzya sativa*	NP_001047190
OsKSL6	*Orzya sativa*	ABH10733
OsKSL7	*Orzya sativa*	NP_001047186
OsKSL8	*Orzya sativa*	NP_001067887
OsKSL10	*Orzya sativa*	NP_001066799
OsKSL11	*Orzya sativa*	Q1AHB2
TaKS	*Triticum aestivum*	BAL41693
TaKSL1	*Triticum aestivum*	BAL41688
TaKSL2	*Triticum aestivum*	BAL41689
TaKSL3	*Triticum aestivum*	BAL41690
TaKSL4	*Triticum aestivum*	BAL41691
HvKS	*Hordeum vulgare*	AAT49066
ZmKSL1	*Zea mays*	AFW61735
ZmKSL2	*Zea mays*	DAA54948
ZmKSL3	*Zea mays*	DAA36069
ZmKSL4	*Zea mays*	DAA49845
HvKSL4	*Hordeum vulgare*	BAK01991

Table S4 List of CYP sequences used for phylogenetic analysis in Figure S1

Accession no.	Name	Organism	Function
AB014459	AtCYP51A2	*Arabidopsis thaliana*	
Q93Z79	AtCYP714A1	*Arabidopsis thaliana*	
Q6NKZ8	AtCYP714A2	*Arabidopsis thaliana*	
AF318500	AtKAO1	*Arabidopsis thaliana*	Kaurenoic acid oxidase (KAO)
AF318501	AtKAO2	*Arabidopsis thaliana*	Kaurenoic acid oxidase (KAO)
AF047719	AtKO	*Arabidopsis thaliana*	Kaurene oxidase (KO)
Q42602.2	AtCYP89A2	*Arabidopsis thaliana*	unknown function
HQ658173	CamKAO	*Castanea mollissima*	
ACQ99375	CaKO	*Coffea arabica*	Kaurene oxidase (KO)
KT382342	CfCYP71D381	*Coleus forskohlii*	Forskolin biosynthesis
KT382346	CfCYP76AH10	*Coleus forskohlii*	Forskolin biosynthesis
KT382349	CfCYP76AH11	*Coleus forskohlii*	Forskolin biosynthesis
KT382358	CfCYP76AH15	*Coleus forskohlii*	Forskolin biosynthesis
KT382359	CfCYP76AH16	*Coleus forskohlii*	Forskolin biosynthesis
KT382360	CfCYP76AH17	*Coleus forskohlii*	Forskolin biosynthesis
KT382348	CfCYP76AH8	*Coleus forskohlii*	Forskolin biosynthesis
KT382347	CfCYP76AH9	*Coleus forskohlii*	Forskolin biosynthesis
NP_001267703	CsKO	*Cucumis sativus*	Kaurene oxidase (KO)
AF212991	CumKAO	*Cucurbita maxima*	Kaurenoic acid oxidase (KAO)
AF212990	CumKO	*Cucurbita maxima*	Kaurene oxidase (KO)
KR350668	ElCYP71D445	*Euphorbia lathyris*	Casbene oxidase
KR350669	ElCYP726A27	*Euphorbia lathyris*	Casbene oxidase
KX428471	EpCYP71D365	*Euphorbia peplus*	Casbene oxidase
KJ026362	EpCYP726A19	*Euphorbia peplus*	Casbene synthase
KF986823.1	EpCYP726A4	*Euphorbia peplus*	Casbene oxidase
KF773141	GbCYP716B	*Ginkgo biloba*	taxoid-9α-hydroxylase
KHN31869	GsKO	*Glycine soja*	Kaurene oxidase (KO)
FR666915	HaKAO1	*Helianthus annuus*	Kaurenoic acid oxidase (KAO)
FR666916	HaKAO2	*Helianthus annuus*	Kaurenoic acid oxidase (KAO)
AF326277	HvKAO1	*Hordeum vulgare*	Kaurenoic acid oxidase (KAO)
A0A287GY22	HvCYP89E31	*Hordeum vulgare*	Hordediene oxidase
A0A287GY21	HvCYP99A66	*Hordeum vulgare*	Hordediene oxidase
A0A287GY30	HvCYP99A67	*Hordeum vulgare*	Hordediene oxidase
AK249794	HvCYP99A68	*Hordeum vulgare*	Hordetriene oxidase
KX060559	JcCYP71D495	*Jatropha curcas*	Casbene oxidase
KF986815	JcCYP726A20	*Jatropha curcas*	Casbene oxidase
KF986816	JcCYP726A21	*Jatropha curcas*	
KF986818	JcCYP726A23	*Jatropha curcas*	
KF986819	JcCYP726A24	*Jatropha curcas*	
KX060558	JcCYP726A35	*Jatropha curcas*	Casbene oxidase
JF929910	JcKO	*Jatropha curcas*	Kaurene oxidase (KO)
AB370238	LsKAO	*Lactuca sativa*	Kaurenoic acid oxidase (KAO)

KF437682	MdKAO	*Malus domestica*	Kaurenoic acid oxidase (KAO)
AY563549	MdKO	*Malus domestica*	Kaurene oxidase (KO)
XM_013607618	MtKAO	*Medicago truncatula*	Kaurenoic acid oxidase (KAO)
ADE06669	McKO	*Momordica charantia*	Kaurene oxidase (KO)
XP_010089925	MnKO	*Morus notabilis*	Kaurene oxidase (KO)
AF116915	NtCYP51	*Nicotiana tabacum*	obtusifoliol 14-alpha demethylase
AF166332	NtCYP71D16	*Nicotiana tabacum*	CBT-ol oxidase
Q7XHW5	OsCYP714B1	*Oryza sativa*	
Q0DS59	OsCYP714B2	*Oryza sativa*	
AK109526	OsCYP714D1	*Oryza sativa*	
AK107418	OsCYP71Z6	*Oryza sativa*	
AK070167	OsCYP71Z7	*Oryza sativa*	Cassadiene oxidase
AK059010	OsCYP76M5	*Oryza sativa*	
AK101003	OsCYP76M6	*Oryza sativa*	Oryzalexin synthase
AK105913	OsCYP76M7	*Oryza sativa*	
AK069701	OsCYP76M8	*Oryza sativa*	Oryzalexin synthase
AK071864	OsCYP99A2	*Oryza sativa*	Pimaradiene oxidase
AK071546	OsCYP99A3	*Oryza sativa*	Pimaradiene oxidase
Q5VRM7	OsKAO	*Oryza sativa*	Kaurenoic acid oxidase (KAO)
Q5Z5R4	OsKO2	*Oryza sativa*	Kaurene oxidase (KO)
AY579214	OsKOL4	*Oryza sativa*	Kaurene oxidase (KO)
AY660664	OsKOL5	*Oryza sativa*	Kaurene oxidase (KO)
BAK19917	PhpKO	*Physcomitrella patens*	Kaurene oxidase (KO)
HM245408	PsiCYP720B10	*Picea sitchensis*	
HM245397	PsiCYP720B12	*Picea sitchensis*	Hydroxyl abietene oxidase
HM245398	PsiCYP720B15	*Picea sitchensis*	
HM245399	PsiCYP720B16	*Picea sitchensis*	
HM245402	PsiCYP720B2	*Picea sitchensis*	Hydroxyl abietene oxidase
HM245403	PsiCYP720B4	*Picea sitchensis*	Diterpene C-18 oxidase
HM245406	PsiCYP720B7	*Picea sitchensis*	
HM245407	PsiCYP720B8	*Picea sitchensis*	
HM245410	PsiCYP720B9	*Picea sitchensis*	
KJ845667	PbCYP720B2	*Pinus banksiana*	Hydroxyl abietene oxidase
KJ845671	PcCYP720B1	*Pinus contorta*	Abietadienol/abietadienal oxidase
KJ845675	PcCYP720B11	*Pinus contorta*	
KJ845676	PcCYP720B12	*Pinus contorta*	Hydroxyl abietene oxidase
KJ845672	PcCYP720B2	*Pinus contorta*	Hydroxyl abietene oxidase
AY779541	PtaCYP720B1	*Pinus taeda*	Abietadienol/abietadienal oxidase
AF537321	PsaKAO1	*Pisum sativum*	Kaurenoic acid oxidase (KAO)
AF537322	PsaKAO2	*Pisum sativum*	Kaurenoic acid oxidase (KAO)
AAP69988	PsaKO	*Pisum sativum*	Kaurene oxidase (KO)
XP_006386514	PtrKO	*Populus trichocarpa*	Kaurene oxidase (KO)
AEK01241	PcKO	*Pyrus communis*	Kaurene oxidase (KO)
HM003112	PypKO	*Pyrus pyrifolia*	Kaurene oxidase (KO)

KF986809	RcCYP726A13	*Ricinus communis*	
KF986810	RcCYP726A14	*Ricinus communis*	Casbene oxidase
KF986811	RcCYP726A15	*Ricinus communis*	Neocembrene oxidase
KF986812	RcCYP726A16	*Ricinus communis*	Casbene oxidase
KF986813	RcCYP726A17	*Ricinus communis*	Casbene oxidase
KF986814	RcCYP726A18	*Ricinus communis*	Casbene oxidase
KP091843	RoCYP76AH22	*Rosmariuns officinalis*	Hydroxyferruginol synthase
KP091844	RoCYP76AH23	*Rosmariuns officinalis*	Hydroxyferruginol synthase
	RoCYP76AH4	*Rosmariuns officinalis*	Hydroxyferruginol synthase
KX431219	RoCYP76AK7	*Rosmariuns officinalis*	C20 oxidase
KX431220	RoCYP76AK8	*Rosmariuns officinalis*	C20 oxidase
KP091842	SfCYP76AH24	*Salvia fruticosa*	Hydroxyferruginol synthase
KX431218	SfCYP76AK6	*Salvia fruticosa*	C20 oxidase
JX422213	SmCYP76AH1	*Salvia miltiorrhiza*	Ferruginol synthase
KR140168	SmCYP76AH3	*Salvia miltiorrhiza*	Hydroxyferruginol synthase
KR140169	SmCYP76AK1	*Salvia miltiorrhiza*	C20 oxidase
KP337688	SmCYP76AK2	*Salvia miltiorrhiza*	
KP337689	SmCYP76AK3	*Salvia miltiorrhiza*	
KJ606394	SmKO	*Salvia miltiorrhiza*	Kaurene oxidase (KO)
KT157042	SpCYP71BE52	*Salvia pomifera*	C2 oxidase
KT157044	SpCYP76AH24	*Salvia pomifera*	Hydroxyferruginol synthase
KT157045	SpCYP76AK6	*Salvia pomifera*	C20 oxidase
XP_034572432.1	SvCYP89A2-like	*Setaria viridis*	unknown function
Solyc08g005650.2.1	SlCYP71BN1	*Solanum lycopersisum*	
U74319	SbCYP51	*Sorghum bicolor*	obtusifoliol 14-alpha demethylase
AY364317	SrKO1	*Stevia rebaudiana*	Kaurene oxidase (KO)
AY995178	SrKO2	*Stevia rebaudiana*	Kaurene oxidase (KO)
AY518383	TcaCYP725A6, T2OH	*Taxus canadensis*	taxoid-2α-hydroxylase
AF318211	TcuCYP725A1, T10OH	*Taxus cuspidata*	taxoid-10β-hydroxylase
AY056019	TcuCYP725A2, T13OH	*Taxus cuspidata*	taxoid-13α-hydroxylase
AY188177	TcuCYP725A3, T14OH	*Taxus cuspidata*	taxoid-14β-hydroxylase
AY289209	TcuCYP725A4, T5OH	*Taxus cuspidata*	
AY307951	TcuCYP725A5, T7OH	*Taxus cuspidata*	taxoid-7β-hydroxylase
ADZ55286	TaKO	*Triticum aestivum*	Kaurene oxidase (KO)
KAF6985951	TaCYP89A2-like	*Triticum aestivum*	unknown function
MG696754.1	VacCYP76BK1	*Vitex agnus-castus*	
JQ086553	VvKO	*Vitis vinifera*	Kaurene oxidase (KO)
ACG38493	ZmKO	*Zea mays*	Kaurene oxidase (KO)

Table S5 NMR data of hordediene (compound 1) (C_6D_6)

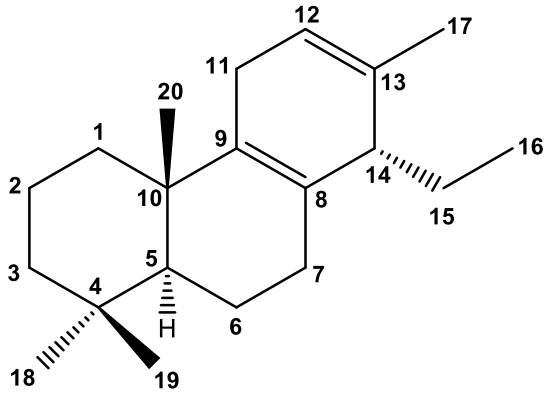

Pos.	^{13}C: δ [ppm]	^{1}H: δ [ppm] m (J[Hz])	selected HMBC (H → C)	ROE[c]
1	37.38	1.66[a] β; 1.043 ddd (13.0/13.0/3.7) α		20;
2	19.37	1.565[b] α; 1.40[a] β		
3	42.01	1.39[a] β; 1.148 ddd (13.7/13.2/4.1) α		18[d]
4	33.39	---		
5	52.49	1.210 dd (12.5/2.0) α		1α[d],7α[d],18[d]
6	19.20	1.687[b] α; 1.503 m β	10; 5,7,10	18;
7	30.81	2.189 m α; 1.750 br dd (17.1/6.2) β		5[d],15[d],16[d],18[d]; 14[d]
8	126.41	---		
9	138.22	---		
10	37.86	---		
11	26.41	2.53[a]		20
12	121.84	5.611 m		11[d],17[d]
13	133.66	---		
14	46.64	2.462 m	8,9,12,13,15	7α[d],7β[d],15[d]
15	21.41	1.61[a]		
16	22.89	0.763 t (7.4)	14,15	
17	7.72	1.656 qd (1.7/0.5)	12,13,14	
18	33.44	0.921 s	3,4,5,19	
19	21.94	0.877 s	3,4,5,18	20
20	19.42	1.014 s	1,5,9,10	

[a] ^{1}H chemical shift of HSQC correlation peaks; [b] ^{1}H chemical shift from selective TOCSY spectrum; [c] each NOE is listed only once; [d] correlations (H → H) from selective ROESY spectra.

14*S* configuration is more likely because of NOE H-7β/H-14 und H-7α/H-15.

Table S6 NMR data of hordetriene (compound 5) (C_6D_6)

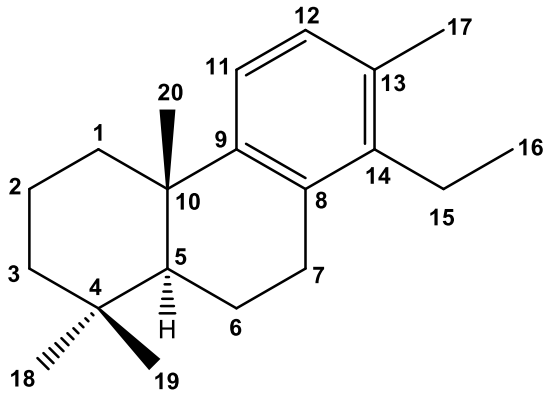

Pos.	^{13}C: δ [ppm]	^{1}H: δ [ppm] m (J[Hz][a])	HMBC (H →C)	ROE[d]
1	39.6	2.206 m β; 1.344 td-like (13.2/3.8) α		11,20;
2	19.8	1.670 qt-like (13.9/3.4) β; 1.5054 m α	1 4,10	20;
3	41.9	1.409 m β; 1.138 td-like (13.5/4.0) α	 4	
4	33.4	---		
5	50.0	1.243 dd (12.6/2.2) α		18
6	19.7	1.797 ddt-like (13.2/7,8/1.9) α; 1.613 m β		
7	28.0	2.849 ddd (17.1/6.6/1.3) β; 2.643 ddd (17.1/11.6/7.8) α		
8	132.5[b]	---		
9	148.5	---		
10	38.1	---		
11	122.4	7.092 d (8.0)		
12	128.4[c]	7.020 d (8.0)		17
13	132.6[b]	---		
14	140.2	---		
15	22.4	2.52 m	16	
16	13.4	1.035 t (7.5)	14,15	
17	19.5	2.209 s	12,13,14	
18	33.4	0.923 s	3,4,5,19	
19	21.8	0.899 s	3,4,5,18	20
20	25.2	1.197 br s	1,5,9,10	

[a] "-like" multiplicities: the given value represents the distance of the multiplet lines, not the exact coupling constant; [b] might be interchanged; [c] ^{13}C chemical shift of HSQC correlation peak; [d] each NOE is listed only once.

Table S7 NMR data of compound 8 (C_6D_6)

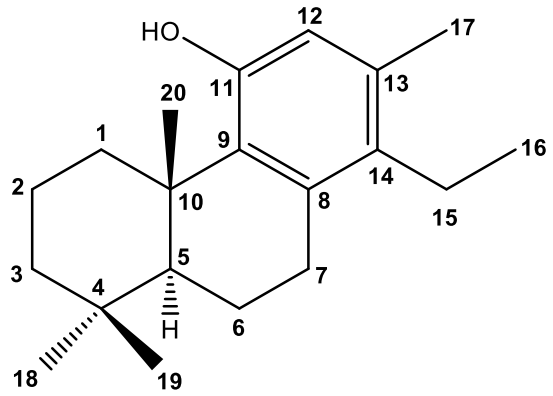

Pos.	^{13}C: δ [ppm]	^{1}H: δ [ppm] m (J[Hz][a])	HMBC (H → C)	ROE (H ↔ H)[b]
1	37.26	3.848 br dt (13.4/3.7) β; 1.350 td (13.4/3.7) α	2,3,5,10; 2,10	20;
2	19.98	1.824 dtt (14.0/13.4/3.7) β; 1.582 dt-like (14.0/3.7) α	1,3,4,10; 4,10	20;
3	41.83	1.453 dtd-like (13.1/3.5/1.5) β; 1.234 td-like (13.4/4.2) α	2,4; 2,4,18,19	
4	33.77	---		
5	52.88	1.276 dd (12.2/1.3) α	4,6,10,18,20	18
6	19.64	1.769 br dd-like (12.9/6.8) α; 1.521 qt-like (12.5/5.4) β	8,10; 5,10	18,19; 19
7	30.64	2.791 ddd (16.8/5.4/1.5) β; 2.614 ddd (16.8/12.6/6.8) α	5,6,8,9,14; 6,8	15;
8	136.02	---		
9	133.62	---		
10	39.72	---		
11	152.11	---		
12	116.67	5.668 br s	9,11,14,17	11-OH,17
13	133.29	---		
14	132.84	---		
15	21.99	2.475 q (7.5)	8,13,14,16	17
16	13.74	1.030 t (7.5)	14,15	
17	19.12	2.097 br s	12,13,14	
18	33.88	0.960 s	3,4,5,19	
19	22.36	0.954 s	3,4,5,18	20
20	20.05	1.549 s	1,5,9,10	
11-OH	---	3.726 s	9,11,12	

[a] "-like" multiplicities: the given value represents the distance of the multiplet lines, not the exact coupling constant; [b] each NOE is listed only once.

Table S8 NMR data of compound 6 (C_6D_6)

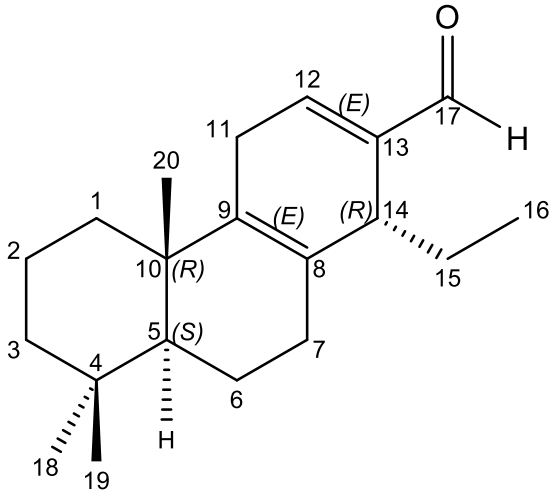

Pos.	^{13}C: δ [ppm]	^{1}H: δ [ppm] m (J[Hz][a])	HMBC (H →C)	COSY	ROE[d]
1	37.33	0.927 m α 1.514 m β	3, 10, 2 2, 10	2	; 20, 11
2	19.26	1.400 m α 1.520 m β	4, 1, 10,3 10, 1		; 20
3	41.84	1.102[c] dt-like (4.3, 13.5) α 1.380 m[c] β	2,4,19 5, 19, 2		
4	33.30	---			
5	52.26	1.076 dd (2.1,12.6) α	10, 19, 7, 20	6	18
6	18.88	1.329[c] qd-like (6.4, 12.4) β 1.552[c] br dd-like (7.3, 12.6) α	7, 10, 5 7, 10, 5, 8	7,5	 18
7	30.41	1.636[c] br dd like (6.4, 17.5) β 2.066 m α	6, 8, 9, 5 6, 8, 9	6	
8	127.65	---			
9	136.16	---			
10	37.70	---			
11	27.25	2.432 m	8,9,13, 12	12	20
12	148.83	6.214 dd (4.4, 3.3)	11, 14, 17, 9	11	17
13	142.69	---			
14	39.17	3.272 m	7, 8, 9, 12, 13, 15, 16, 17	15	7β
15	24.47	1.872 m [c] 1.613 m [c]	16, 14, 8, 13; 16, 14, 8, 13	14,16	
16	8.27	0.609 t (7.5)	14, 15	15	7β, 5
17	191.91	9.350 s	12, 13, 8, 14		
18	33.34	0.869 s	3,4,5,19		6α
19	21.82	0.836 s	3,4,5,18		6α, 20
20	19.14	0.891 s	1, 9, 5, 10		

[a] "-like" multiplicities: the given value represents the distance of the multiplet lines, not the exact coupling constant; [c] ^{1}H chemical shift of HSQC correlation peak; [d] each NOE is listed only once. 14R configuration is more likely because of NOE H-7β/H-14

Table S9 NMR data of compound 19 (C_6D_6)

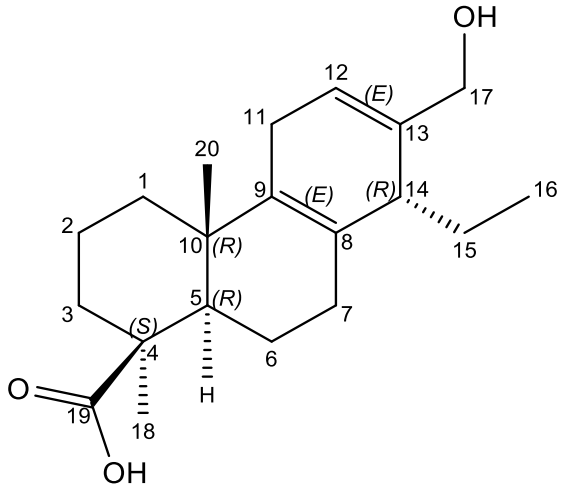

Pos.	^{13}C: δ [ppm]	^{1}H: δ [ppm] m (J[Hz][a])	HMBC (H →C)	COSY	ROE[d]
1	37.61	1.656[c] m β 0.974[c] m α	2, 3, 5,10, 20 2, 3, 5, 9, 10, 20	2	11;
2	19.90	1.451[c] m α 2.079[c] m β	1, 3, 4, 10,	3	; 20
3	37.65	2.308 dt-like (13.4, 3.2) β 0.860 td-like(13.7, 4.4) α	1, 2, 4, 5; 1, 2, 4, 5, 18, 19	2	
4	43.87	---			
5	53.92	1.287[c] dd (3.3, 10.7) α	3, 4, 6, 7, 9, 10, 18, 19, 20	6	1α, 3α
6	20.92	2.030[c] m	8, 5, 7, 10	5, 7	20
7	31.62	2.104[c] m α 1.760 brdd-like (16.0, 2.8) β	; 6, 8, 9	6	
8	127.56	---			
9	136.92	---			
10	38.62	---			
11	26.12	2.435 br-s	---	12	20
12	122.16	5.711 t-like (3.4)	9, 11, 14, 17	11	17, 11
13	137.92	---			
14	42.64	2.704 m	7, 8, 9, 12, 13, 15, 16	15	7β
15	23.42	1.564 m	8, 13, 14, 16		7α
16	7.86	0.709 t (7.4)	14, 15	15	
17	64.91	3.871[c] m	12, 13, 14		
18	28.49	1.150 s	5, 4, 3, 4, 5, 19		3, 6
19	182.42	---			
20	17.38	1.043 s	9, 10, 5, 1		1β

[a] "-like" multiplicities: the given value represents the distance of the multiplet lines, not the exact coupling constant; [c] ^{1}H chemical shift of HSQC correlation peak; [d] each NOE is listed only once.

14R configuration is more likely because of NOE H-7β/H-14

Table S10 NMR data of compound 21 (C_6D_6)

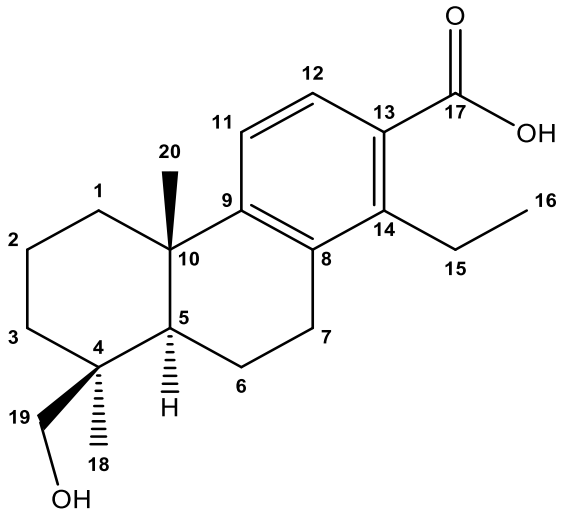

Chemical Formula: $C_{20}H_{28}O_3$

Pos.	^{13}C: δ [ppm]	^{1}H: δ [ppm] m (J[Hz])	selected HMBC (H → C)	ROE[c]	COSY
1	39.20	1.990 dt-like (8.4, 3.5) β 1.153 m α	6, 20, 3, 10	2, 11	2
2	19.29	1.40[e] m 1.48[e] m			3
3	35.30	1.833[a] β 0.814[a] α	2, 4, 19		
4	38.84	---			
5	50.08	1.163[a] α	10, 19, 7, 20, 6	6	
6	19.28	1.761 α 1.427[a] β	6, 5, 10, 7	7α; 7β	5
7	28.18	2.715 dd (17.2, 6.2) β 2.429 ddd α	9, 14, 8, 5, 6	16, 6, 15; 6α, 15	6
8	134.24	---			
9	154.97	---			
10	38.63	---			
11	122.73	6.998 d(8.5)	13, 8, 10	1β	12
12	129.19	7.914 d(8.4)	17, 9, 14		11
13	126.32	---			
14	145.28	---			
15	23.05	3.147 2.946	16, 13, 8, 14	7β 7α	16
16	14.72	1.285 t (7.4)	14, 15		15
17	170.34	---			
19	64.83	3.506 d (10.6) 3.226 dd (10.6, 1.2)	18, 3, 10, 5	20 6β	20
18	26.96	0.950 s	4, 3, 5, 19		6α
20	25.54	0.987 s	9, 5, 10, 1	19	

[a] ^{1}H chemical shift of HSQC correlation peaks; [b] ^{1}H chemical shift from selective TOCSY spectrum; [c] each NOE is listed only once; [e] 1H chemical shift from TOCSY

Acknowledgement

Many to say, many thanks I want to say, but firstly I would like to share a short story that happened to me. It was on my first day in Europe. When I arrived at the airport, I saw so many Europeans for the first time. Then I sent a message to my friend. I said I was surrounded by foreigners. But immediately I realized that I am the foreigner now. Also at that moment, I knew that it's time to change my mind now.

My foremost gratitude goes to my supervisors **Prof. Dr. Alain Tissier** and **PD Dr. Gerd Balcke** for accepting me as a PhD student and unending supports for this thesis project. I thank them for supervision, guidance and constant encouragement during my research.

I am very grateful to my collaborators in Köln. I want to thank **Prof. Dr. Alga Zuccaro** for being a member of my thesis committee, and for valuable insights, discussions on this project. I want to thank **Lisa Mahdi** for providing barley root samples and the supports on establishing the workflow of infection assay in IPB. I would like to thank **Dr. Ivan Acosta** (MPI for Plant Breeding Research, Köln) for providing CRISPR lines of barley.

I would like to thank the reviewers for investing their time and energy to review my thesis. Many thanks go to thesis committee members for evaluating my research.

I want to thank all the former and present lab members for their help and support, and for keeping the great atmosphere of the lab. I want to thank **Dr. Ulschan Bathe** for the guide of yeast expression. I want to thank **Dr. Tom Schreiber** for the introduction of Golden Gate Cloning and the transient expression. I would like to thank **Dr. Heena Yadav**, **Dr. Maximilian Frey**, **Dr. Changqing Yang**, **Dr. Khabat Vahabi** for great discussions and suggestions on the project. I want to thank **Dr. Micha Gracianna Devi**, **Kathleen Helmstedt**, **Jayanth Gopinatha Bharadwaj**, **Robert Säbel**, **Alejandro Brand Duran, Dario Esposto** for all kinds of help in the experiments. I want to thank the technicians, **Petra Schäfer**, **Anja Prange**, specially to **Anja Scherr-Henning** for her tremendous supports on the lab work.

I have great pleasure to thank all the members of **SZB** department, especially **AG Sylvestre Marillonnet** for providing all the vectors for Golden Gate Cloning, and **AG Bettina Hause** for conducting mycorrhiza assay. I want to thank **PD Dr. Thomas Vogt** for discussions and comments during my progress report. A special thanks goes to **Esther Harding** for proofreading of my thesis.

I want to thank my friends in Halle and in China, **Zihao, Yi, Marc**, **Ahyoung, Xiyuan, Yunjing, Arianna** specially to **Mingdan** for their kindness and emotional support. It is so much fun to gather together with you.

I greatly acknowledge the funding from the **DECRyPT** project (SPP 2125).

I am very grateful to my parents and my sister for their unconditional love and support on my decisions. They are my biggest source of strength and motivation.

Curriculum Vitae

Name: Yaming Liu
Nationality: Chinese
Gender: Male
Email: lymzzu2009@gmail.com

Education and Working Experience

2019-present	**PhD Candidate** Leibniz Institute of Plant Biochemistry, Halle (Saale) Thesis: Characterization of the molecular mechanism underlying defense responses of barley against pathogenic infection Supervisor: Prof. Dr. Alain Tissier, PD Dr. Gerd Balcke
2016-2019	**Bioinformatician** BGI, Shenzhen, China
2013-2016	**Master of Engineering (Bioengineering)** University of Chinese Academy of Sciences, Beijing, China Thesis: Development of an MSn spectra database for N-linked oligosaccharides Supervisor: Prof. Dr. Yan Li
2009-2013	**Bachelor of Science (Biotechnology)** Zhengzhou University, Zhengzhou, China

Conference and Workshop

BOTANIK-TAGUNG — Bonn, Germany, 2022

Poster, ‘A barley gene cluster for the biosynthesis of diterpenoid phytoalexins’

CliMetabolomics Workshop — France/Germany, 2022

Plant Science Student Conference — Halle, Germany, 2019 and 2021

Oral Talk and Poster, 2019, ‘Metabolic response of barley root upon plant-pathogen interaction’
Poster, 2021, ‘A barley gene cluster for the biosynthesis of diterpenoid phytoalexins’

TERPNET — Halle, Germany, 2019

Poster, ‘Characterization of the molecular mechanism underlying defense responses of barley against pathogenic infection’

List of publications

1) **Liu, Y.**, Balcke, G.U., Porzel, A., Mahdi, L., Scherr-Henning, A., Bathe, U., Zuccaro, A. and Tissier, A., 2021. A barley gene cluster for the biosynthesis of diterpenoid phytoalexins. bioRxiv.

2) Sun, S., Huang, C., Wang, Y., **Liu, Y.**, Zhang, J., Zhou, J., Gao, F., Yang, F., Chen, R., Mulloy, B. and Chai, W., 2018. Toward automated identification of glycan branching patterns using multistage mass spectrometry with intelligent precursor selection. Analytical chemistry, 90(24), pp.14412-14422.

3) Zhao, Q., Zhan, T., Deng, Z., Li, Q., **Liu, Y.**, Yang, S., Ji, D. and Li, Y., 2018. Glycan analysis of colorectal cancer samples reveals stage-dependent changes in CEA glycosylation patterns. Clinical proteomics, 15(1), pp.1-11.

4) Huang, C., **Liu, Y.**, Wu, H., Sun, D. and Li, Y., 2017. Characterization of IgG glycosylation in rheumatoid arthritis patients by MALDI-TOF-MSn and capillary electrophoresis. Analytical and Bioanalytical Chemistry, 409(15), pp.3731-3739.

5) Huang, C., Zhan, T., **Liu, Y.**, Li, Q., Wu, H., Ji, D. and Li, Y., 2015. Glycomic profiling of carcinoembryonic antigen isolated from human tumor tissue. Clinical proteomics, 12(1), pp.1-7.

Eidesstattliche Erklärung

Hiermit erkläre ich, dass ich die vorliegende wissenschaftliche Arbeit selbständig und ohne fremde Hilfe angefertigt habe. Ich erkläre, dass ich keine anderen als die von mir angegebenen Quellen und Hilfsmittel benutzt habe und die den Werken wörtlich und inhaltlich entnommenen Stellen als solche kenntlich gemacht habe. Ich versichere weiterhin, dass ich mich erstmals mit dieser Arbeit um die Erlangung des Doktorgrades bewerbe. Diese Arbeit wurde an keiner anderen Fakultät oder Universität zur Begutachtung eingereicht.

Halle (Saale), den 16.01.2023
Yaming Liu